Proton-Catalyzed Oligomerization, non-Stokesian Diffusion, and the Slaving Effect of Glycerol on Protein Folding and Dynamics

A Thesis Submitted for the Degree of

DOCTOR OF PHILOSOPHY

By

KIRTHI JOSHI



School of Chemistry
University Of Hyderabad
Hyderabad - 500 046
INDIA

JULY 2023

Dedicated to My parents

And

My Chemistry Teacher, S. Narsing Reddy

CONTENTS

		Page No
STATEME	ENT	I
DECLARA	ATION	П
CERTIFIC	CATE	Ш
ACKNOW	LEDGEMENT	V
List of Abb	previations and symbols	VII
Chapter 1	Introduction	
	1.1. Overview	1
	1.2. Structure, Bonding and Chemical properties	1
	1.3. Glycerol as a cryoprotectant and stabilizing agent for protein molecules	2
	1.4. Earlier reports on water-glycerol binary system and water-protein-glycerol ternary system	3
	1.5. Native and Quasi-native states of protein	4
	1.6. Diffusion and Hydrodynamic radius	4
	1.7. Internal Dynamics of protein	5
	1.8. References	6
Chapter 2	H ⁺ -Catalyzed glycerol condensation, preferential compe exclusion, and water clustering in water-glycerol binary	
	Abstract	10
	2.1. Introduction	11
	2.2. Materials and methods	12

	2.3. Results and Discussions	2
	2.4. Discussion	27
	2.5. References	30
Chapter 3	Quasi-native transition and self-diffusion of proteins in water-glycer mixture	ol
	Abstract	35
	3.1. Introduction	35
	3.2. Materials and methods	37
	3.3. Results	38
	3.4. Discussion	56
	3.5. Conclusion and Prospect	64
	3.6. References	64
Chapter 4	Glycerol-slaved volume fluctuations and NMR cross-relaxations in lysozyme	
	Abstract	73
	4.1. Introduction	73
	4.2. Experimental section	75
	4.3. Results and Discussion	76
	4.4. Discussion	.87
	4.5. Conclusions	94
	4.6. References	.95
Publications	s and Presentations	102



School of Chemistry
University of Hyderabad
Hyderabad – 500 046

STATEMENT

I hereby declare that the matter embodied in thesis is the result of investigations carried out by me at School of Chemistry, University of Hyderabad, Hyderabad, under the supervision of **Prof.** Abani K. Bhuyan.

In keeping with the general practice of reporting scientific observations, due acknowledgements have been made whenever the work described is based on the finding of other investigators. Any omission which might have occurred by oversight or error is regretted.

Hyderabad

July 2023

Kisthijoshi

Kirthi Joshi

(17CHPH02)



DECLARATION

I, Kirthi Joshi, hereby declare that the thesis entitled, "Proton-Catalysed Oligomerization, non-Stokesian Diffusion, and the Slaving Effect of Glycerol on Protein Folding and Dynamics" submitted by me under the supervision of Prof. Abani K. Bhuyan, is a bonafide research work which is free from plagiarism. I also declare that it has not been submitted previously in part or in full to this University or any other university or institution for the award of any degree or diploma. I hereby agree that my thesis can be deposited in Shodhganga/INFLIBNET.

A report on plagiarism from the University Library is enclosed.

Date: 27/07/2023

Kirthi Joshi

Reg. No. 17CHPH02

Kithijoshi
Signature of the student

Signature of the Supervisor

ABANI K. BHUYAN, Ph.D. Professor

Dani W

University of Hyderabad School of Chemistry Hyderabad - 500 046. Prof Abani K. Bhuyan School of Chemistry University of Hyderabad Hyderabad – 500 046



Phone: +91-40-2313 4810 (O) Fax: +91-40-2301-2460

Email: akbsc@uohyd.ac.in

<u>CERTIFICATE</u>

This is to certify that the thesis entitled, "Proton-Catalysed Oligomerization, non-Stokesian Diffusion, and the Slaving Effect of Glycerol on Protein Folding and Dynamics" submitted by Ms. Kirthi Joshi bearing registration number 17chph02 in partial fulfillment of the requirements for the award of Doctor of Philosophy (Ph.D.) is a bonafide work carried out by her under my supervision and guidance in the School of Chemistry, University of Hyderabad. This thesis is free from plagiarism and has not been submitted previously in part or in full to this or any other University or Institution for the award of any degree or diploma.

Further, the student has two publications before submission of the thesis adjudication and has produced evidences for the same in the form of reprints.

Parts of this thesis have been published in the following one publication

1. Joshi, K.; Bhuyan, A. K. *Biophysical Chemistry*. **2020**, 257, 106274

She has also made presentations in the following conferences

1. Poster: "The effect of Glycerol on the structure of Protein" at CHEMFEST - 2019: Annual In-house symposium at School of Chemistry, University of Hyderabad.

 Presentation: "NMR and Optical Spectroscopic Studies of binary and ternary aqueous systems containing glycerol as a component" at CHEMFEST- 2021: Annual In-house Symposium at School of Chemistry, University of Hyderabad.

The student has passed the following courses towards the fulfilment of coursework requirement for Ph.D.

Sl. No.	Course No.	Title of the Course	No. of Credits	Result
1	CY801	Research Proposal	4	Pass
2	CY805	Instrumental Methods - A	4	Pass
3	CY806	Instrumental Methods - B	4	Pass

Abani Wy.

Prof. Abani K. Bhuyan

(Thesis Supervisor)

ABANI K. BHUYAN, Ph.D.

Professor

University of Hyderabad School of Chemistry Hyderabad - 500 046. Almi Mengre Dean

School of Chemistry

University of Hyderabad

Dean

SCHOOL OF CHEMISTRY University of Hyderabad Hyderabad-500 046.

Acknowledgement

I express my heartfelt gratitude to my Ph.D. supervisor Prof. Abani K. Bhuyan who is mainly responsible for the completion of my thesis. I'm grateful to him for teaching me the research skills and the importance of ethics in research. I would love to inculcate many of his qualities in my life, three most important being his organizational skills, extraordinary skills of record keeping and most importantly his simplicity. I personally adore his oratory skills, beautiful handwriting and scientific rigor.

I would like to extend my heartfelt gratitude to the members of my doctoral committee, Prof. Tushar Jana and Dr. Manju Sharma. Their insightful suggestions, constructive criticism and intellectual engagement have enriched the quality of work.

I want to thank present and former Deans, School of Chemistry, University of Hyderabad and all the faculty members of School of Chemistry for their help and support on various occasions. I thank all the faculty who taught me during my coursework.

I want to acknowledge DST-INSPIRE for the financial support during my Ph.D. tenure.

I was extraordinarily fortunate to work with a very good company of people in the laboratory. I thank my friend Noorul who always stood by me through thick and thin. I thank him for teaching me the importance of updating oneself with the current technical skills and knowledge to stay stay relevant in current times. I admire his empathetic nature and cheerful personality. I thank my friend Mujahid for always motivating me in tough times. I admire his calm personality, deep thinking and I enjoy listening to his philosophical interpretations of scientific phenomena. I thank Ramesh who has taught me the importance of networking and social skills for growth in life. I thank Shanti mam for teaching me protein purification techniques and for being with me whenever I was ill and hospitalized. I will be indepted to my labmates for their kindness, love and support showered upon me. I thank Shashi sir for the valuable discussions and helpful suggestions.

I thank the project students, Sarita, Koustav, Kavya and Athira who had worked with me during my tenure and offered so much to learn.

I'm grateful to Dr. Prakash Prabhu for allowing me to use densitometer in his lab. I also thank Brahmini mam, Tejaswi sir, Pratibha for helping me with Densitometer. A special thanks to Sanjay who has helped me with Circular Dichroism when it was really urgent.

I thank my School teachers who had taught me basic science, mathematics and life skills. I thank Gajanan sir for improving my mathematics, Sudeep sir who had taught me English, my School Principal D. Vinayak Rao sir who equally emphasized on education, discipline and values. I thank Ms. Veena who introduced me to the basics of chemistry like writing electronic configurations of the elements. I would be indebted to late Narsing Reddy Sarsan, my chemistry

teacher, who inculcated curiosity in my mind for chemistry. He is an example of how one could speak less and yet be so influential. His accomplishments in his life set an example that it's not the long life that matters but a fulfilling life. I really feel fortunate to have been taught by such a wonderful person. I'm grateful to Mallikarjun sir and Kama Shastri sir for their wonderful classes on Chemistry and Mathematics. I thank Ms. Hari Padmashri mam, Sowmya mam (Mathematics) and Sowmya mam (Chemistry), who were extremely kind and helpful to me during my Bachelors study. A special thanks to Hari Padmashri mam, who had shown concern towards my health and career.

A special thanks to my friend and a genius researcher, Dr. Vinod Mouli who has inspired me to step into research. All the discussions regarding chemistry, I had with him have always benefited me in research.

I thank God for blessing me with a wonderful family. I thank my Aayee (mother), Ms. Vijaya Joshi, who had been selflessly making sacrifices for my well being and happiness. Her kind and empathetic nature and modern outlook has a great role in shaping my personality. I thank her for always encouraging me to dream high and work hard towards achieving it. I thank my pappa, Mr. Krishanand Joshi who had never compromised on providing us with good education inspite of the financial constrains. I like the way he switches his role from a father to a friend and carefully listens to my insecurities and distress and I'm very fond of the small meaningful anecdotes that he narrates to me to teach great lessons of life. I cannot imagine my life without my beautiful sisters Dolly (Shravani Joshi) and kalyantai (Kalyani Joshi Samudre) who have been a constant strong supports in my personal and professional life. I thank my elder sister for teaching me to have a broader perspective towards life, I thank her for taking our responsibility and caring like a mother. I thank my younger sister Dolly for being my best friend all these years and also for being with me in every walk of life and helping me in taking correct decisions. I thank my brother-in-law, Mr. Parikshit Samudre who have always supported and guided me like an elder brother. Above all I thank my little nephew Puchku (Samihan Samudre) who have always been my stress buster and helped me stay happy in the most stressful period of my life.

I'm indebted to my dear friends, Jhansi and Prasannatha for always helping me when I was ill. I thank Prasannatha for helping me with the academic stuff. I thank Girija mam, Rina, Sonali, Rani, Bhavana, Arun Anna - the best listener I know, for all the good memories during my stay of six years in this campus. I thank all my well-wishers whom I could not name due to space constrain.

Kirthi Joshi July 2023.

ABBREVIATIONS

CD Circular Dichroism

UV Ultraviolet

NMR Nuclear Magnetic Resonance

PFG Pulsed Field Gradient

NOE Nuclear Overhauser Effect

MSD Mean Square Displacement

RMS Root Mean Square

m/z mass/charge

au atomic unit

R_H Hydrodynamic Radius

D_s Translational Diffusion Coefficient

V_M Intrinsic Volume

a_{glycerol} Activity of glycerol

N_w Native state

D_{gly} Quasi-native state

η Viscosity

 β_p Adiabatic Compressibility

β_s Isothermal Compressibility

Trp Tryptophan

M Methionine

K Lysine

W Tryptophan

Y Tyrosine

R Argnine

S Serine

G Glycine

C Cysteine

N Asparagine

D Aspartic acid

T Threonine

INTRODUCTION

1.1. Overview

Glycerol has numerous applications in industries that involve the production of dynamite, storage of industrial products, drugs and cosmetics. But the utility of glycerol in the area of biophysical chemistry as a molecular crowder, viscogen in friction related studies of proteins, as a cosolvent to enhance the stability of protein¹⁸ and cryoprotectant for biological molecules, cells, clones and embryos⁴ raises some serious concerns with regard to glycerol properties themselves. This thesis focuses particularly on the structure and dynamics of protein in aqueous glycerol. Studies have revealed that glycerol thermodynamically stabilizes protein by excluding itself from the vicinity of the protein.⁵ The conformational changes induced by glycerol makes one wonder if protein dynamics, relaxation and conformational substates studied in the presence of glycerol solvent truly report on the native state of the protein. Likewise, to what extent glycerol changes protein conformation in cryoprotected material remains unknown. It is therefore necessary to study the binary water-glycerol system to find out the mole fraction dependent properties of glycerol and the ternary system: water-protein-glycerol to understand the effects on protein structure, stability and dynamics. For example, the caveat of using glycerol to study protein properties at low pH is that glycerol monomers undergo proton-assisted oligomerization whose effect on solvent and protein properties is little understood. The thesis examines oligomerization of glycerol at moderately low pH, a condition used widely to not only study proteins but also preserve foodstuffs and biomaterials at low temperatures. Since protein is preferentially hydrated in aqueous glycerol, 6 the thesis also studies how glycerol in the bulk controls relaxations and internal motions in proteins.

1.2. Structure, Bonding and Chemical properties of Glycerol

Glycerol, Propane-1,2,3-triol is a three carbon aliphatic alcohol with three hydroxyl groups. It is highly soluble in water and other alcohols because of its ability to form intermolecular H-bonding. The aliphaticity of carbons in glycerol renders the molecule a complicated

conformational behavior. The presence of three –OH groups allows the molecule to form a rich inter- and intra-molecular H-bond network. It is this strong network of H-bond that is responsible for the viscosity of 1.412×10^3 cP at 20 °C for pure glycerol⁷. Glycerol has a long liquid range temperature with melting point of 18 °C and boiling point of 290 °C. The presence of C–O and O–H polar bonds imparts a net dipole moment of 2.56 D to the molecule. The molecular structure of glycerol is shown below.

1.3. Glycerol as a cryoprotectant and stabilizing agent for protein molecules

The adaptation of living organisms in harsh environmental conditions of extremely low temperatures has always been a fascinating area of research. Many studies investigated the biochemical response and changes in the metabolites of these freeze tolerant animals to decrease in the temperature with seasonal changes. A study conducted on metabolites of liver of animals from Kolyma populations reveal that the concentrations of glycerol in fall is $\leq 0.5\%$, the three day long freezing at -5 °C results the concentration of glycerol increase to 2%, a gradual decrease in temperature to -20 °C for 20 days raised the concentration of glycerol to 7% and glycerol content as high as 18% was observed on long exposure to temperature below -20 °C which demonstrates the role of glycerol as a natural cryoprotectant in these organisms. In vitro and also for biomolecules like proteins and DNA. The low temperature studies on protein molecules are generally carried out in the presence of glycerol as a cryoprotectant because it is known to decrease the freezing point of water inhibiting the formation of ice and maintaining the structure of protein at low temperatures. But the knowledge of detailed transformations in the

conformation of protein at secondary and tertiary levels that glycerol could otherwise induce at room temperature will help gain deeper insights on the mechanistic approach of the role of glycerol as a cryoprotectant and preservant.

1.4. Earlier reports on the study of water-glycerol binary system and waterprotein-glycerol ternary system

1.4.1. Water-glycerol binary system

The cryoprotective property and protein stabilizing ability of higher concentration of aqueous glycerol makes the water-glycerol mixture a fascinating system to study. It is crucial to explore the physical chemistry of water-glycerol binary system to unravel its function as a cryoprotectant and stabilizing cosolvent. Studies reveal that at low concentrations of glycerol in the water-glycerol binary mixture, water undergoes crystallization at low temperature but an inhibition in the crystallization of water was observed at high concentration of glycerol which indicates that the ability of water-glycerol mixture to inhibit water crystallization at low temperature is linked to the concentration of glycerol and hydrogen bonding patterns of these solutions.⁴ The H-bonding of water-glycerol mixture at different composition have been extensively studied using Molecular Dynamics Simulations (MDS)¹⁵ and IR spectroscopy.¹⁶ The study of protein reactions in glycerol also employs specific pH conditions to maintain the native state of the protein and hence the manner in which pH affects the physical chemistry of the binary mixture from pH 2–7 is explored in the chapter 2 of the thesis.

1.4.2. Water-protein-glycerol ternary system

Water has always been employed as a natural medium to carry out protein folding and unfolding studies. Since proteins are only marginally stable and can undergo partial unfolding with slightest stimulation from the environment which can affect the functionality of proteins *in vitro*

and *in vivo*, polyols are often employed as cosolvents owing to their ability to enhance the stability of the protein.

One of the most widely used polyols to stabilize protein in aqueous solvent is glycerol. Although not much is known regarding the mechanism by which the cosolvents induce protein stability, earlier reports on the study of water-protein-glycerol ternary system have shown that glycerol shifts the native conformation of protein to a more compact and ordered states. Some reports also refer to the preferential interaction theory to provide a thermodynamic framework to account for the effect of glycerol on the stability of protein. The often encountered problem during protein refolding is the aggregation of protein, and glycerol is also known to inhibit the aggregation of protein. Reports also show that glycerol protects the protein from thermal induced aggregation.

1.5. Native and Quasi-native states of Protein

The native state of a protein is the folded form which has all the four levels of protein structure properly assembled whereas the quasi-native state which appears in glycerol has higher propensity of secondary structure when compared to the native state. Also, the tertiary structure of the quasi-native state could be more compact or a little expanded depending on the protein and its native pH condition. These pH specific changes pertaining to tertiary structure is due to different physical properties of the binary mixture water-glycerol at different pH conditions. At low pH, the binary mixture is extremely heterogeneous in terms of the glycerol oligomers and water clusters which could affect the hydration of protein, consequently affecting its tertiary structure and Stoke's radius.

1.6. Diffusion and Hydrodynamic radius

Diffusion allows molecules to find one another in the cell – enzymes to find the substrates, membrane proteins to find membranes, and transcription factors to find sites on DNA. The proper functioning of cell depends significantly on the diffusion of the cellular components. Therefore, diffusion studies of proteins in cells, cell membranes, and in vitro have always been a

core area of research in biophysical chemistry. Diffusion related studies act as an interface between biology and physics.

If the Brownian motion is the manifestation of the thermal motions of fluid molecules, then the motion should obey the law of diffusion which is linear proportionality of Mean-squared displacement with time to yield a translational diffusion constant $(D_s)^{21}$

$$D_{\rm S} = \frac{k_{\rm B}T}{c\pi r\eta} \tag{1}$$

depending on the absolute temperature (T), radius of the particle (r) and viscosity of the fluid (η) . The other symbols in eq 1 have the usual meaning; k_B is Boltzmann constant and c is a constant that depends on the nature of the solvent. Since the sizes of the proteins make them susceptible to Brownian motion, Einstein's equation of translational diffusion is applicable to protein molecules.

Molecular dimension of the proteins is of considerable importance to characterize native and non-native states of proteins in a solution. Hydrodynamic radius which is also referred to as Stoke's radius is a measure of dimension of a molecule determined by means of a translational diffusion coefficient. Hydrodynamic radius is a key parameter beyond just sizing of the molecule which provides vital information on numerous crucial biomolecular properties including conformational changes, affinity, oligomerization, and degradation. There are numerous techniques to probe the hydrodynamics of a protein molecule that includes small angle scattering studies using neutrons and X-rays,²² dynamic light scattering,²³ and fluorescence correlation spectroscopy.²⁴ Our study invariably employs pulsed field gradient (PFG) NMR²⁵ to determine Stoke's radius of proteins via translational diffusion coefficient.

1.7. Internal Dynamics of Protein

The extreme specificity in the functionality of protein is a consequence of the specific threedimensional structure of protein. The protein-enzyme reactions occasionally require the adaptation of changes in the 3D structure of protein. This adaptability demands high order of flexibility in protein molecule. The internal dynamics is a protein specific intrinsic property which offers this flexibility to the protein molecule. The internal dynamics of protein is strongly affected by external parameters, like temperature and hydration in particular. Experiments have shown that density of water in the hydration shell impacts the functioning of enzyme by perturbing its internal dynamics.²⁶ In the thesis we study the impact of high bulk viscosity of the solvent (glycerol) on internal dynamics, mean-squared volume fluctuation and diffusion of proteins. The internal dynamics of protein in glycerol is probed using transient 2D NOESY NMR to understand the slaving of internal dynamics of protein molecule by Debye relaxation of glycerol.²⁷

1.8. References

- 1. Pagliaro, M.; Ciriminna, R.; Kimura H.; Rossi, M.; Della Pina, C. From glycerol to value-added products. *Angew. Chem., Int. Ed. Engl.* **2007**, *46*, 4434-4440.
- 2. Chau, C. C.; Radford, S. E.; Hewitt, E. W.; Actis, P. Macromolecular crowding enhances the detection of DNA and proteins by a solid-state nanopore. *Nano Lett.* **2020**, *20*, 5553–5561.
- 3. Fologea, D.; Uplinger, J.; Thomas, B.; McNabb, D. C.; Li, J. Slowing DNA translocation in a solid state nanopore. *Nano Lett.* **2005**, *5*, 1734–1737.
- Dashnau, J. L.; Nucci, N. V.; Sharp, K. A.; Vanderkooi, J. M. Hydrogen Bonding and Cryoprotective properties of Glycerol/Water Mixtures. J. Phys. Chem. B. 2006, 110, 13670-13677.
- 5. Timasheff, S. N. The control of Protein Stability and Association by Weak-Interactions with Water: How Do Solvents Affect These Processes? *Annu. Rev. Biophys. Biomol. Struct.* **1993**, 22, 67-69
- 6. Timasheff, S. N. Protein Hydration, Thermodynamic Binding, and Preferential Hydration. *Biochemistry*, **2002**, *41*, *46*, 13473-13482.
- 7. Segur, J. B.; Oberstar, H. E. Viscosity of Glycerol and its Aqueous Solutions. *Ind. Eng. Chem.*

- **1951**, *43*(9), 2117-2120.
- 8. Bormashenko, E. Why are the values of surface tension of most organic liquids similar? *Amer. J. Phys.* **2010**, 78, 1309-1311.
- 9. Churchill, T. A.; Storey, K. B. Effects of dehydration on organ metabolism in the frog Pseudacris crucifer: Hyperglycemic responses to dehydration mimic freezing-induced cryoprotectant production. *J. Comp. Physiol. B.* **1994**, *164*, 492-498.
- 10. Costanzo, J. P.; Lee, R. E. Jr. Avoidance and tolerance of freezing in ectothermic vertebrates. *J. Exp. Biol.* **2013**, *216*, 1961-1967.
- 11. Berman, D. I.; Meshcheryakova, E. N.; Bulakhova, N. A. Extreme negative temperatures and body mass loss in the Siberian salamander (Salamandrella Keyserlingii, Amphibia, Hynobiidae). *Dolk. Biol. Sci.* **2016**, *468*, 137-141.
- 12. Berman, D. I.; Leirikh, A. N.; Meshcheryakova, E. N. The Schrenck newt (Salamandrella schrenckii, Amphibia, Caudata, Hynobiidae) is the second amphibian that withstands extremely low temperatures. *Dokl. Bio. Sci.* **2010**, *431*, 131-134.
- 13. Berman, D. I.; Meshcheryakova, E. N.; Bulakhova, N. A. The Japanese tree frog (Hyla japonica), one of the most cold resistant species of amphibians. *Dokl. Biol. Sci.* **2016**, *471*, 276-279.
- Shekhovtsov, S. V.; Bulakhova, N. A.; Tsentalovich, Y. P.; Zelentsova, E. A.;
 Meshcheryakova, E. N.; Poluboyarova, T. V.; Berman, D. I. Biochemical Response to
 Freezing in Siberian Salamander Salamandrella Keyserlingii. *Biology.* 2021, 10, 1172.
- 15. Egorov, A. V.; Lyubartsev, A. P; Laaksonen, A. Molecular dynamics simulation study of glycerol-water mixtures. *J. Phys. Chem. B.* **2011**, *115*(49), 14572-14581

- 16. Kataoka, Y.; Kitadai, N.; Hisatomi, O.; Nakashima, S. Nature of hydrogen bonding of water molecules in aqueous solutions of glycerol by attenuated total reflection (ATR) infrared spectroscopy. *Applied Spectroscopy*, **2011**, *65*(*4*), 436-441.
- 17. Vagenende, V.; Yap, M. G.; Trout, B. L. Mechanisms of protein stabilization and prevention of protein aggregation by glycerol. *Biochemistry*, **2009**, *48* (*46*), 11084-11096.
- 18. Vagenende, V.; Yap, M. G.; Trout, B. L. Molecular anatomy of preferential interaction coefficients by elucidating protein solvation in mixed solvents: methodology and application for lysozyme in aqueous glycerol. *J. Phys. Chem. B.* **2009**, *113*(*34*), 11743-11753.
- 19. Khan, M. V.; Ishtikhar, M.; Rabbani, G.; Abdelhameed, A. S.; Khan, R. H.; Polyols (Glycerol and Ethylene glycol) mediated amorphous aggregate inhibition and secondary structure restoration of metalloproteinase-conalbumin (ovotransferrin). *Int. J. Biol. Macromol.* **2017**, *94* (PtA) 290-300.
- 20. Joshi, K.; Bhuyan, A. K. Quasi-native transition and self-diffusion of proteins in water-glycerol mixture. Biophysical Chemistry. **2020**, 257, 106274.
- 21. Einstein, A. Uber die von der molecularkinetischen Theorie der Warme geforderte Bewegung von in ruhenden Flussigkeiten suspendierten Teilchen *Ann. Phys.* **1905**, 549-560.
- 22. Meisburger, S. P.; Thomas, W.C.; Watkins, M.B.; Ando, N. X-ray scattering studies of protein structural dynamics. *Chem. Rev.* **2017**, *117*, 12, 7615-7672.
- 23. Lorber, B.; Fischer, F.; Baily, M.; Roy, H.; Kern, D. Protein analysis by dynamic light scattering: Methods and techniques for students. *Biochem Mol Biol Educ.* **2012**, *40*(6), 372-382.

- 24. Sherman, E.; Itkin, A.; Kuttner, Y. Y.; Rhoades, E.; Amir, D.; Haas, E.; Haran, G. Using Fluorescence correlation spectroscopy to study conformational changes in denatured proteins. *Biophys J.* **2008**, *94*(*12*), 4819-4827.
- 25. Wilkins, D. K.; Grimshaw, S. B.; Receveur, V.; Dobson, C. M.; Jones, J. A.; Hydrodynamic radii of native and denatured proteins measured by pulse field gradient NMR techniques. *Biochemistry*. **1999**, *38*(*50*), 16424-16431.
- 26. Rupley, J. A.; Gratton, E.; Careri, G. Water and globular proteins. *Elsevier Biomedical Press.* **1983**, *8*(*1*), 18-22.
- 27. Puzenko, A.; Hayashi, Y.; Ryabov, Y. E.; Balin, I.; Felsman, Y.; Kaatze, U.; Behrends, R. Relaxation Dynamics in Glycerol-Water Mixtures: I. Glycerol-Rich Mixtures. *J. Phys. Chem. B.* **2005**, 6031-6035.

H⁺-catalyzed glycerol condensation, preferential component exclusion, and water clustering in water-glycerol binary mixture

Abstract

Studies on pH sensitivity of glycerol in its binary mixture with water reveal cooperative formation of oligoglycerol catalyzed homogeneously by H⁺ under mild acidic condition at 25 °C. The oligo species predominantly occur as di, tri, and tetraglycerol, suggesting that the intended effect of glycerol in foods, pharmaceuticals, cosmetics, and the likes can be achieved simply by adding an optimized level of glycerol under mild acidic conditions. A survey of mean sizes of oligoglycerol and water clusters across the 2-7 pH range in 4.5-54.5 % glycerol (w/v) show enhancement in both oligomerization and water clustering as the glycerol content in the binary mixture increases, suggesting increasing mutual exclusion of the two components. While the two mutually excluded components plausibly exist by hydrogen bonding between the molecules of individual components under neutral pH conditions, glycerol largely undergoes oligomerization under acid condition with concomitant increase in the size of hydrogen-bonded water clusters. The preferential interactions of glycerol and water are explained invoking the concept of composition fluctuation that states that the thermodynamic interaction between the larger solute (glycerol) and the smaller solute (water) causes the former to produce composition fluctuation with respect to the latter to the same extent as the composition fluctuation with respect to the former itself.

2.1. Introduction

Glycerol (propane-1,2,3-triol) is one of the most widely studied compounds due to its structural uniqueness and diverse applications in numerous areas of science, technology, and industry. The three -OH groups on glycerol make it readily soluble in water and alcohols, but not hydrocarbons. Glycerol is a saturated compound which makes it more flexible, imparting a vast conformational range and also makes it a good glass former. It has a long liquid range temperature (T_{melting} =18 $^{\circ}$ C and T_{boiling} =290 $^{\circ}$ C) and can be supercooled to -86 $^{\circ}$ C which makes it acceptable as a cryoprotectant solvent to preserve proteins, biomolecules, and specimen. Because of the extraordinary properties of glycerol, including flexibility, viscosity, conformational behavior, and the ability to form inter and intramolecular H-bonds, the water-glycerol mixture forms an attractive system to study the physical properties of the binary mixture. In the process, the fundamental principles of physical chemistry are tested, glycerol reactions are explored, and possible caveats in the application of glycerol are examined.

Experiments conducted on diverse areas of properties and reactions of glycerol and its interactions with solutes in binary and ternary mixtures are too vast to cite even a small fraction of the available literature. Nevertheless, some previous studies on water-glycerol system involved computational and experimental methods to study H-bond pattern at different concentrations of glycerol, and some experimental studies have focused on the H-bond status, diffusion, and cluster formation as a function of glycerol concentration. Barring a few dedicated reports (ref 11, 12, for example), the preferential solvent exclusion role of glycerol that thermodynamically stabilizes solutes has not been discussed. The phenomenon of preferential interaction of glycerol with solution components, which is deeply rooted in the principle of composition fluctuation in multicomponent systems 13,14 is important because it contains often neglected terms arising from inter-solute thermodynamic interactions. The magnitude of composition fluctuation and hence the thermodynamic interactions are expected to change to a large extent when the hydrodynamic sizes of glycerol or water or both increase, leading to mutual exclusion of the components.

In studies of mutual exclusion of water and glycerol in their binary mixture here, it is found that formation of glycerol oligomers can be homogeneously catalyzed by protons at ambient temperature, i.e., by simply changing the pH of the aqueous solution from neutral to the range of 4–2. While this process is similar to Brønsted and Lewis acid-catalyzed condensation of glycerol at ~150 °C,¹⁵ retrospection also shows heterogeneously catalyzed production of oligoglycerol by the use of solid acid catalysts and cation exchange resins at temperatures ≥100 °C.^{16–18} Our approach of oligomerizing glycerol at ~25 °C is thus simple and unassuming compared to the requirements of much higher temperature in both latter methods. We carry out a series of dimensional analysis of the glycerol oligomers and water clusters to demonstrate increasing mutual exclusion of the two components as glycerol concentration in the binary mixture increases. It is also inferred that changes to certain applications of glycerol, in pharmaceutical and food industries in particular, can be achieved simply by holding the glycerol containing solution under mildly acidic conditions.

2.2. Materials and methods

Glycerol from Sigma was 99.5% as determined by gas chromatography. Aqueous solutions of glycerol in the 4.5–54.5% (w/v) range were prepared in deionized water and held at different pH from 2 to 7 by using HCl and NaOH. The NMR samples were prepared in ~10% D_2O , and simple 1D spectra were recorded using a relaxation delay of 5 s. Pulsed field gradient (PFG) experiments used diffusion gradients (*z*-gradient) in the range 0–15 Gauss cm⁻¹. The gradient pulse duration δ was 200 μ s, and the time delay between two pulses was set to 30 ms. All spectra were recorded at 25°C in a 500 MHz ASCEND Bruker spectrometer. The same samples were used to take IR spectra using a FTIR-ATR instrument (ThermoFisher Scientific).

2.3. Results and discussion

2.3.1. ¹H NMR spectrum of glycerol.

The neutral-pH proton spectrum of aqueous glycerol contains resonances from three different sets of alkyl protons that we have labeled H¹, H^{1'}, and H², of which the two protons each of H¹

and H^{1'} labels are assumed to be non-equivalent (Figure 2.1). The H¹ and H^{1'} protons give rise to two doublet-of-doublet upfield resonances, one centered at ≈ 3.63 (J=4.35 Hz) and the other at ≈ 3.54 ppm (J=11 Hz), arising from ${}^3J_{(1,2)}$, ${}^2J_{(1,1')}$ and ${}^3J_{(1',2)}$, ${}^2J_{(1',1)}$ couplings. The downfield-shifted resonances centered at ≈ 3.75 ppm (Figure 2.1) are assigned to H². Albeit insufficiently resolved, the 3.75 ppm resonance should have a triplet-of-triplet structure due to ${}^3J_{(2,1)}$, ${}^3J_{(2,1')}$ splitting of H².

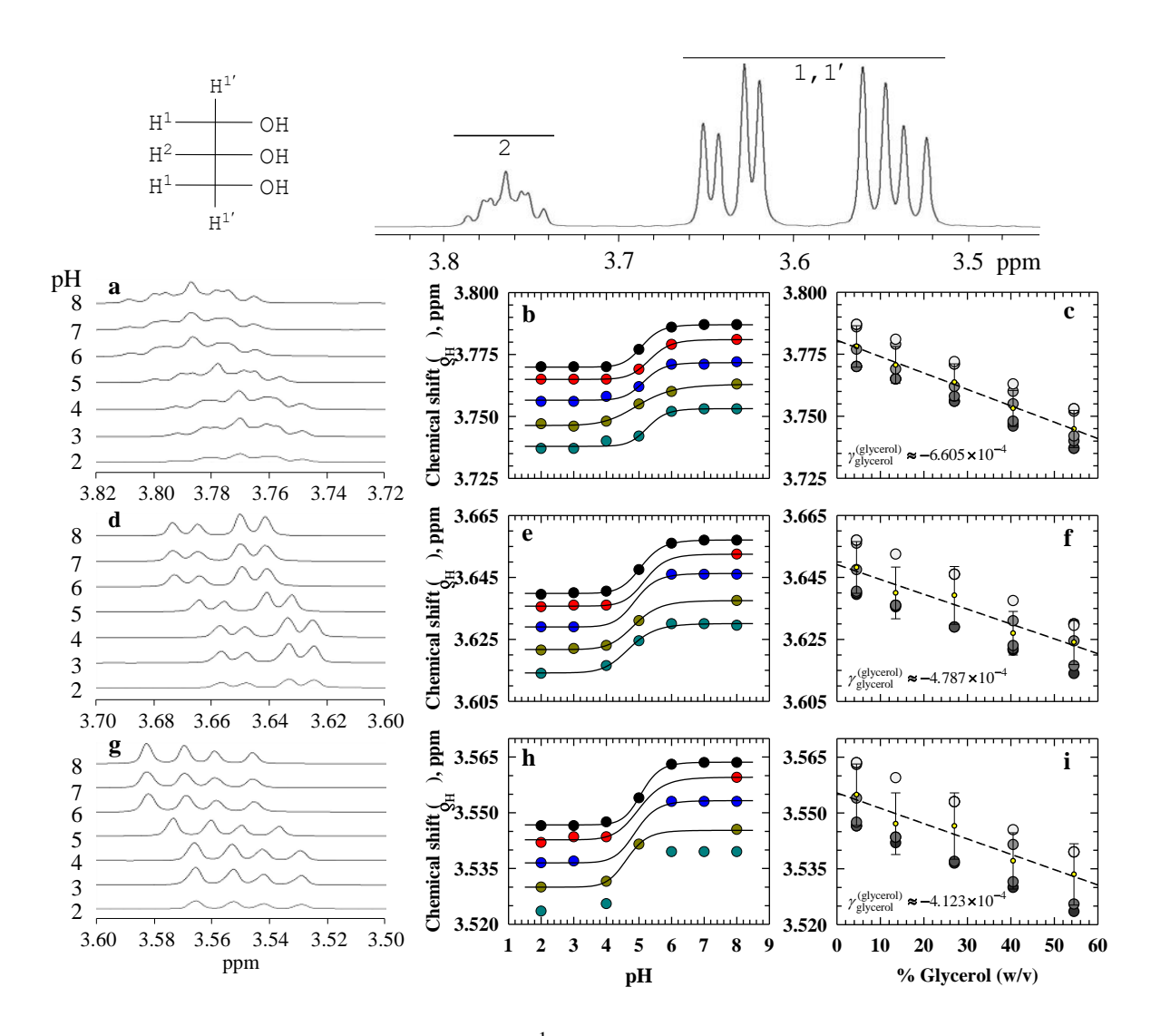


Figure 2.1. *Top*, alkyl proton labels and the ${}^{1}H$ NMR spectrum of 4.5% glycerol, pH 6. (a–c) The shift of the H^{2} triplet-of-triplet resonances at the indicated pH values, pH-cooperative resonance shift shown for 4.5 (black), 13.5 (red), 27.0 (blue), 40.5 (dark yellow) and 54.5 (dark

cyan) % glycerol, and glycerol dependence of chemical shift at pH 2, 3, 4, 5, 6, and 7 plotted with increasing gray shade. The slope of the dashed line in (c) measures the glycerol coefficient, $\gamma_{\text{glycerol}}^{\text{(glycerol)}}$, of glycerol chemical shifts according to Eq 2. The coefficients are listed in Table 5. (d-f) and (g-i) depict the same description in the same order as in (a-c) for the H¹ and H^{1'} or H^{1'} and H¹ resonances. The fits of data to acid titration of the chemical shifts shown in b, e, and h are given by Eq 1.

2.3.2. Acid-induced cooperative oligomerization of glycerol.

The chemical shifts (δ) of all alkyl protons regardless of the concentration of glycerol used titrate upfield (shielding or low frequency shift) cooperatively as acidic conditions are approached (Figure 2.1b,e,h). The acid titration of δ is assumed to represent a proton-consuming oligomerization transition depicted by Scheme 1. We note that aggregated population of glycerol may be present even at neutral pH, especially at higher %glycerol, but the formation of such aggregates do not require the assistance of protons. In the proton-assisted oligomerization, protonated glycerol leads to the formation of oxirane ring which is opened by another glycerol monomer to yield diglycerol ether. The process can continue to yield [glycerol]_n, where n is the number of monomers in the oligoglycerol whose population is presumably heterogeneous in terms of the n value (Scheme 1). This proposition requires the appearance of more than two resonances in the ¹³C NMR spectrum of glycerol at acid pH which we did not observe in titration experiments. The appearance of only two ¹³C lines influences us to assume that the linear aggregates of glycerol condense further to produce crown ether-like cyclic glycerol.

Considering this putative mechanism (Scheme 1) of glycerol oligomerization in acidic medium we chose to analyze the acid titration of chemical shifts by the modified Hill equation in the form of the logistic four-parameter regression model

$$\delta(pH) = a + \frac{m_{pH}^{n}}{p^{n} + pH^{n}}, \tag{1}$$

where a is the completely titrated upfield chemical shift or shielding of the glycerol protons, m (= $\Delta\delta$ ppm) is the total change of δ across the titration, n is the slope (Hill coefficient) of the

transition that brings about the observed shielding of glycerol protons at acid pH, and p is the midpoint of the transition (Figure 2.1b,e,h). The value of each of the m and p fit parameters is nearly the same for all protons in different % glycerol (Table 1), indicating H⁺-induced oligomerization independent of glycerol concentration. Specifically, the Hill coefficient averaged over the glycerol concentrations is ~13(\pm 2) for all the resonances measured, suggesting that the formation of the initial oligomer cooperatively leads to the formation of other oligomers, each requiring a proton to produce the first oxirane ring. The subsequent cyclization of the oligomers does not consume protons.

Scheme 1. Proton assisted oligomerization of glycerol.

Table 1. Logistic Hill equation fit parameters for pH titrations of chemical shifts of glycerol protons, 298 K

Proton	%glycerol	Parameters			
		a	$m (=\Delta \delta)$, ppm	n	p
1,1' (or 1',1)	4.50	3.55	0.017	14.8	5.1
	13.5	3.55	0.017	11.2	5.0
	27.5	3.54	0.017	13.0	4.9
	40.5	3.53	0.016	12.8	4.6
	54.5	3.53	0.016	12.3	5.0
1',1 (or 1,1')	4.50	3.64	0.017	13.3	5.1
, , , ,	13.5	3.64	0.017	13.9	5.2
	27.5	3.63	0.017	13.0	4.9
	40.5	3.62	0.016	11.3	4.9
	54.5	3.61	0.016	9.7	4.7
2	4.50	3.76	0.017	14.4	5.1
	13.5	3.76	0.016	14.6	5.3
	27.5	3.76	0.015	14.9	5.1
	40.5	3.75	0.017	8.1	5.0
	54.5	3.74	0.015	15.0	5.3
Water protons	4.50*	_	_	_	_
•	13.5	4.81	0.02	18.7	5.2
	27.5	4.81	0.05	18.7	5.2
	40.5	4.81	0.09	18.5	5.2
	54.5	4.81	0.12	17.9	5.2

^{*} The change $\Delta\delta$ across the pH scale is insufficient for fitting the data.

Although the size of the chemical shift change for glycerol ($m = \Delta \delta^{(\text{glycerol})}$) across the pH range is very similar (Table 1), the glycerol coefficient for shielding of the glycerol protons

$$\gamma_{\text{glycerol}}^{(\text{glycerol})} = \left(\frac{\Delta \delta^{(\text{glycerol})}}{\Delta_{\text{glycerol}}}\right)_{\text{pH,T,P}},\tag{2}$$

where $\Delta_{glycerol}$ is the range of %glycerol, for the H^2 proton (Figure 2.1c) is larger than those for protons H^1 and $H^{1'}$ (Figure 2.1f,i) by $\sim 2.15 \times 10^{-4}$ ppm %glycerol⁻¹. The larger shielding of the H^2 proton but relatively deshielded H^1 and $H^{1'}$ (Figure 2.1c,f,i) is presumably due to the involvement of carbon bearing these protons in the etherial linkage (Scheme 1).

Seeking additional support for acid-induced glycerol oligomerization, we took IR spectra of 27% glycerol held in the pH range 2–8 (Figure 2.2a). The IR absorption intensities of the indicated vibrational modes appear to titrate with acidity of the medium (Figure 2.2b,c,d). The absorption of the stretching mode of C–O in –CH₂OH in particular titrates out distinctly (Figure 2.2b). This is the same –CO group involved in the etherial linkages in the cyclic aggregate. Unconstrained fit of the titration according to

$$I = A + \frac{\Delta I}{1 + 10^{n(pH-pK_a)}} \tag{3}$$

where I is IR absorption, A the initial untitrated baseline absorption, ΔI the change in absorption across the pH range, and n the number of protons titrated, yields the involvement of $1.5(\pm 0.5)$ protons for the formation of the acid oligomers.

It is also pertinent to ask as to how the IR absorbance might increase as the pH of the medium is reduced from neutral to acidic, i.e., when the aggregates turn larger. The IR absorbance for a single-quantum excitation of C-O stretching for example is given by

$$I = \left(\frac{\partial \mu(r)}{\partial r}\right)_{r=r_e} \int_{-\infty}^{+\infty} \psi_v^*(r - r_e) \,\psi_{v'} \,dr \tag{4}$$

where v' and v refer to vibrational levels in the ground and excited electronic surfaces, r is the internuclear $C^{\delta+}-O^{\delta-}$ distance specific to the stretching mode and r_e is the equilibrium separation. The first-order derivative of the dipole is expected to be larger in larger aggregates, i.e., at lower pH, because the reduced intermolecular distances in the aggregates that increase the intermolecular interactions also leads to an increase in the magnitude of μ of $C^{\delta+}-O^{\delta-}$; for example, the net dipole moment of two nearby -CO groups will be the vector sum of the two dipole moments. This increase in the magnitude of μ is compensated little by the change in the C-O bond length. In other words, the oscillation of the C-O bond from the equilibrium position

changes only marginally in the larger aggregates than in the smaller ones. The larger value of the dipole derivative then leads to more intense absorption of the large-size aggregates forming at low pH than that of the smaller ones occurring at higher pH.

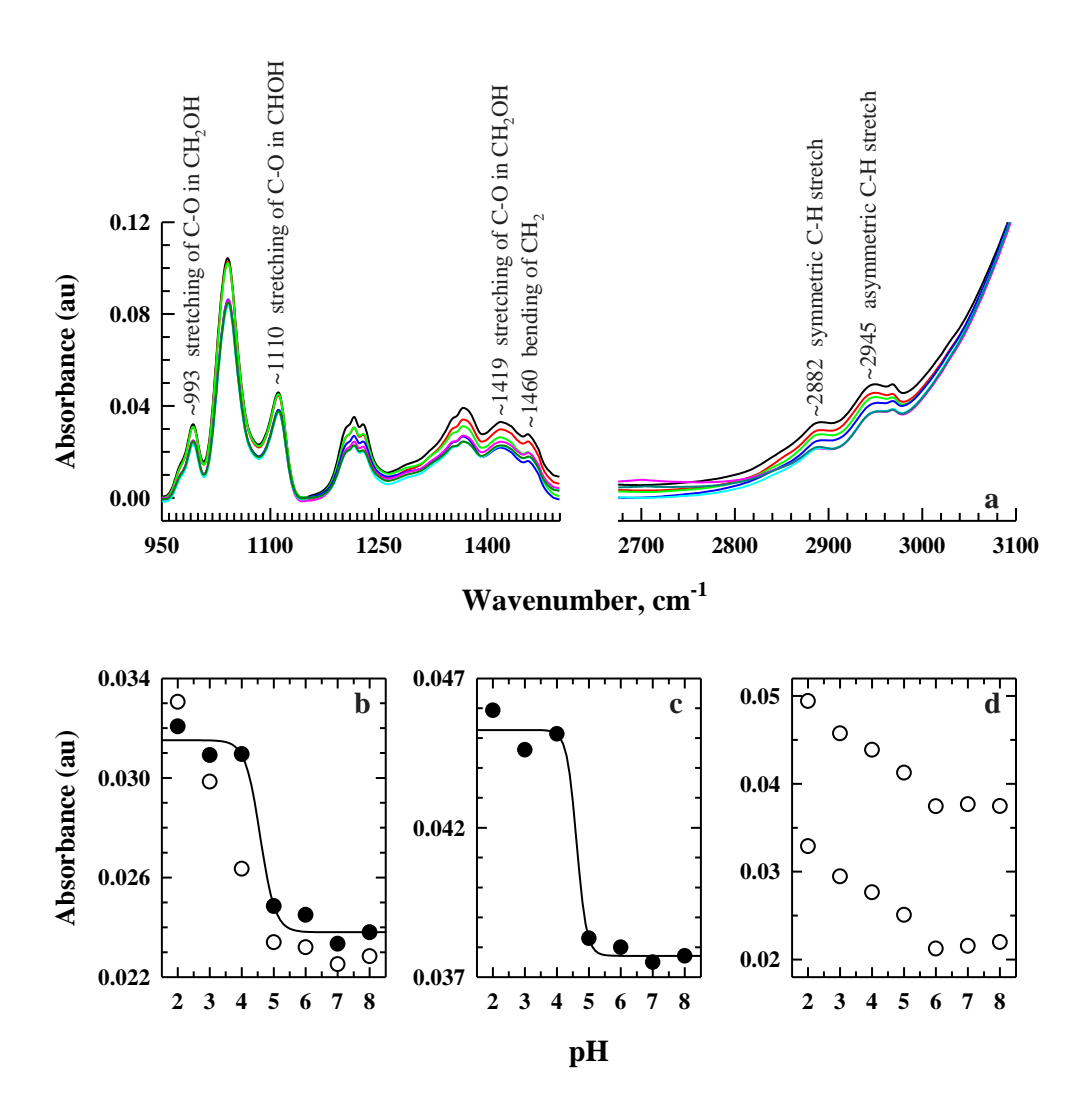


Figure 2.2. (a) IR spectra of 27% glycerol in the pH range 2-8 (in the order of decreasing absorbance) indicating a few mode assignments. The absorbance with pH is shown for the bands at 993 (solid) and 1418 (open) cm⁻¹ (b), 1110 cm⁻¹ (c), and 2894 and 2949 cm⁻¹ (d). The solid lines are fits to data according to equation 3.

2.3.3. Confirmation of oligomerization of glycerol in acidic pH using mass spectrometry

The mass spectra of 50% (w/v) aqueous glycerol at pH 2.63, 3.7 and 6.24 were recorded (Figure 2.3). The peaks of m/z values higher than the peaks of mono glycerol (m/z upto 800) were observed in the spectra recorded at pH mentioned above. These peaks must correspond to the fragments of higher oligomers of glycerol. Thus the appearance of these peaks in the mass spectrum confirm the oligomerization of glycerol at acidic pH. According to the Table 1, the mass spectrum of 50% (w/v) aqueous glycerol at the aforementioned pH values should show peaks corresponding to the m/z of cyclic glycerol oligomers of size 5-9 along with smaller oligomers. However, molecular ion peaks of oligomers of size 8 and 9 are not prominent in the spectra probably due of their instablity. The molecular ions of oligomers in 50% (w/v) aqueous glycerol observed in the spectra at pH 2.63, 3.7 and 6.24 are listed below.

Table 2. The mass spectra data of oligomers at pH 2.63

pH 2.63							
Observed	Identification	Molecular	Oligomer	Oligomer	Theoritical	I%	Error
m/z		formula	type	size	m/z		(ppm)
167.0930	M+H	$C_6H_{14}O_5$	linear	2	167.0919	27	6.5
189.0750	M+Na	$C_6H_{14}O_5$	linear	2	189.0739	23	5.8
184.1199	$M+NH_4$	$C_6H_{14}O_5$	linear	2	184.1185	4.5	7.6
388.1970	M	$C_{15}H_{32}O_{11}$	linear	5	388.1944	0.4	6.7
463.4937	M+H	$C_{18}H_{38}O_{13}$	linear	6	463.4952	0.3	-3.2
610.3074	M	$C_{24}H_{50}O_{17}$	linear	8	610.3048	0.2	4.2
149.0819	M+H	$C_6H_{12}O_4$	cyclic	2	149.0814	4.2	3.3
171.0633	M+Na	$C_6H_{12}O_4$	cyclic	2	171.0642	1	-5.2
245.1001	M+Na	$C_9H_{18}O_6$	cyclic	3	245.1016	6.8	-6.1
240.1447	M+NH ₄	$C_9H_{18}O_6$	cyclic	3	240.1470	0.5	-9.6
319.1368	M+Na	$C_{12}H_{24}O_{8}$	cyclic	4	319.1371	0.7	0.9
319.3059	M+Na	$C_{12}H_{24}O_{8}$	cyclic	4	319.3044	6.9	4.7
370.3928	M	$C_{15}H_{30}O_{10}$	cyclic	5	370.3933	0.2	-1.3
319.1368	M+Na	$C_{15}H_{30}O_{10}$	cyclic	5	319.1371	0.7	-0.9
319.3059	M+Na	$C_{15}H_{30}O_{10}$	cyclic	5	319.3044	6.9	4.7
541.5422	M+Na	$C_{21}H_{42}O_{14}$	cyclic	7	541.5404	0.8%	3.3
666.3370	M	$C_{27}H_{54}O_{18}$	cyclic	8	666.3370	0.2	0

Table 3. The mass spectra data of oligomers at pH 3.7

pH 3.7							
Observed	Identification	Molecular	Oligomer	Oligomer	Theoritical	I%	Error
m/z		formula	type	size	m/z		(ppm)
167.0921	M+H	$C_6H_{14}O_5$	linear	2	167.0919	19.3	1.1
189.0744	M+Na	$C_6H_{14}O_5$	linear	2	189.0739	65.7	2.6
263.1107	M+Na	$C_9H_{20}O_7$	linear	3	263.1106	2.4	0.3
258.1555	$M+NH_4$	$C_9H_{20}O_7$	linear	3	258.1553	0.3	0.7
337.1473	M+Na	$C_{12}H_{26}O_9$	linear	4	337.1474	0.5	-0.2
332.1927	$M+NH_4$	$C_{12}H_{26}O_9$	linear	4	332.1920	0.2	2.1
633.6333	M+Na	$C_{24}H_{50}O_{17}$	linear	8	633.6343	0.2	-1.5
149.0812	M+H	$C_6H_{12}O_4$	cyclic	2	149.0814	4.8	-1.3
171.0641	M+Na	$C_6H_{12}O_4$	cyclic	2	171.0633	2.9	4.6
223.1181	M+H	$C_9H_{18}O_6$	cyclic	3	223.1182	1.2	-0.4
245.1003	M+Na	$C_9H_{18}O_6$	cyclic	3	245.1001	17.3	0.8
240.1453	M+NH ₄	$C_9H_{18}O_6$	cyclic	3	240.1447	0.4	2.4
319.1360	M+Na	$C_{12}H_{24}O_8$	cyclic	4	319.1368	0.6	-2.5
393.1748	M+NH ₄	$C_{15}H_{30}O_{10}$	cyclic	5	393.1736	0.4	3.0
462.2576	M+NH ₄	$C_{18}H_{36}O_{12}$	Cyclic	6	462.2550	0.2	5.6
541.2462	M+Na	$C_{21}H_{42}O_{14}$	cyclic	7	541.2472	0.2	-1.8

Table 4. The mass spectra data of oligomers at pH 6.24

	pH 6.24						
Observed	Identification	Molecular	Oligomer	Oligomer	Theoritical	I%	Error
m/z		formula	type	size	m/z		(ppm)
167.0919	M+H	$C_6H_{14}O_5$	linear	2	167.0920	18.7	-0.5
189.0742	M+Na	$C_6H_{14}O_5$	linear	2	189.0739	100	1.5
184.1185	M+NH ₄	$C_6H_{14}O_5$	linear	2	184.1185	3	0
263.1107	M+Na	$C_9H_{20}O_7$	linear	3	263.1109	7.1	-0.7
258.1539	M+NH ₄	$C_9H_{20}O_7$	linear	3	258.1553	0.6	-5.4
337.1477	M+Na	$C_{12}H_{26}O_9$	linear	4	337.1474	0.8	0.8
149.0814	M+H	$C_6H_{12}O_4$	cyclic	2	149.0817	5	-2.0
171.0634	M+Na	$C_6H_{12}O_4$	cyclic	2	171.0633	2.7	0.5
223.1180	M+H	$C_9H_{18}O_6$	cyclic	3	223.1181	29	-0.4
240.1432	M+NH ₄	C ₉ H ₁₈ O ₆	cyclic	3	240.1447	0.4	-6.2
319.3048	M+Na	$C_{12}H_{24}O_8$	cyclic	4	319.3044	7.6	1.2
541.5396	M+Na	$C_{21}H_{42}O_{14}$	cyclic	7	541.5404	0.8	-1.4

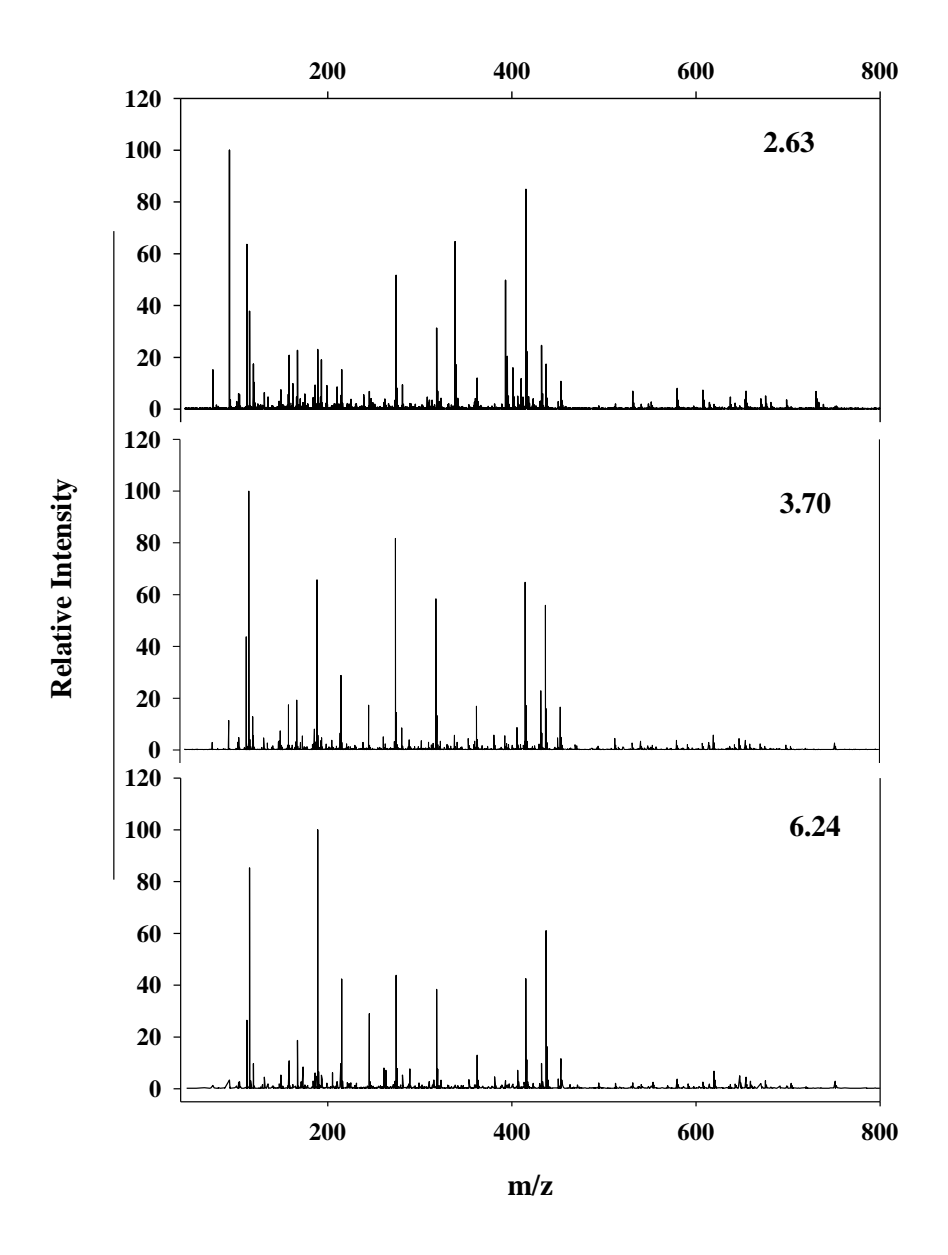


Figure 2.3. The mass spectra of glycerol at three different acidic pH

2.3.4. Mutually inclusive water clustering.

An interesting observation is the formation of water clusters concurrent with glycerol oligomerization. The clue to water clustering is provided by deshielding (high-frequency shift) titration of the water protons as the pH of the water-glycerol solution is reduced from 6 to 4, registering pH \sim 5.3(\pm 0.15) as the titration midpoint p (Figure 2.4a, Table 1). Deshielding is

associated with water clustering because the network of H-bonds in the water cluster decreases the electron density on the participating protons. Unlike the same size of shielding of the glycerol protons ($\Delta\delta^{(glycerol)}$) at low pH regardless of %glycerol used (Figure 2.1b,e,h), the deshielding of water protons ($\Delta\delta^{(water)}$) at low pH strongly depends on the concentration of glycerol in the water-glycerol mixture (Figure 2.4a), suggesting that water clustering is increasingly favorable with glycerol concentration or, equivalently, with decreasing water content (Figure 2.4b). To see this, we consider the glycerol coefficient of water deshielding, i.e., the slope of $\Delta\delta^{(water)}$ with glycerol content at different pH

$$\gamma_{\text{glycerol}}^{(\text{water})} = \left(\frac{\Delta \delta^{(\text{water})}}{\Delta_{\text{glycerol}}}\right)_{\text{pH,T,P}}.$$
 (5)

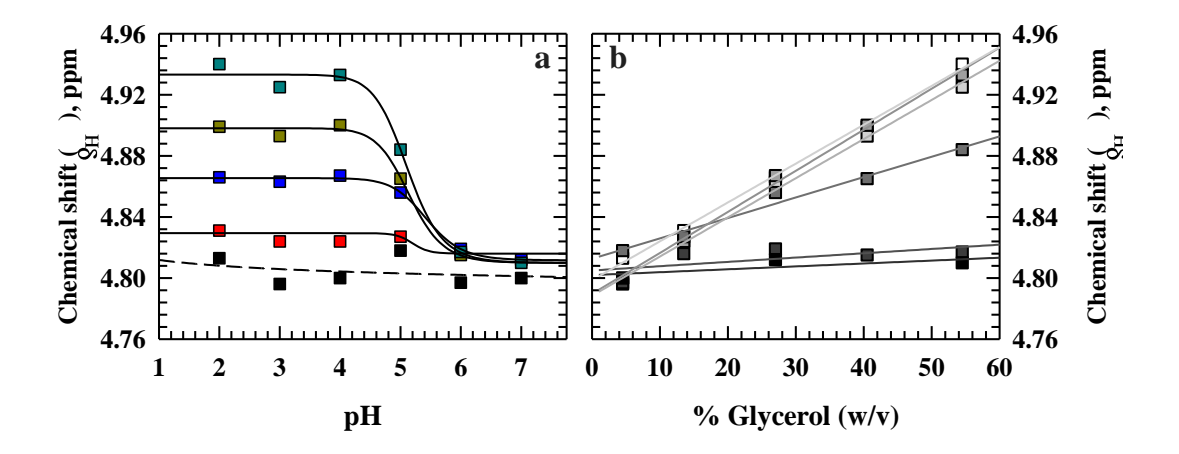


Figure 2.4. (a) pH-dependent chemical shift of water protons in the binary solution of 4.5 (black), 13.5 (red), 27.5 (blue), 40.5 (dark yellow), and 54.5 (dark cyan) % glycerol. The solid lines are drawn according to equation 1. The dashed line for 4.5% glycerol indicates insufficiency of data for a fit. (b) Glycerol dependence of the chemical shift of water protons at pH 2, 3, 4, 5, 6, and 7 plotted with increasing gray shade. The slopes defined as glycerol coefficient of water chemical shift, $\gamma_{\text{glycerol}}^{(\text{water})}$, are listed in Table 5.

Table 5. Glycerol coefficients ($\gamma_{glycerol}$) in ppm %glycerol⁻¹ for chemical shift changes ($\Delta\delta$)

pН	$\gamma_{ m glycerol)}^{(m glycerol)}_*$	$\gamma_{ m glycerol}^{ m (water)}$
Averaged	$-6.605 \times 10^{-4} (\text{H}^2)$ $-4.787 \times 10^{-4} (\text{H}^1 \text{ or H}^{1'})$ $-4.123 \times 10^{-4} (\text{H}^{1'} \text{ or H}^1)$	
2 3 4		2.544×10^{-3} 2.563×10^{-3} 2.687×10^{-3}
5		1.336×10^{-3}
6 7		$2.820 \times 10^{-3} 1.900 \times 10^{-3}$

^{*} Negative signs for the coefficients indicate shielding of glycerol protons with increasing glycerol.

The results plotted in Figure 2.4b and listed in Table 1. show that water protons are deshielded more with glycerol content in the solution, suggesting that water clustering and glycerol oligomerization are concurrent phenomena.

It is also useful to analyze the titration of $\gamma_{\text{glycerol}}^{(\text{water})}$ of water deshileding with pH (Figure 2.5) by equation 4 mentioned above. Explicitly,

$$\gamma_{\text{glycerol}}^{(\text{water})} = A + \frac{\Delta \gamma_{\text{glycerol}}^{(\text{water})}}{1 + 10^{n(\text{pH-pK}_a)}},\tag{6}$$

in which A is the ordinate value at pH 7, n the number of protons titrated, and $\Delta \gamma_{\rm glycerol}^{\rm (water)}$ is the total change in $\gamma_{\rm glycerol}^{\rm (water)}$ across the pH range. The n=1.3(± 0.2) from the fit suggests a single proton-mediated water clustering, and pK_a=5.0 is close to the midpoint of pH titration of glycerol chemical shift (p) given in Table 1, further indicating the mutual inclusiveness of glycerol aggregation and water clustering.

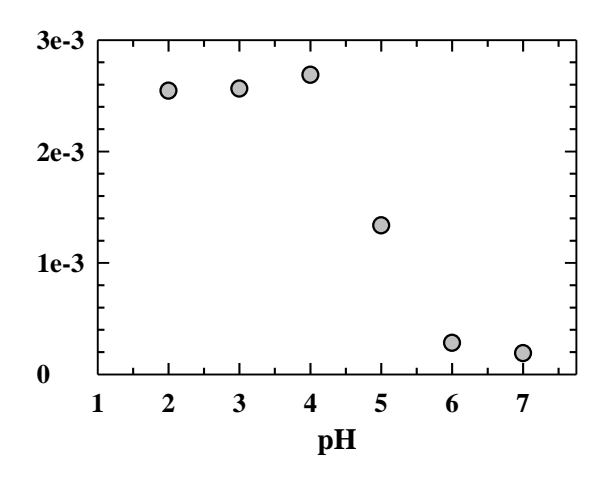


Figure 2.5. pH-titration of glycerol coefficient for deshielding of water protons. The fit through the data yields $n=1.3(\pm0.2)$ and pK_a=5.0 (Eq 5).

2.3.5. Sizes of glycerol oligomers and water clusters.

The sizes were determined by a series of pulsed-field-gradient (PFG)-NMR experiments with water-glycerol binary mixtures of 4.5, 13.5, 27, 40.5, and 54.5% glycerol contents, each at unit interval of pH from 2 to 7. A sample of spectra is shown in Figure 2.6a, and the details of calculation of translational diffusion coefficient (D_s) are supplied as Supporting Information. Cluster sizes were estimated from the Stokes-Einstein relation

$$D_{\rm S} = \frac{k_{\rm B}T}{c\pi r\eta},\tag{7}$$

in which the symbols have the usual meaning, and we assume the particle-liquid sticking condition (c=6). The sizes of glycerol clusters given as Stokes diameter increase as the pH decreases from 7 to 2 (Figure 2.6b). There are however neutral-pH aggregates as well, the sizes of which increase with glycerol level in the solution. To estimate the size of an aggregate it is useful to consider the size of a glycerol monomer, which can be estimated from the molecular volume

$$V = \frac{4}{3}\pi r^3 \text{ with } V = \frac{m}{N_A \rho},\tag{8}$$

where r is the radius of the molecular volume, m the molecular mass (\sim molecular weight), $N_{\rm A}$ Avogadro number, and ρ the density of glycerol ($\approx 1.255~{\rm g~ml}^{-1}$); the diameter of the monomer is roughly 0.81 nm. At pH 7 for example, the mean size of glycerol in its 4.5% solution is 1.46 nm

corresponding to a dimer, and the size in the 54.5% solution increases to 6.34 nm. This result is consistent with earlier reports of the existence of neutral-pH aggregates which are held together by H-bonding, ¹⁹ and whose size scales up with the glycerol content in the binary solution. ²⁰ We see similar behavior with the sizes of water clusters (Figure 2.6d). The diameters for both glycerol and water at different % glycerol and pH values and the corresponding glycerol repeats calculated by taking ~0.81 as the monomer diameter are listed in Table 6.

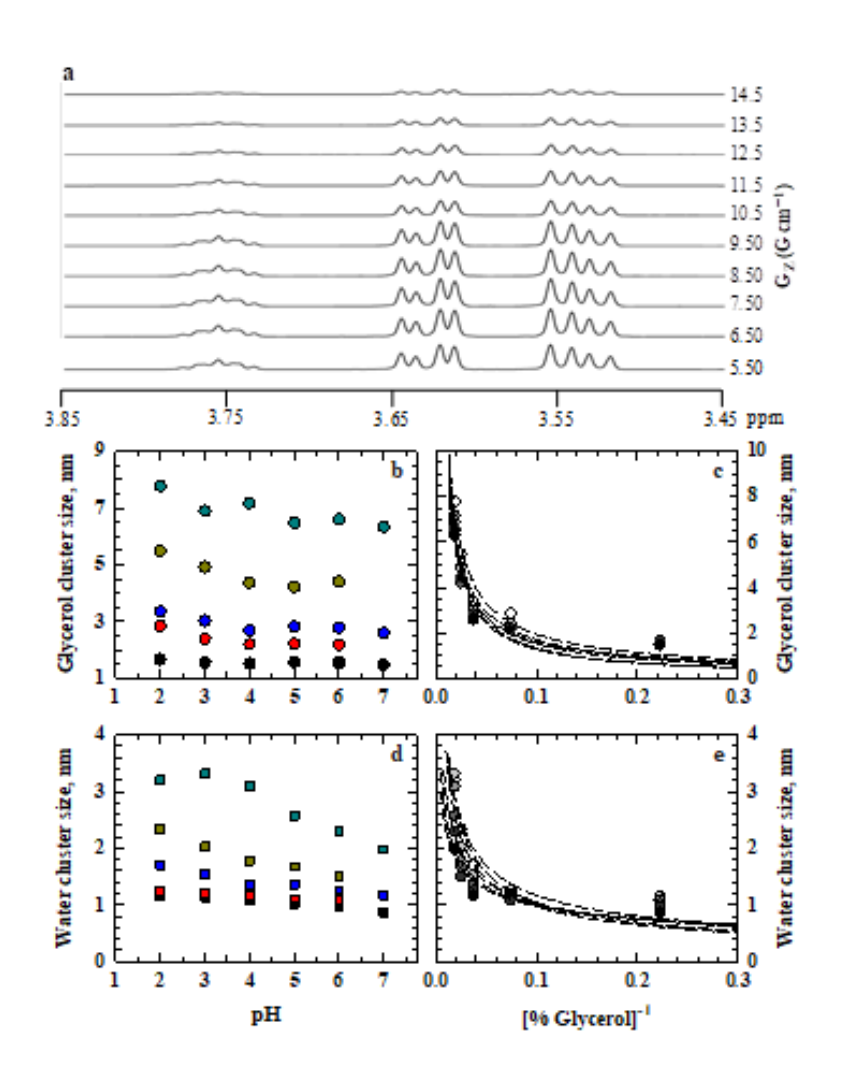


Figure 2.6. Size estimation of glycerol aggregates and water clusters in water-glycerol binary mixture. (a) PFG-NMR spectra of 13.5% glycerol showing the decrease in resonance intensities of glycerol with field gradient. (b) Stokes diameter of glycerol aggregates in 4.5 (black), 13.5 (red), 27 (blue), 40.5 (dark yellow), and 54.5 (cyan) % glycerol at different pH. (c) Stokes diameter of glycerol aggregates at pH 7, 6, 5, 4, 3, and 2 (decreasing gray shade in the order) with inverse glycerol. The dashed lines, one for each pH, represent fits to data according to equation 9, yielding an average power law

coefficient, $\kappa \sim 0.85$ (SD 0.07). (d) and (e) show water cluster diameters with the same description given for (b) and (c), respectively. For water clustering, $\kappa \sim 0.49$ (SD 0.09).

Table 6. Stokes diameter (in nm) of glycerol and water clusters, 298 K. The numbers in *italics* within parentheses provide the approximate repeat size of glycerol in the oligomers/aggregates.

% glycerol	рН								
	2	3	4	5	6	7			
	Glycerol								
4.5	1.6521(2)	1.5501(2)	1.5092(2)	1.5523(2)	1.5427(2)	1.4675(2)			
13.5	2.8406(3)	2.3835(3)	2.1997(2/3)	2.2149(2/3)	2.1721(2/3)	_			
27.0	3.3459(4)	3.0089(4)	2.6881(3)	2.8262(3)	2.7600(3)	2.5996(3)			
40.5	5.4900(7)	4.9087(6)	4.3719(5)	4.2152(5)	4.4147(5)	_			
54.5	7.7778(9)	6.8987(8/9)	7.1690(9)	6.4742(8)	6.6014(8)	6.3350(8)			
	Water								
4.5	1.1541	1.1398	1.0842	1.0198	0.9556	0.8656			
13.5	1.2357	1.2019	1.1674	1.1079	1.0890	_			
27.0	1.7040	1.5348	1.3567	1.3592	1.2560	1.1702			
40.5	2.3376	2.0239	1.7797	1.6757	1.4983	_			
54.5	3.2032	3.3093	3.1016	2.5809	2.3049	1.9786			

The sizes of both glycerol oligomers and water clusters irrespective of the pH vary with inverse glycerol concentration by a power law dependence

$$2r = \left(\frac{1}{\% \text{ glycerol}}\right)^{-\kappa},\tag{9}$$

the coefficient κ taking values of 0.85 and 0.49 for glycerol and water, respectively (Figure 2.6c,e). This behavior is similar to that observed for polymers, where the radius of gyration has a dependence on the number of monomers raised to a power (Flory 1949).²¹ The power law behavior observed for both glycerol oligomers and water clusters is a manifestation of mutual exclusion by which the two avoid each other; the larger value of κ for the former appears because of their larger size relative to those of the latter. Thermodynamically, the interaction between water and glycerol becomes less favorable when glycerol concentration in the binary solution increases, leading to exclusion of water molecules from the vicinity of glycerol species that in turn favors clustering of water molecules.

2.4. Discussion

2.4.1. Oligomerization of glycerol catalyzed by solvent H^+ .

Glycerol oligomerization catalyzed directly by solvent H^+ in the range of $\sim 1 \times 10^{-4}$ to 1×10^{-2} mol L^{-1} (pH \lesssim 4) at ambient temperature has a distinct overall advantage over the hitherto shown oligomerization carried out by homogeneous catalysts such as strong Brønsted and Lewis acids 15,17 and heterogeneous catalysts including Nafion-like acid ionomers and zeolites. 16,18 The latter approaches suggest the use of high temperature, $\gtrsim 100$ °C, with the rationale that elevated thermal energy may facilitate the formation of glycidol epoxide 17 that we have called oxirane. The results we produce however show redundancy of elevating the temperature to such a high level without compromising on the time required to produce the glycerol oligos; condensation of glycerol under our ambient condition occurs within $\sim 4-6$ h of lowering the pH to the 2–4 range. This possibility of generating oligoglycerol renders *in situ* use of glycerol in acidic foodstuff, cosmetics, and certain pharmaceutical products that are maintained in the 2–5 range of pH to achieve antimicrobial activitity.

Porous solid catalysts such as ionomers are thought to induce shape-selective effects on oligomerization, often preventing repeated condensation and cyclization so as to produce lesser number of repeats in the oligomer. On the other hand, the high temperature conditions applied in heterogeneously catalyzed oligomerization also leads to ion leaching and deactivation of even physical degradation of the catalyst. It must be said that the explicit reaction conditions for obtaining lower repeats of glycerol is not available apriori; instead the initial % glycerol as the reactant, the catalyst load, and the reaction time up to the point of consumption of about half of the initial glycerol are optimized. In any event, physical data of glycerol oligos routinely declare the presence of di, tri, tetra, and penta to nonaglycerols. Generally, triglycerol dominates, and penta to nonaglycerol species account for ~10% of the overall yield. Our simple non-catalytic approach yields a mixture of di- to tetraglycerol at acid pH with the initial glycerol contained within ~27% (Table 6).

2.4.2. Preferential interaction of water-glycerol components.

The key result that glycerol oligomerization and water clustering is mutually inclusive can be explained qualitatively by considering the physical properties of water-glycerol binary solution. When the molecules of two fluid components obey the van der Waals equation of state they share similarity in their behavior at the same reduced pressure and temperature – called corresponding state principle (CSP), which has already been generalized to predict the surface tension of liquid mixtures (Rice& Teja, 1982). If the surface tension of aqueous glycerol solution decreases with increasing mole fraction of glycerol, ²⁴ then the decrease should occur for both water and glycerol, and it is known that glycerol slightly decreases the surface tension of water. ¹¹ The reduced surface tension lowers the respective Gibbs free energy barrier for water clustering and glycerol aggregation.

On a quantitative footing, one may refer to the concept of composition fluctuation of multicomponent systems, according to which the thermodynamic interaction between the larger solute molecules (glycerol) and the smaller solute molecule (water) should cause the former to produce composition fluctuation with respect to the latter to the same extent as the composition fluctuation with respect to the former itself. To suit the context of the water-glycerol binary mixture, we provide a concise and simple picture of the outcome of the otherwise rigorous thermodynamic treatment. Denoting the nonelectrolyte components water and glycerol by '1' and '2', respectively, the liquid solute behavior can be represented by the individual excess chemical potentials which when expanded in a power series in the component concentration c read

$$\mu_{i} = \mu_{i}^{0}(T, P) + \log \gamma_{i} c_{i} \qquad i = 1, 2$$

$$\log \gamma_{1} = A_{11}c_{1} + A_{12}c_{2}$$

$$\log \gamma_{2} = A_{21}c_{1} + A_{22}c_{2}, \qquad (10)$$

where A_{11} , A_{12} , A_{21} , and A_{22} are thermodynamic interaction coefficients that measure the perturbation of γ of one component by the other. The perturbation could be in the intra- and inter-component interactions as well as in the freedom of motion of the molecules, both are

mutual. The vector equation $\log \gamma = Ac$ obtained from eq (10) explicitly provides the matrix for thermodynamic interaction coefficients

$$\begin{pmatrix} \log \gamma_1 \\ \log \gamma_2 \end{pmatrix} = \begin{pmatrix} A_{11} & A_{12} \\ A_{21} & A_{22} \end{pmatrix} \begin{pmatrix} c_1 \\ c_2 \end{pmatrix}. \tag{11}$$

The off diagonal coefficients, well known as coherence transfer coefficients for two coupled species, in the present case should be negative because when interpreted from a molecular standpoint the two components preferentially exclude each other.

2.4.3. Caveat on the use of glycerol in acid pH.

Glycerol has been employed as a macromolecular crowder, ²⁵ and as a viscogen in studies of frictional effects on DNA translocation, ²⁶ RNA transcription, ²⁷ protein and enzyme reaction rates, ²⁸ and protein dynamics, conformational substates, and energy landscape. ^{29–40} Although the results of these studies are generally acceptable, the reducing effect of glycerol remains accountable. Glycerol is a reducing agent, and hence the iron-containing proteins, e.g., myoglobin and cytochrome *c*, which have been used extensively in studies cited above are invariably in the reduced or ferro form. ⁴⁰ In such cases, the already prevailing protein-stabilizing effect of glycerol ¹¹ is augmented by the reductive stabilization of heme proteins. At the same time, the preferential hydration of proteins by aggregated species of glycerol vis a vis its monomer remain unknown. In other words, glycerol not only increases the viscosity and reduces the surface tension of the solvent, but also modifies the physicochemical properties of proteins. This study recognizes another caveat of using glycerol to study protein properties at low pH (ref 41–43, for example) where repeats of glycerol monomers in the form of oligomers whose effect on solvent and protein properties is little understood. This limitation will apply also to studies with glycerol at alkaline pH, where OH⁻ catalyzes condensation to produce oligomers.

2.5. References

- 1. Mizuno, K.; Miyashita, Y.; Shindo, Y.; Ogawa, H. NMR and FT-IR studfies of hydrogen bonds in ethanol-water mixtures. *J. Phys. Chem.* **1995**, *99*, 3225–3228.
- 2. To, E. C. H.; Davies, J. V.; Tucker, M.; Westh, P.; Trandum, C.; Suh, K. S. H.; Koga, Y. Excess chemical potentials, excess partial molar enthalpies, entropies, volumes, and isobaric thermal expansivities of aqueous glycerol. *J. Solution Chem.* **1999**, 28, 1137–1157.
- 3. Marcus, Y. Some thermodynamic and structural aspects of mixtures of glycerol with water. *Phys. Chem. Phys.* **2000**, *2*, 4891–4896.
- 4. Parsons, M. T.; Westh, P.; Davies, J. V.; Trandum, C.; To, E. C. H.; Chiang, W. M.; Yee, E. G. M.; Koga, Y. J. A thermodynamic study of 1-Propanol-Glycerol-H₂O at 25°C: effect of glycerol on molecular organization of H₂O. *Solution Chem.* **2001**, *30*, 1007–1028.
- 5. Döss, A.; Paluch, M.; Sillescu, H.; Hinze, G. From strong to fragile glass formers: secondary relaxation in polyalcohols. *Phys. Rev. Lett.* **2002**, *88*, 095701.
- Zelent, B.; Nucci, N. V.; Vanderkooi, J. M. Liquid and ice water and glycerol/water glasses compared by infrared spectroscopy from 295 to 12K. J. Phys. Chem. A 2004, 108, 11141–11150.
- 7. Fabri, D.; Williams, M. A. K.; Halstead, T. K. Water T2 relaxation in sugar solutions. *Carbohydr. Res.* **2005**, *340*, 889–905.
- 8. Vanderkooi, J. M.; Dashnau, J. L.; Zelent, B. Temperature excursion infrared (TEIR) spectroscopy used to study hydrogen bonding between water and biomolecules. *Biochim. Biophys.* Acta **2005**, *1749*, 214–233.
- 9. Dashnau, J. L.; Nucci, N. V.; Sharp, K. A.; Vanderkooi, J. M. Hydrogen bonding and the

- cryoprotective properties of glycerol/water mixtures. J. Phys. Chem B, 2006, 110, 13670–13677.
- 10. Vegenende, V.; Yap, M. G. S.; Trout, B. L. Mechanism of protein stabilization and prevention of proein aggregation by glycerol. *Biochemistry* **2009**, *48*, 11084–11096.
- 11. Gekko, K.; Timasheff, S. N. Mechanism of protein stabilization by glycerol: preferential hydration in glycerol-water mixtures. *Biochemistry* **1981**, *20*, 4667–4676.
- Timasheff, S. N. Protein-solvent preferential interactions, protein hydration, and the modulation of biochemical reactions by solvent components. *Proc. Natl. Acad. Sci. U.S.A.* 2002, 99, 9721–9726.
- 13. Kirkwood, J. G.; Goldberg, R. J. Light scattering arising from composition fluctuations in multicomponent systems. *J. Chem. Phys.* **1950**, *18*, 54–57.
- 14. Stockmeyer, W. H. Light scattering in multi-component systems. *J. Chem. Phys.* **1950**, *18*, 58–61.
- Sayoud, N.; De Oliviera Vigier, K.; Cucu, T.; De Meulenaer, B.; Fan, Z.; Lai, J.; Clacens, J-M.; Liebens, A.; Jerome, F. Homogeneously-acid catalyzed oligomerization of glycerol. *Green Chem.* 2015, 17, 4307–4314.
- 16. Martin, A.; Richter, M. Oligomerization of glycerol a critical review. *Eur. J. Lipid Sci. Technol.* **2011**, *113*, 100–117.
- 17. Salehpour, S.; Dube, M A. Towards the sustainable production of higher-molecular-weight polyglycerol. *Macromol. Chem. Phys.* **2011**, *212*, 1284–1293.
- 18. Martin, A.; Chesinski, M. P.; Richter, M. Tuning of diglycerol yield and isomer distribution in oligimerization of glycerol supported by DFT calculations. *Catalysis*

- Commun. **2012**, 25, 130–135.
- 19. Towey, J. J.; Soper, A. K.; Dougan, L. The structure of glycerol in the liquid state: a neutron diffraction study. *Phys. Chem. Chem. Phys.* **2011**, *13*, 9397–9406.
- 20. Elamin, K.; Swenson, J. Brownian motion of single glycerol molecules in an aqueous solution as studied by dynamic light scattering. *Phys. Rev. E* **2015**, *91*, 032306.
- 21. Flory, P. J. The configuration of eral polymer chains. *J. Chem. Phys.* **1949**, *17*, 303–310.
- 22. Parvulescu, A. N.; Mores, D.; Stavitski, E.; Teodorescu, C. M.; Bruijnincx, P. C. A.; Klein Gebbink, R. J. M.; Weckhuysen, B. M. Chemical imaging of catalyst deactivation during the conversion of renewables at the single particle level: etherification of biomass-based polyols with alkenes over H-beta zeolites. *J. Am. Chem. Soc.* 2010, 132, 10429–10439.
- 23. Plasman, V.; Caulier, T.; Boulos, N. B. Polyglycerols. Versatile ingredients for personal care. *HAPPI* magazine, Ramsey, NJ, November **2004**, 94–97.
- 24. Takamura, K.; Fischer, H.; Morrow, N. R. Physical properties of aqueous glycerol solutions. *J. Petroleum Sci. Engg.* **2012**, *98*–*99*, 50–60.
- 25. Chau, C. C.; Radford, S. E.; Hewitt, E. W.,; Actis, P. Macromolecular crowding enhances the detection of DNA and proteins by a solid-state nanopore. *Nano Lett.* **2020**, *20*, 5553–5561.
- 26. Fologea, D.; Uplinger, J.; Thomas, B.; McNabb, D. C.; Li, J. Slowing DNA translocation in a solid state nanopore. *Nano Lett.* **2005**, *5*, 1734–1737.
- 27. Demidenso, A.A.; Lee, J.; Powers, T. R.; Nibert, M. L. Effects of viscogens on RNA

- transcription inside reovirus particles. J. Biol. Chem. 2011, 286, 29521–29530.
- 28. Sashi, P.; Bhuyan, A. K. Viscosity dependence of some protein and enzyme reaction rates: seventy-five years after Kramers. *Biochemistry* **2015**, *54*, 4453–4461.
- 29. Austin, R. H.; Beeson, K. W.; Eisenstein, L.; Frauenfelder, H.; Gunsalus, I.C. Dynamics of ligand binding to myoglobin. *Biochemistry* **1975**, *14*, 5355–5373.
- 30. Caliskan, G.; Kisliuk, A.; Tsai, A. M.; Soles, C. L.; Sokolov, A. P. Protein dynamics in viscous solvents. *J. Chem. Phys.* **2003**, *118*, 4230–4236.
- 31. Agmon, N. Coupling of protein relaxation to ligand binding and migration in myoglobin. *Biophys. J.* **2004**, 87, 1537–1543.
- Caliskan, G.; Mechtani, D.; Roh, J. H.; Kisliuk, A.; Sokolov, A. P.; Azzam, S.; Cicerone, M. T.; Lin-Gibson, S.; Peral, I. Protein and solvent dynamics: how strongly are they coupled. *J. Chem. Phys.* 2004, 121, 1978–1983.
- 33. Dirama, T. E.; Carri, G. A.; Sokolov, A. P. Coupling between lysozyme and glycerol dynamics: microscopic insights from molecular-dynamics simulations. *J. Chem. Phys.* **2005**, *122*, 244910.
- 34. Frauenfelder, H.; Chen, G.; Berendzen, J.; Fenimore, P. N.; Jansson, H.; McMahon, B. H.; Stroe, I. R.; Swenson, J.; Young, R. D. A unified model of protein dynamics. *Proc. Natl. Acad. Sci. USA* **2009**, *106*, 5129–5134.
- 35. Jansson, H.; Bergman, R.; Swenson, J. Role of solvent for the dynamics and the glass transition of proteins. *J. Phys. Chem. B* **2011**, *115*, 4099–4109.
- 36. Kumar, R.; Jain, R.; Kumar, R. Viscosity dependent structural fluctuation of the M80-containing Ω -loop of horse ferrocytochrome *c. Chem. Phys.* **2013**, *418*, 57–64.

- 37. Sashi, P.; Ramakrishna, D.; Bhuyan, A. K. Dispersion forces and the molecular origin of internal friction in protein. *Biochemistry* **2016**, *55*, 4595–4602.
- 38. Ronsin, O.; Caroli, C.; Baumberger, T. Preferential hydration fully controls the renaturation dynamics in water–glycerol sovents. *Eur. Phys. J. E* **2017**, *40*, 55.
- 39. Librizzi, F.; Carrotta, R.; Peters, J.; Cupane, A. The effects of pressure on the energy landscape of proteins. *Sci. Rep.* **2018**, *8*, 2037.
- 40. Joshi, K.; Bhuyan, A. K. Quasi-native transitin and self-diffusion of proteins in water-glycerol mixture. *Biophys. Chem.* **2020**, 257, 106724.
- 41. Santucci, R.; Polizio, F.; Desideri, A. Formatin of a molten globule-like state of cytochrome *c* induced by high concentration of glycerol. *Biochimie* **1999**, *81*, 745–750.
- 42. Bongiovanni, C.; Sinibaldi, F.; Ferri, T.; Santucci, R. Glycerol induced formation of the molten globule from acid-denatured cytochrome *c*: implication for hierarchical folding. *J. Protein Chem.* **2002**, *21*, 35–41.
- 43. Rahamtullah; Ahmadi, A.; Mishra, R. Polyol and sugar osmolytes stabilize and inhibit amyloid fibril formation. *Biochim. Biophys. Acta Proteins Proteiom.* **2022**, *1870*, 140853.

Quasi-native transition and self-diffusion of proteins in waterglycerol mixture

Abstract

An orderly investigation of the levels of secondary and tertiary structures, kinetics of tertiary structural changes, and self diffusion coefficient of lysozyme and cytochrome c in the 0–70% (weight/volume) range of glycerol is reported. While secondary structural propensity of both proteins is larger in glycerol, results for tertiary structure and translational diffusion coefficient with increasing glycerol provide two contrasting depictions – lysozyme becomes increasingly compact, plausibly due to disulfide bridge constraints, but cytochrome c expands and loses the tertiary structure. The chain expansion and contraction corresponding to loss and reformation of tertiary structure of cytochrome c are ultrafast that occur in the sub-millisecond bin. Changes in protein conformation appear in as little as 2% glycerol, and the results suggest that glycerol does not unfold the protein but reversibly destabilizes to quasi-native state(s). These observations make one ponder whether results of studies on protein dynamics, relaxation, and conformational sub-states reported in literature can be associated with native-state properties.

3.1. Introduction

Glycerol, an exceedingly viscous alcohol with complex conformational and dynamical properties is widely used in dynamite production, storage of industrial products, drugs and cosmetics, enzyme-catalyzed semi-synthesis of proteins, and as a cryoprotectant for biological molecules, cells, clones, and embryos. The highly elastic property of glycerol renders its use as a general glass matrix¹ that has been employed for a long time in studies of low-temperature protein dynamics, conformational sub-states and energy landscape²⁻⁹, and plasticization of protein-based films¹⁰. Even though the extraordinary properties of glycerol itself and its effect on solutes have drawn attention for a long time, of particular interest has been the structure, conformation, kinetics of conformational changes, and thermodynamic properties of proteins in

water–glycerol mixture. Following initial observations of glycerol effect on enzyme activity¹¹⁻¹³ and conformational change¹⁴, the influential work of Gekko and Timasheff¹⁸⁻¹⁹ heralded a great deal of interest in the chemistry of the three-component water–protein–glycerol system. Ensuing experimental and theoretical studies²⁰⁻²⁶ have substantially added to the understanding of protein stabilization by glycerol. It has also become apparent that a part of the glycerol effect involves its influence on the order, structure, and hydrogen bonding of water.^{7,27} Although protein–glycerol interactions involve both electrostatic and hydrophobic bonding²², more recent investigations are focusing on the interplay of osmolytes, in general, with hydrophobic interactions within the protein.^{28,29} Stabilization by glycerol against cold denaturation of proteins has also been discussed very recently.^{28,30}

Despite such significant advances in the area questions still arise as to what extent glycerol might change the structure and conformation of proteins, and whether the induced changes are similar for different proteins. How fast the conformational changes might occur in response to a transfer of the aqueous protein to glycerol solutions? How can the structural and conformational changes in the presence of glycerol be related to increased protein stability, which is explained in thermodynamic terms? Is 15-17,22,28 It was reported that high concentration of glycerol transforms both native and acid denatured cytochrome c to a low-spin heme-containing molten globule-like state that is rich in α -helix but lacks tertiary structure. Chen et al have reported that glycerol stabilizes lysozyme and β -lactoglobulin, but destabilizes α -lactalbumin and lactoferrin. Bonincontro et al find a slight reduction of hydrodynamic radius of lysozyme in 0–70% (w/w) range of glycerol, indicating compaction of the protein. Scharnagle et al state that there is no unique molecular model for the influence of glycerol on protein stability.

Here we have conducted simple experiments for a systematic review of secondary and tertiary structures of lysozyme and cytochrome c placed in 0–70% glycerol solutions, determined the self diffusion coefficient for the two proteins in glycerol, and considered the rate of conformational changes when the aqueous protein solution is transferred to water–glycerol mixture. The secondary structural propensity of both proteins has been found to increase in glycerol, but tertiary structural changes and translational diffusion coefficients indicate that lysozyme becomes more compact and dense while cytochrome c expands concomitant with

considerable loss of tertiary contacts. Glycerol-induced conformation loss and chain expansion of the latter are also supported by kinetic results. The structural changes are modeled as a two-state native \rightleftharpoons quasi-native transition, and the changes in the free energy are calculated. We also discuss the instances where our data appear inconsistent with those reported earlier.

3.2. Materials and methods

Horse cytochrome c (Sigma) and hen lysozyme (Calbiochem) were used without further purification. Glycerol (Sigma) was 99.5% in minimum assay by gas chromatography. Aqueous solutions of glycerol were prepared by weighing glycerol. All experiments were performed at 25°C in water at pH 3.8 (lysozyme) and 15 mM phosphate buffer, pH 7 (cytochrome c).

3.2.1. Equilibrium titration

Protein titration with glycerol was carried out by mixing two stock solutions that were identical in pH, buffer, and protein content, except that one contained glycerol and the other not. Samples containing variable glycerol (w/v %) were prepared by mixing the two stock solutions appropriately. Final protein concentrations were 8 and 10 µM of cytochrome *c* and lysozyme, respectively. Samples for near-UV CD measurements contained 50 µM protein. All measurements were done after equilibrating the samples at 25°C for ~12 h. Tryptophan fluorescence spectra (excitation 280 nm) were recorded in a JASCO FP-8300 instrument, far-UV CD measurements were done using a AVIV SF420 spectropolarimeter, and visible absorption spectra were taken in a CARY 100 UV-Visible spectrophotometer.

3.2.2. Stopped-flow kinetics

Kinetics of protein conformational changes in glycerol were studied by diluting the aqueous solution of the protein with the glycerol solution. In the reverse experiment, the protein initially dissolved in the glycerol solution was diluted by mixing with the buffer. The mixing ratio of protein to buffer solutions was 1:7. Fluorescence-monitored kinetics were measured in a BioLogic SFM400 instrument using a high-density mixer and a 0.8 mM cuvette. The instrument

dead time, determined at the actual flow rate of solutions, was $\sim 1.8(\pm 0.2)$ ms. Each kinetic trace analyzed was an average of 8–10 traces.

3.2.3. NMR Spectroscopy

The samples were 15% D₂O solutions of 2 mM protein containing variable glycerol. Lysozyme samples were held at pH 4, and cytochrome *c* samples were buffered with 15 mM sodium phosphate, pH 7. Pulsed-field-gradient NMR (PFG NMR) diffusion measurements were carried out with diffusion gradient (*z*-gradient) in the range of 1-40 Gauss cm⁻¹. All spectra were recorded at 25°C in a 500 MHz Avance HD Bruker spectrometer.

3.3. Results

3.3.1. Glycerol increases the propensity of secondary structure

The effect of glycerol, expressed in terms of activity (Figure 3.1), on the secondary structure of lysozyme and cytochrome c was probed by 222 and 207-nm CD (Figure 3.2). To read a large number of samples with better signal-to-noise time-averaged CD values at 222 and 207 nm were taken instead of acquiring the entire far-UV spectrum. The changes in ellipticity angles with the natural logarithm of glycerol activity (Figure 3.3a,b,d,e) clearly show an increase in the secondary structure for both proteins. We note that a previous study reported little change in the CD of lysozyme in 0–50% (v/v) range of glycerol⁴⁵. It is not clear how the authors missed out the changes, and whether data presented were averaged adequately.

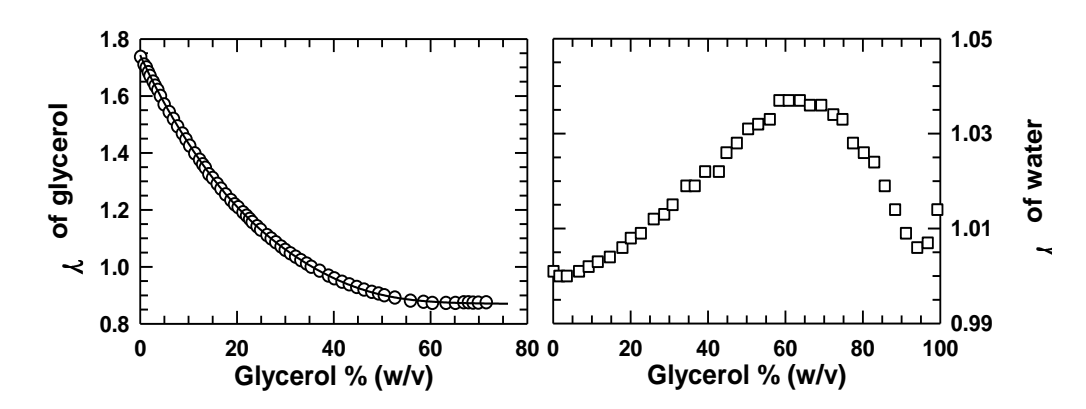


Figure 3.1. Simulated glycerol-water binary mixture data to obtain the empirical relations (Equations 1 and 2). The data are reproduced from the work of Yi, F. and Axelbaum, R. L. (Oxy-

combustion of low-volatility fuel with high water content. Eastern States Section Meeting of the Combustion Institute, 2013).

$$\gamma_{\text{glycerol}} = a + be^{-cx} + de^{-ex^2} + fe^{-gx^3}$$
 (1)

Where α =0.869137, b=0.485583, c=0.077251, d=0.169208, e=3.100230e-3, f=0.219587, g=1.835472e-5

$$\gamma_{\text{water}} = a + be^{-cx} - de^{-ex^2} + fe^{-gx^3} - he^{-ix^4}$$
 (2)

Where a=132.374134, *b*=0.019929, *c*=21.138945, *d*=131.938407, *e*=3.147335e-7, *f*=0.744960 *g*=1.531386e-6, *h*=0.181720, *i*=5.967701e-8

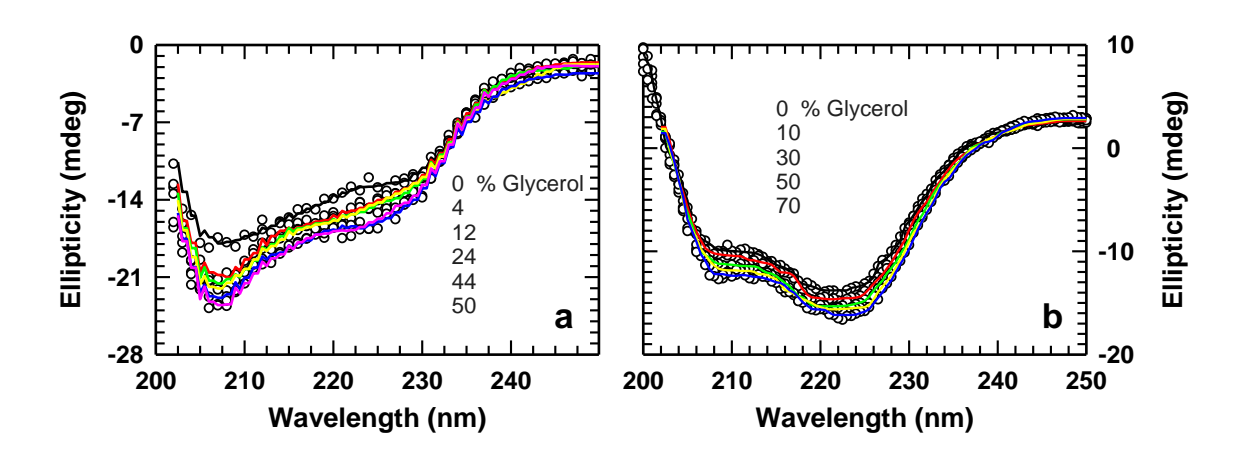


Figure 3.2. Far-UV CD spectra of (a) lysozyme, and (b) cytochrome c at different glycerol. Each spectrum is an average of two scans.

The 222 and 207-nm bands do not distinguish between helical and β -structures, their rotational strength originating from the $n\rightarrow\pi^*$ and $\pi\rightarrow\pi^*$ transitions, respectively, of the peptide chromophore. However the argument that the contribution of α -helical structure to the 207-nm ellipticity is more than that of β -structure is often used as a first approximation of the α -helix content through R_{θ} , defined as the ratio of 207 to 222 nm ellipticities. The variation of R_{θ} with glycerol suggests no increase of α -helix for lysozyme (Figure 3.3c), contrary to the result for cytochrome c (Figure 3.3f). It thus appears that glycerol induces β -structural propensity in

lysozyme but α -helical propensity in cytochrome c. We call this 'reversible secondary structure transition' $(N_w \rightleftharpoons D_{gly})$ that transforms the native state in water (N_w) to a quasi-native state in glycerol (D_{gly}) , which is richer in secondary structure content.

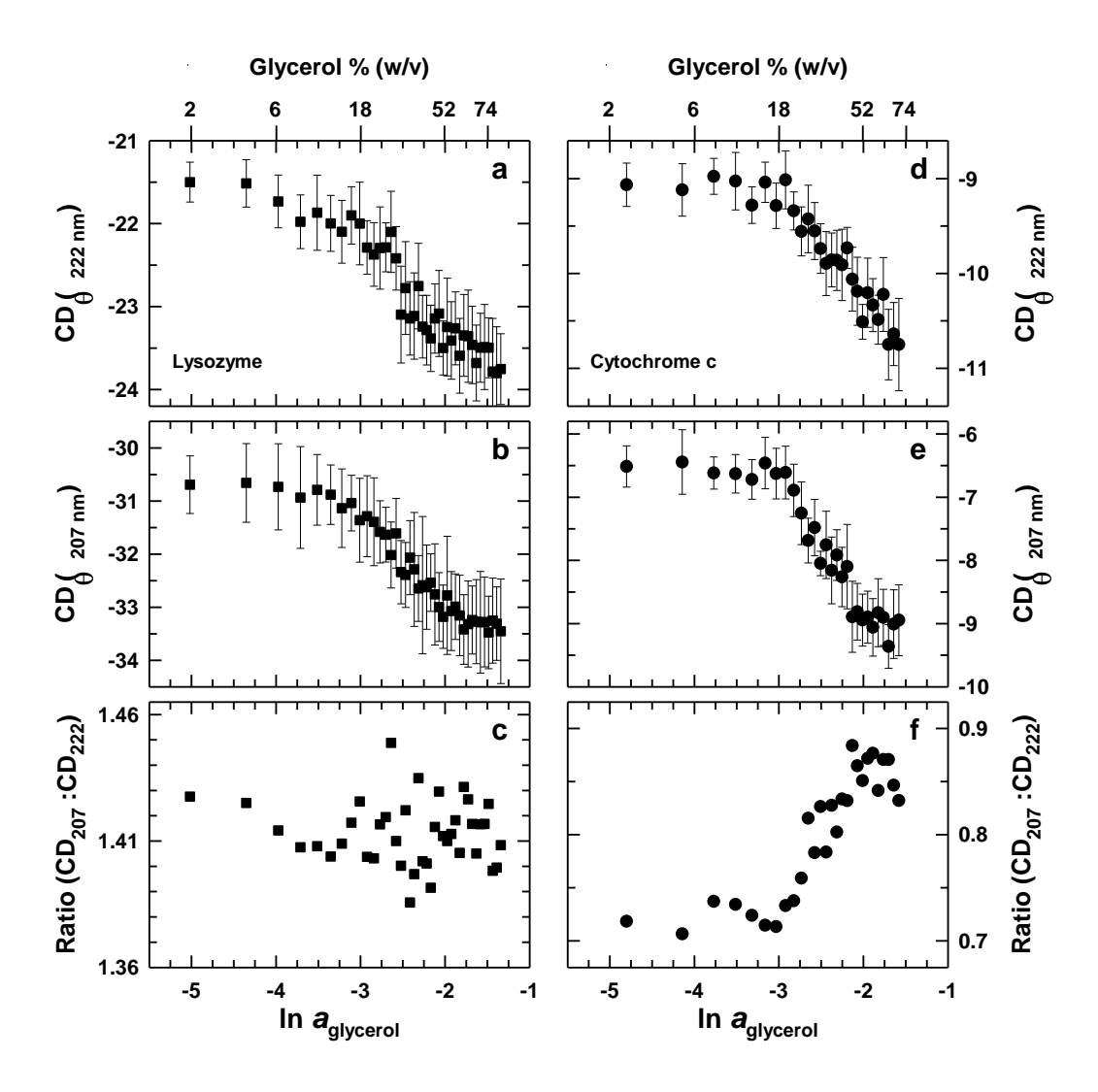


Figure 3.3. Secondary structure probed by far-UV CD for lysozyme (a–c) and cytochrome c (d–f) plotted with the natural logarithm of the activity of glycerol (ln $a_{\rm glycerol}$). The weight-percent values corresponding to $\ln a_{\rm glycerol}$ are shown on top.

3.3.2. Significant changes in tertiary structure

Tertiary structure was probed first by fluorescence using the same samples that were used for far-UV CD experiments. In the 0-80% range of glycerol the wavelength of maximum emission, λ_{max} , for lysozyme undergoes Stokes shift from 337 to 329 nm (Figure 3.4a), consistent with earlier reports. 37,38 The λ_{max} of the model chromophore 5-methoxyindole in glycerol-water mixture shows little shift (Figure 3.5a,b), suggesting that the observed shift for lysozyme may not be due to the surface tryptophans (W 62,63, and 123). In a similar result, the fluorescence of N-acetyl tryptophanamide (NATA) across 0-60% glycerol shows 2.5(±0.5) nm blue shift and ~15% decrease in quantum yield (Figure 3.5c,d), suggesting a minor contribution of the fluorescence of any surface tryptophan to the total fluorescence due to tertiary structural changes to which we did not apply any correction. The blue shift of the protein fluorescence arises from the displacement of the tryptophan side chains into protein interior. Since the protein interior is already apolar and the excited state of the indole has a larger dipole moment than the ground state, 39 the excited state corresponding to the $0\rightarrow0$ fluorescence emission will be energetically less stable. The higher energy of the excited state will produce blue shift in emission λ_{max} . The glycerol-induced protein compaction accompanying burial of the tryptophans should also be the reason for fluorescence quenching shown using the 337-nm emission (Figure 3.4b). As unfolding of lysozyme at pH 3.8 results in fluorescence increase, 40 the quenching seen here might appear to be the reminiscent of folding. However, since the starting state itself is the native state, there is little scope for further conformational folding. The fluorescence quenching therefore reflects a glycerol-induced transition of the compact tertiary structure to more compact states. The compaction leads to tighter packing and hence considerable changes in the tertiary structure.

The change in the tertiary structure with glycerol was also monitored by near-UV CD (Figure 3.4c). The increase in the 290-nm band intensity of lysozyme corresponds to tertiary structure folding, 38,41 but in the present case we associate the transition with compaction of tertiary structure, consistent with the interpretation of the fluorescence results. A simple explanation for the increase in the 290-nm CD intensity can be provided based on the theory of coupled electric transitions. ⁴² If the rotational strength R of an aromatic side chain originates from a coupling of its $\pi \rightarrow \pi^*$ transition with an electric transition of a nearby protein group, then

R is proportional to the distance d between the point dipoles for the aromatic and the nearby group. In the glycerol compacted protein d is expected to decrease which will enhance R, consistent with the observations made (Figure 3.4c).

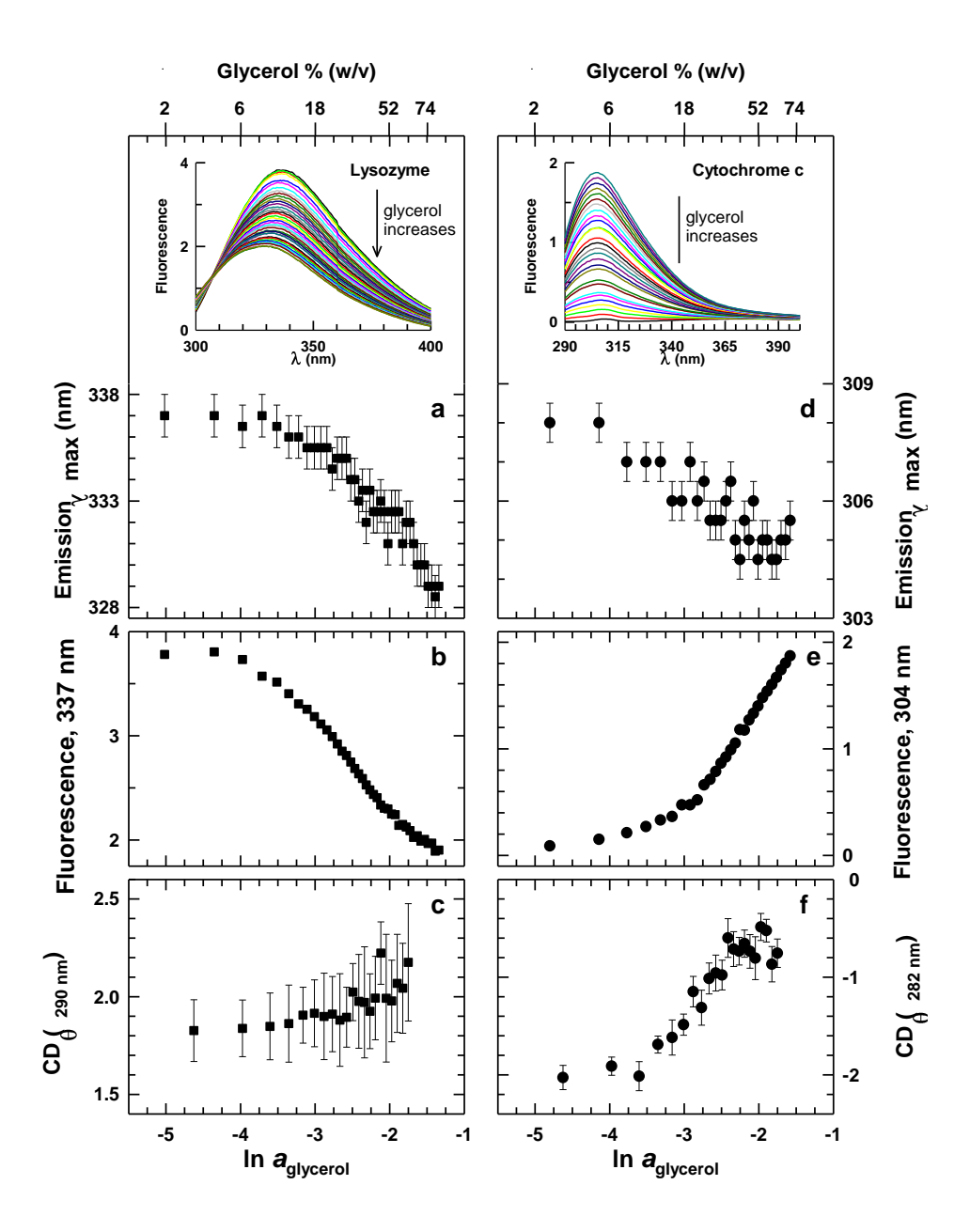


Figure 3.4. Tertiary structure of lysozyme (a–c) and cytochrome c (d–f) with $\ln a_{\rm glycerol}$. Changes in tryptophan fluorescence and near-UV CD correspond to acquisition of additional tertiary structure for lysozyme but unfolding of cytochrome c.

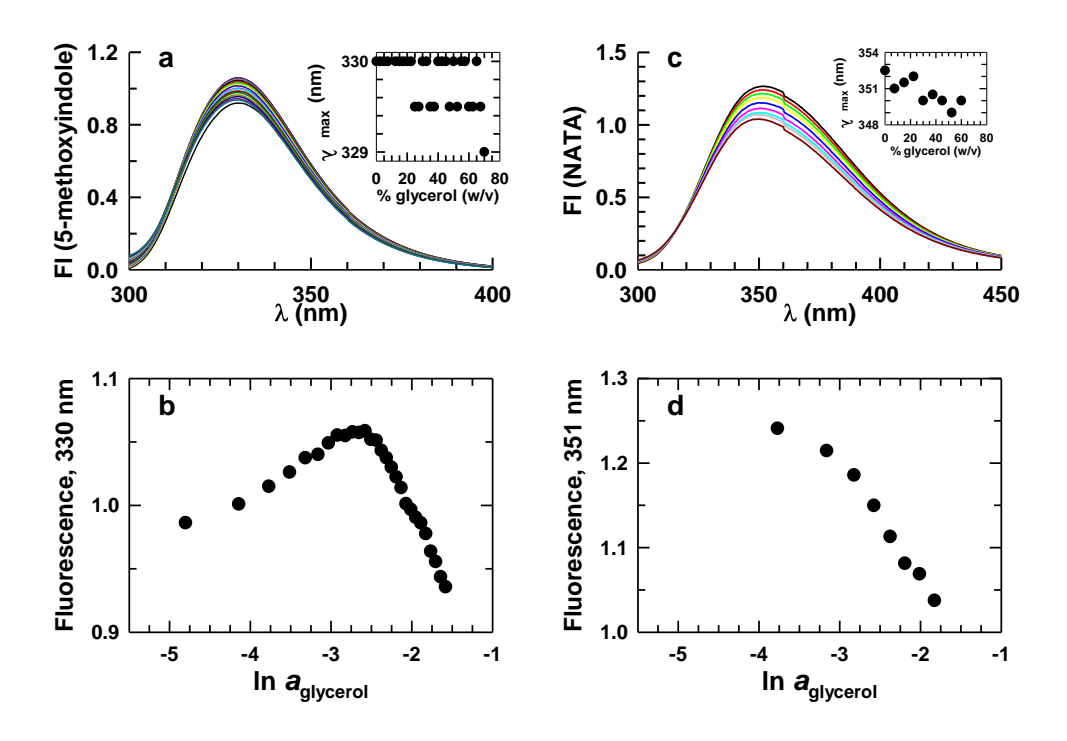


Figure 3.5. (a) Changes in the fluorescence emission spectrum of 5-methoxyindole with glycerol. The *inset* shows no shift (within error) in the wavelength of emission maximum. (b) Quenching of 330-nm emission of 5-methoxyindole intensity due to the solvent effect. (c) Fluorescence of NATA with glycerol, with the λ_{max} shift (*inset*). (d) Quenching of NATA fluorescence at 351 nm with glycerol.

In contrast to the results for lysozyme that have shown glycerol-induced transition of the tertiary structure to more compact states, data for cytochrome c show unfolding of tertiary structure. Fluorescence of the lone tryptophan of native cytochrome c (W59) in water is completely quenched due to resonance energy transfer to the heme, ⁴³ but the emission increases with glycerol accompanying a shift in the λ_{max} from 308 to 305 nm (Figure 3.4d). The 3-nm shift is not substantial, but is an indication of displacement of the tryptophan side chain to a more apolar environment, similar to the explanation given for the blue shift of λ_{max} for lysozyme. However, the result that fluorescence increases with glycerol (Figure 3.4e) suggests an increase in the W59-heme distance and hence unfolding of tertiary structure. It is well known that unfolding of tertiary structure of cytochrome c results in fluorescence increase. ^{43,44}

The loss of tertiary structure in water–glycerol mixture was also probed by near-UV CD (Figure 3.4f). The near-UV CD of cytochrome c originates almost entirely from the Trp 59 side chain. The indole does not possess magnetically allowed transitions, but gains rotational strength through coupling of its electric dipole transition moment with that of the $\pi \rightarrow \pi^*$ transitions of the heme, and possibly peptides and other aromatic chromophores. Since the rotational strength is largely dependent on the indole–heme distance, an increase in the Trp59–heme distance weakens the rotational strength, which is an indicator of tertiary structure unfolding. Thus, fluorescence and near-UV CD results are mutually consistent, and we conclude that the tertiary structure of cytochrome c unfolds in water–glycerol mixture.

3.3.3. Reduction of the heme iron and tertiary structure changes in cytochrome c

During the course of experiments we often observed the color of cytochrome c turn brighter in the water–glycerol mixture which led us to examine the visible optical absorption spectrum of cytochrome c. The Soret band $(\pi \to \pi^*)$ red-shifts from 409 to 412.5 nm in the 0–70% range of glycerol (Figure 3.6a), suggesting reduction of the heme iron Fe³⁺ \to Fe²⁺, consistent with the fact that glycerol is a hydrogen donor.⁴⁷ Also, the decrease in the Soret absorption coefficient with glycerol (Figure 3.6b) indicates destabilization of the tertiary structure, ⁴⁸ consistent with fluorescence and near-UV CD results. These results are made clearer by the much weaker Q bands $(\pi \to \pi^*)$ which were studied with another batch of concentrated samples. The Q bands of reduced cytochrome c (Fe²⁺) appear at 550 nm due to configurational interaction between $a_{1u}\to e_g$ and $a_{2u}\to e_g$, ⁴⁹ and 520 nm which is vibronic. The terms a_{1u} and a_{2u} label the highest occupied π orbitals, and the e_g term refers to the lowest unoccupied π^* orbital. Figure 3.6c shows that cytochrome c is reduced already in the solution containing 3% glycerol.

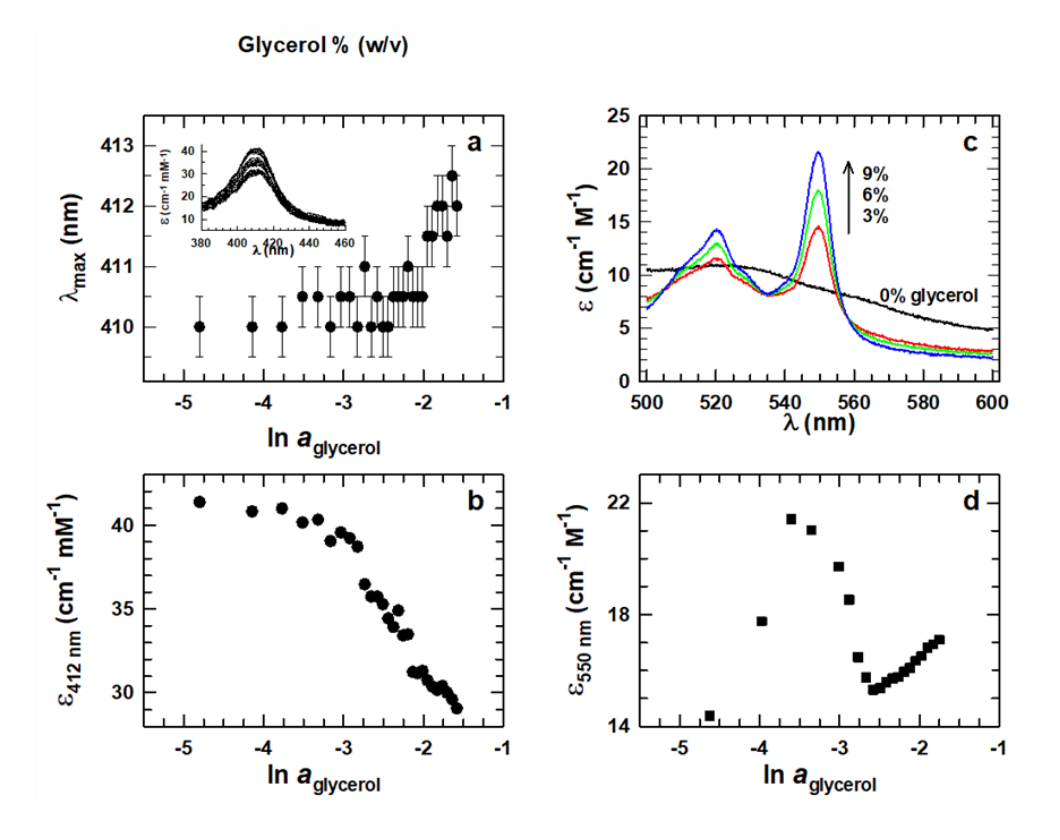


Figure 3.6. Ferric \rightarrow ferrous heme transition and unfolding of cytochrome c probed by heme absorption. Red shift of the Soret absorption maximum with higher glycerol (a) and increased 550-nm absorbance at low concentrations of glycerol (c) are signs of reduction of the heme iron. The decrease in absorption with glycerol (b,d) indicates protein unfolding.

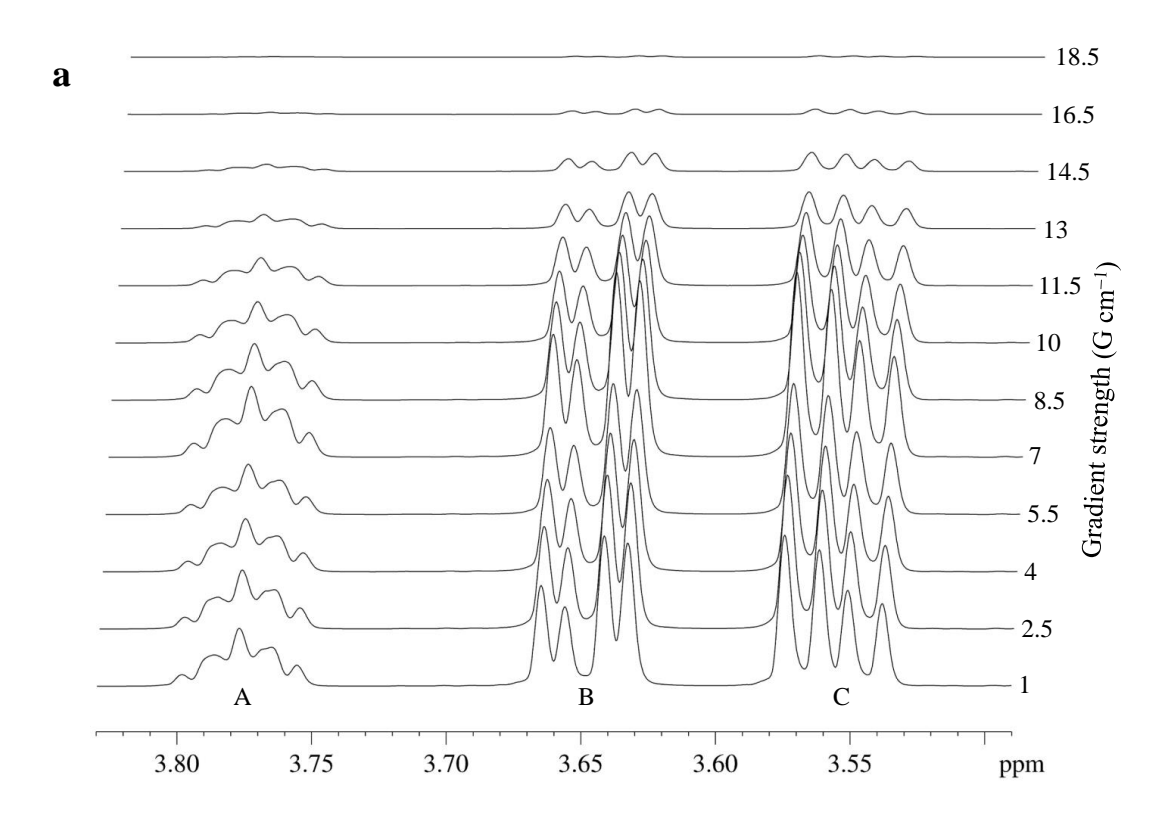
The reduction of the heme of cytochrome c should be due to glycerol, because the trace of any other reducing agent in the solutions was not expected to be significant. The initial increase of the 550-nm absorbance indicates that the protein is fully reduced in ~9% glycerol, which provides the baseline for the reduced protein. At >9% glycerol we observe the conformational changes of the reduced cytochrome c. The absorbance decreases sharply in the 9–30% range of glycerol, suggesting substantial loss of the tertiary structure (Figure 3.6d). Reduced cytochrome c (Fe²⁺) is very stable, and global unfolding of the protein chain by glycerol is unlikely. To summarize, low glycerol reduces cytochrome c and the reduced native state of the protein (N) is reversibly transformed to a quasi-native state (D_{gly}) due to tertiary structure unfolding at high glycerol (N \rightleftharpoons D_{gly}).

3.3.4. Self diffusion and hydrodynamic properties of the proteins

The changes in tertiary structure – compaction for lysozyme but unfolding for cytochrome c, should be reflected in hydrodynamic properties of the proteins in the presence of glycerol. To see this, we measured the translational diffusion coefficient, D_s , for both proteins in water-glycerol solutions by PFG NMR.⁵⁰ The attenuation of resonance amplitudes as a function of pulsed field gradient strength (Figure 3.7) yields D_s according to

$$I(g) = I_0 \exp\left[-(\gamma \delta g)^2 \left(\Delta - \frac{\delta}{3}\right) D_S\right]$$
(3)

in which γ =26.752×10⁷ rad T⁻¹ s⁻¹ is the gyromagnetic ratio of ¹H, δ (=6.3×10⁻³ s) is the duration of the PFG, g is the gradient strength, and Δ (=0.3 s) is the time delay between the PFG pulses. Values of δ and Δ given here are those used in our experiments.



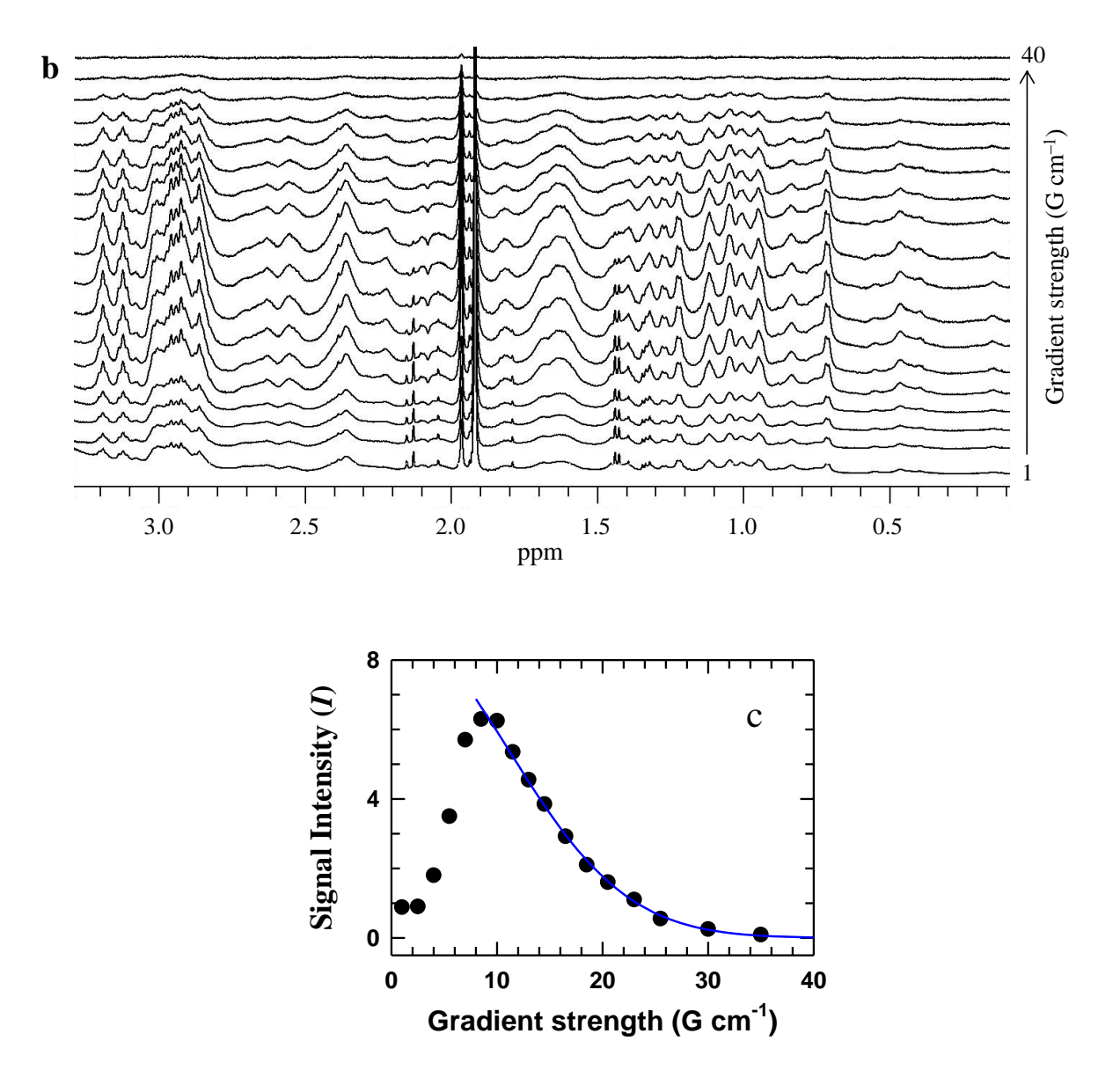


Figure 3.7. (a) Aliphatic region of PFG-NMR spectra of cytochrome c in 20% glycerol. (b) Glycerol resonances in the same set of spectra. (c) Signal attenuation is preceded by a build-up at the lower end of the field gradient, so as to produce a skewed Gaussian. The actual attenuating data are fitted to Equation 3. This illustration is done using data for cytochrome c in aqueous solution.

Figure 3.8 shows the variations of D_s for lysozyme and cytochrome c in water-protein-glycerol system where the glycerol content varies between 0 and 45% (w/v). In both protein solutions the D_s of glycerol decreases, although the values and the extent of decrease are not comparable due to the pH difference of the solutions. However, the measured value of D_s varies from

 $1.1(\pm 0.16) \times 10^{-6}$ to $0.82(\pm 0.24) \times 10^{-6}$ cm² s⁻¹ for lysozyme and $1.05(\pm 0.1) \times 10^{-6}$ to $0.35(\pm 0.24) \times 10^{-6}$ cm² s⁻¹ for cytochrome c, suggesting molecular expansion of the later. This is more clearly seen when the D_s for proteins are converted to hydrodynamic radii (see below).

Considering the general response of protein tertiary structures in water–glycerol mixture we expected cytochrome c also to undergo compaction. The expansion is most likely due to direct binding of glycerol to the heme, in which case not only the heme pocket structure but also the entire tertiary structure will be perturbed. This notion follows from the observation that the heme undergoes reduction in water–glycerol (Figure 3.6), and conforms to an earlier hint that alcohols directly associate with the ferric heme iron of cytochrome c. In spite of the observed expansion of the tertiary fold we feel that certain regions of the protein become more compact locally as was also found in an earlier study of slower flip rate of aromatic rings of cytochrome c in water–glycerol. c

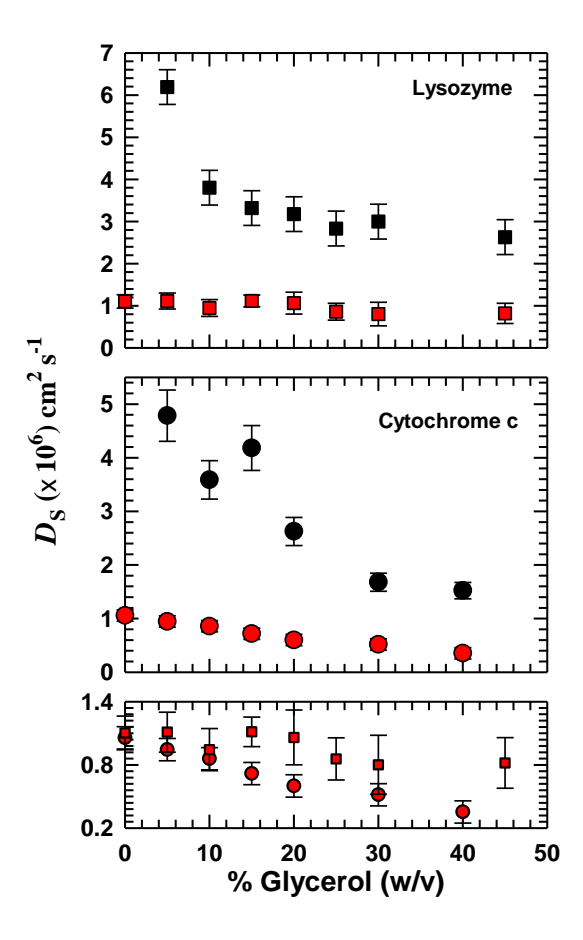


Figure 3.8. NMR-measured self-diffusion coefficients of the proteins (red symbols) in glycerol. Symbols in black show diffusion of glycerol in the respective protein solutions.

3.3.5. The free energy of structural changes, and the effective number of displaced water

The results above have shown that glycerol drives the proteins to non-native states by the $N_w \rightleftharpoons D_{gly}$ transition where D_{gly} -state is rich by α -helix content. But the tertiary structure in the D_{gly} -state is either more compact as for lysozyme or unfolded in the case of cytochrome c. To calculate the free energy of these transitions we carry out an analysis based on the theoretical form of the ligand binding polynomial⁵³ in conjunction with Wyman's linked function.⁵⁴ Because glycerol is thought to interact with surface side chains of proteins by hydrogen bonding²² rather than weak physical interactions, we assume a Langmuir-type of selective binding to independent sites. Using subscripts 1, 2, and 3 to label water, protein, and glycerol components, respectively, the chemical potential of the protein in the presence of glycerol is written as

$$\mu_2 = \mu_2^0 + RT \ln m_2 + RT\beta_2 \tag{4}$$

in which μ_2^0 , m_2 , and β_2 are standard-state chemical potential, molal concentration, and the excess free energy of the protein due to glycerol binding. The quantity β_2 , which is often approximated to the coefficient of thermodynamic binding Γ_{23} for the protein-ligand interaction, is given by ^{55,56}

$$\beta_2 \equiv \Gamma_{23} \cong \left(\frac{\partial m_3}{\partial m_2}\right)_{T,P,\mu_3}.$$

Because the change in the free energy of the protein due to binding of the ligand at two different concentrations is the change in the perturbation of the chemical potential of the protein,

$$\Delta G = \mu_2^{\rm D} - \mu_2^{\rm N} = -RT(\Gamma_{23}^{\rm D} - \Gamma_{23}^{\rm N}) = -RT\Delta\Gamma_{23},$$

where μ_2^D and μ_2^N are chemical potentials of the protein in the glycerol-bound state and the native state in the absence of glycerol. The corresponding thermodynamic binding coefficients are Γ_{23}^D and Γ_{23}^N . When information about Γ_{23} is not available it is estimated from the Wyman linkage equation,⁵⁴ which expressed in terms of glycerol activity is

$$-RT\left(\frac{\partial \ln K}{\partial \ln a_3}\right)_{m_2} = -RT\Delta\Gamma_{23} = \Delta G,\tag{5}$$

where K is the equilibrium constant for the $N_w \rightleftharpoons D_{gly}$ reaction, and a_3 is the activity of glycerol. It is noted that glycerol solution is highly non-ideal, and a large change in the activity coefficient of glycerol takes place over a small change in its % content in the aqueous solution. Therefore, the molar or mole fraction-based scale is inappropriate.

To calculate ΔG by the use of equation 5 we extracted the values of K across the $N_w \rightleftharpoons D_{gly}$ transition from the normalized transition curves. The slope of $\ln K$ vs $\ln a_{glycerol}$ times RT yields ΔG . If the change in the protein effect is assumed to be linear with the natural logarithm of activity of glycerol then the measured ΔG matches $\Delta G_{D,gly}$, the free energy of the quasi-native transition in glycerol. Figure 3.9 illustrates the analysis for the lysozyme $N_w \rightleftharpoons D_{gly}$ transition probed by secondary and tertiary structures. The $\Delta G_{D,gly}$ values obtained for both lysozyme and cytochrome c (Figure 3.10) are listed in Table 1.

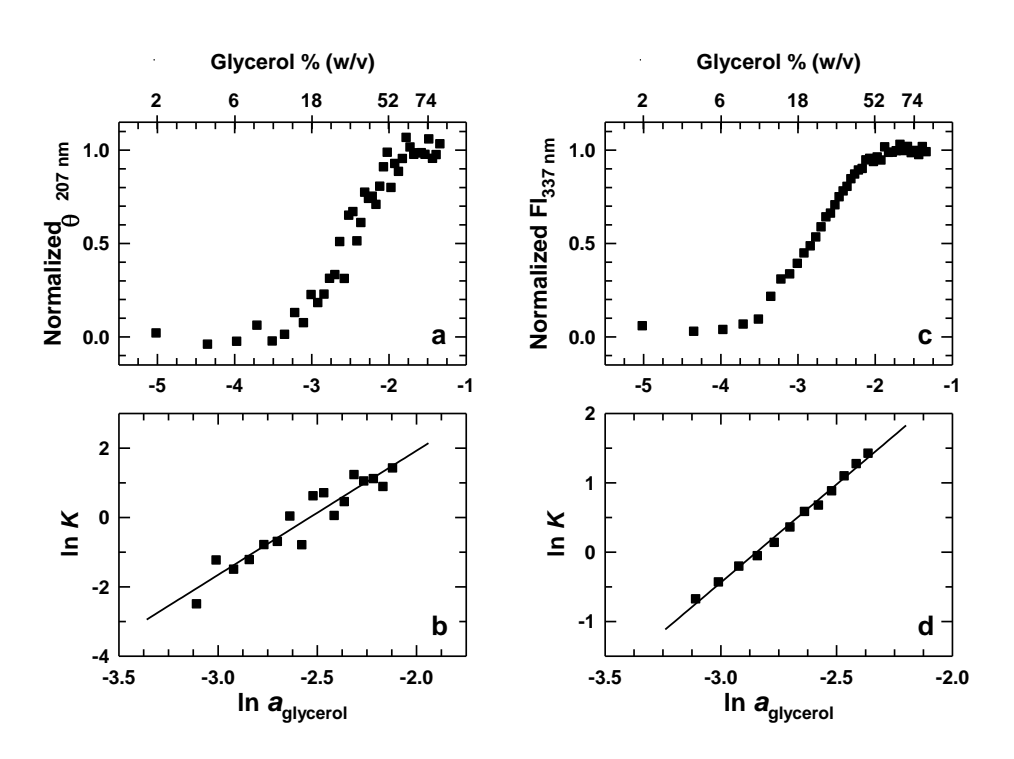


Figure 3.9. Linearity of natural logarithms of the equilibrium constant for the $N_w \rightleftharpoons D_{gly}$ quasinative transition of lysozyme with the natural logarithm of glycerol activity, probed by far-UV CD (a,b) and fluorescence (c,d). The free energy values are listed in Table 1.

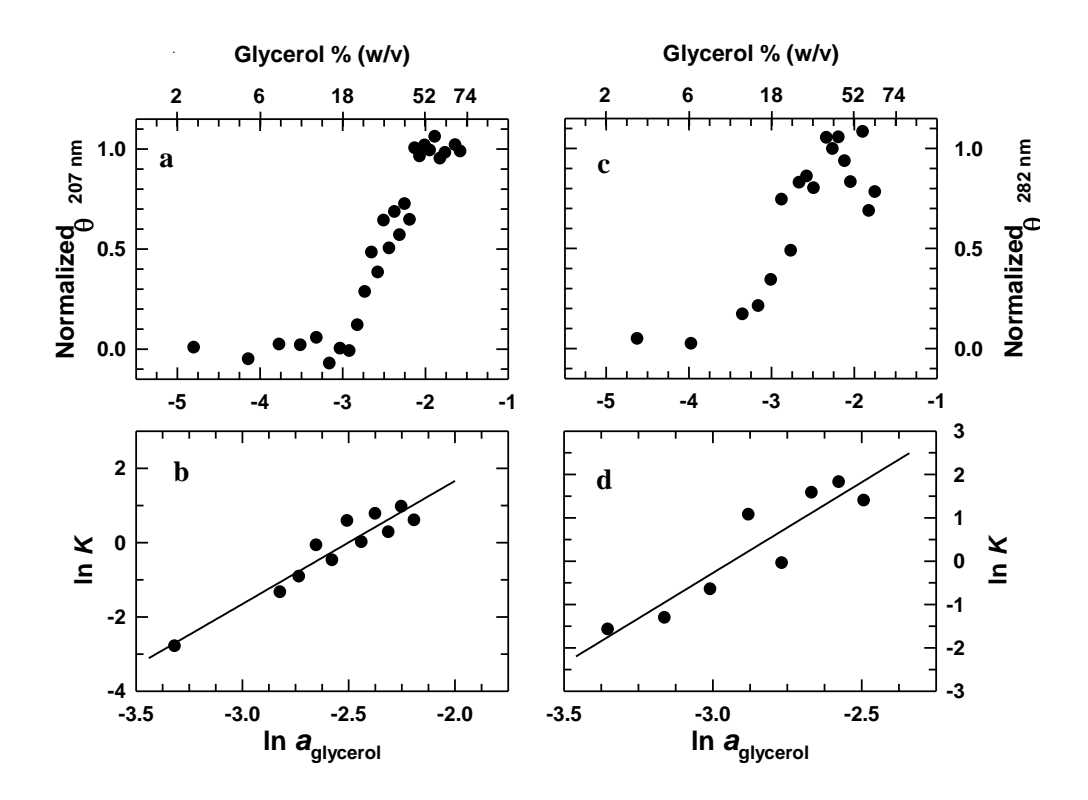


Figure 3.10. Natural logarithms of the equilibrium constant for the $N_w \rightleftharpoons D_{gly}$ denaturation transition of cytochrome c with the natural logarithm of glycerol activity, probed by far- (a,b) and near- (c,d) UV CD. The free energy values are listed in Table 1 of the main text.

The above analysis carried out using the natural logarithm of activity of water ($\ln a_1$), yields the difference in the effective number of preferentially bound water molecules to the native and glycerol-bound non-native states⁵⁶

$$\left(\frac{\partial \ln K}{\partial \ln a_1}\right) = \left(\frac{\partial \ln m_1}{\partial \ln m_2}\right)_{T,P,H_1}^{D} - \left(\frac{\partial \ln m_1}{\partial \ln m_2}\right)_{T,P,H_2}^{N} = \Delta \xi_1,\tag{6}$$

where $\Delta \xi_1$ is the difference between the preferential binding of water and glycerol to the native and non-native states, m_1 and m_2 represent molal concentration of water and protein, respectively, and μ_1 is the chemical potential of water in the water-protein-glycerol system. Figure 3.11, where the activity of water (a_1) is explicitly written as $a_{\rm H_2O}$, shows the analysis using data for lysozyme. Values of $\Delta \xi_1$ for both lysozyme and cytochrome c (Figure 3.12) are given in Table 1.

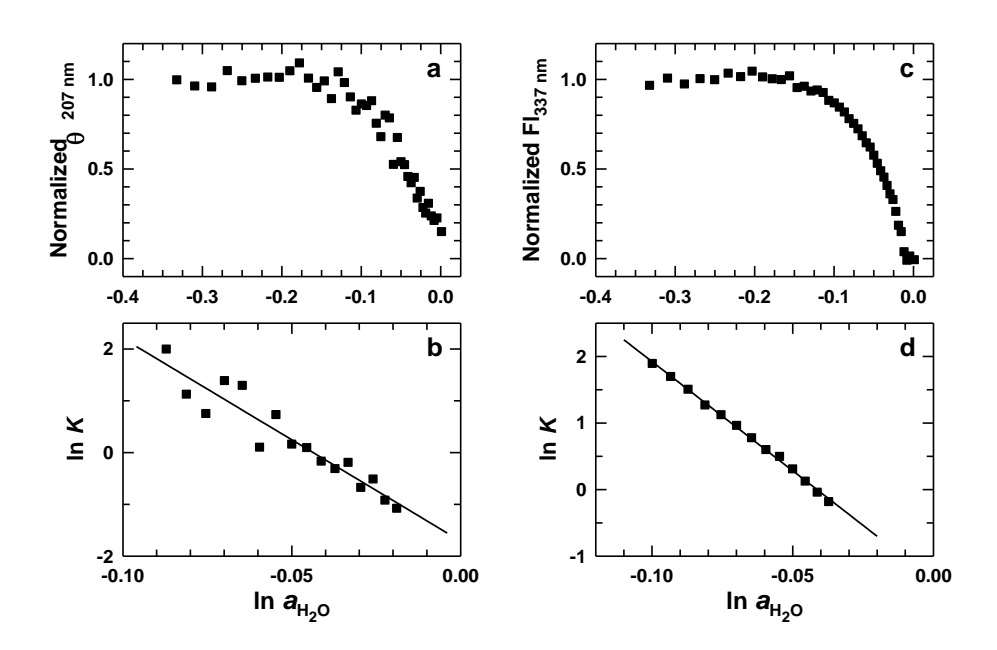


Figure 3.11. The logarithm of equilibrium constants for the $N_w \rightleftharpoons D_{gly}$ transition of lysozyme with logarithm of water activity, probed by far-UV CD (a,b) and fluorescence (c,d). Values of the slope, $\Delta \xi_1$, which represents the change in the effective number of water molecules across the $N_w \rightleftharpoons D_{gly}$ reaction, are listed in Table 1.

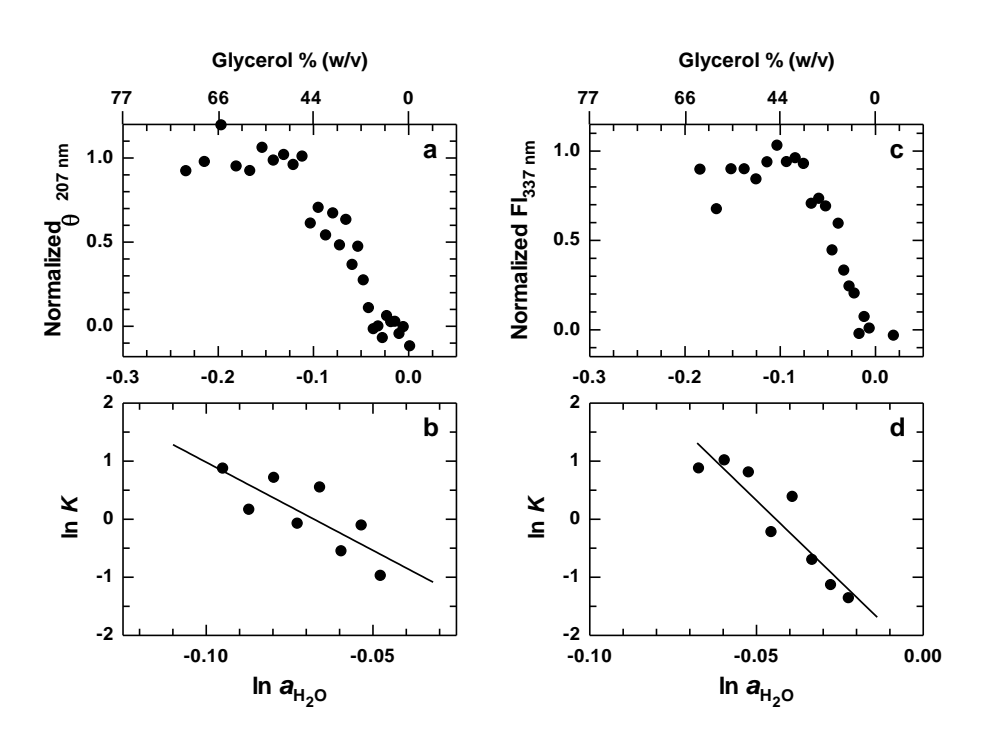


Figure 3.12. The change in the effective number of water molecules across the $N_w \rightleftharpoons D_{gly}$ reaction for cytochrome c transition is obtained from the slope of straight lines ($\Delta \xi_1$) in panels b and d. The values are listed in Table 1.

Table 1. Quasi-native transition free energy ΔG_{gly} and the difference of preferential binding of water to native and Quasi-native states $(\Delta \xi_1)$.

Protein	pН	Charge	$\Delta G_{gly}(\text{Kcal mole}^{-1})$		$(\Delta \xi_1)$	
			Secondary	Tertiary	Secondary	Tertiary
			structure	structure	structure	Structure
Lysozyme	3.8	+16.4	2.11 (±0.3)	$1.70 (\pm 0.2)^*$	39.1 (±4)	32.8 (±2)*
Cytochrome c	7.0	+9.6	1.96 (±0.3)	$2.50 (\pm 0.4)^{\#}$	30.4 (±8)	55.5 (±8) [#]

^{*}From fluorescence at 337 nm

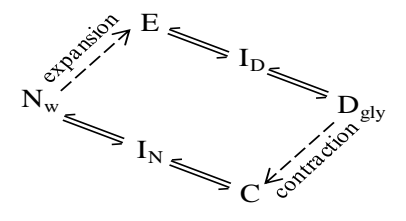
Perusal of the numbers in Table 1 tells that the quasi-native transition free energy in glycerol is modest and roughly matches the folding free energy of structural intermediates commonly observed in guanidinium unfolding of proteins. The $\Delta G_{D,gly}$ values for the $N_w \rightleftharpoons D_{gly}$ transition in glycerol should not be large, because it is not an unfolding transition. The magnitude of $\Delta \xi_1$ reflects the change in the effective number of water molecules in the hydration layer nearest to the protein surface due to interaction of glycerol with surface side chains. The $\Delta \xi_1$ values noted in Table 1 are also modest compared to at least a hundred water molecules involved in the hydration change in protein unfolding, consistent with the results that glycerol interaction does not lead to chain unfolding.

^{*}From near-UV CD

3.3.6. Kinetics of tertiary structural changes in cytochrome c

To find out the timescale for conformational changes across the $N_w \rightleftharpoons D_{gly}$ equilibrium in water-glycerol system we carried out stopped-flow fluorescence measurements. The initial water-protein (N_w) or water-protein-glycerol (D_{gly}) solution was diluted eight-fold into water-glycerol mixture of variable glycerol content. The kinetics entail a single observable phase irrespective of jumps from lower to higher or reverse glycerol content, although the inclusion of a delayed phase (~15-fold slower) improves the fits (Figure 3.13a,e). To note are two interesting observations. One, ~95% of the expected signal is lost in the 1.8 ms dead-time of measurement (Figure 3.8b,f), implying the presence of one or more submillisecond phases. Two, in $D_{gly} \rightarrow N_w$ jumps, the product of the submillisecond kinetics is a contracted protein which then expands in the observable window (Figure 3.13a,b). This inference is based on the fact that expansion of the cytochrome c chain increases the heme–W59 distance causing increased fluorescence of the tryptophan.⁵⁷

In $N_w \rightarrow D_{gly}$ jumps the events are reversed – the native compact state undergoes submillisecond expansion which then contracts in milliseconds (Figure 3.13e,f). With the zero-time signal (S_0) determined by extrapolating the traces to time t=0 we obtained the unobservable fluorescence change corresponding to burst phase kinetics (Figure 3.13c,g). The observable amplitude is <5% across the glycerol scale. The macroscopic rate constants, λ_{obs} , appear to show a transition with a midpoint of ~15% glycerol (Figure 3.13d,h), which is clearer in the experiment in which the water–protein solution was mixed with increasing glycerol-containing buffer where the faster observable phase increases by at least two orders of magnitude (Figure 3.13h). The observations together with the burst phase kinetics leads to the following minimal kinetic mechanism (Scheme 1)



Scheme 1

in which E and C are expanded and contracted burst products, and I_D and I_N are non-native and native-like intermediates, respectively.

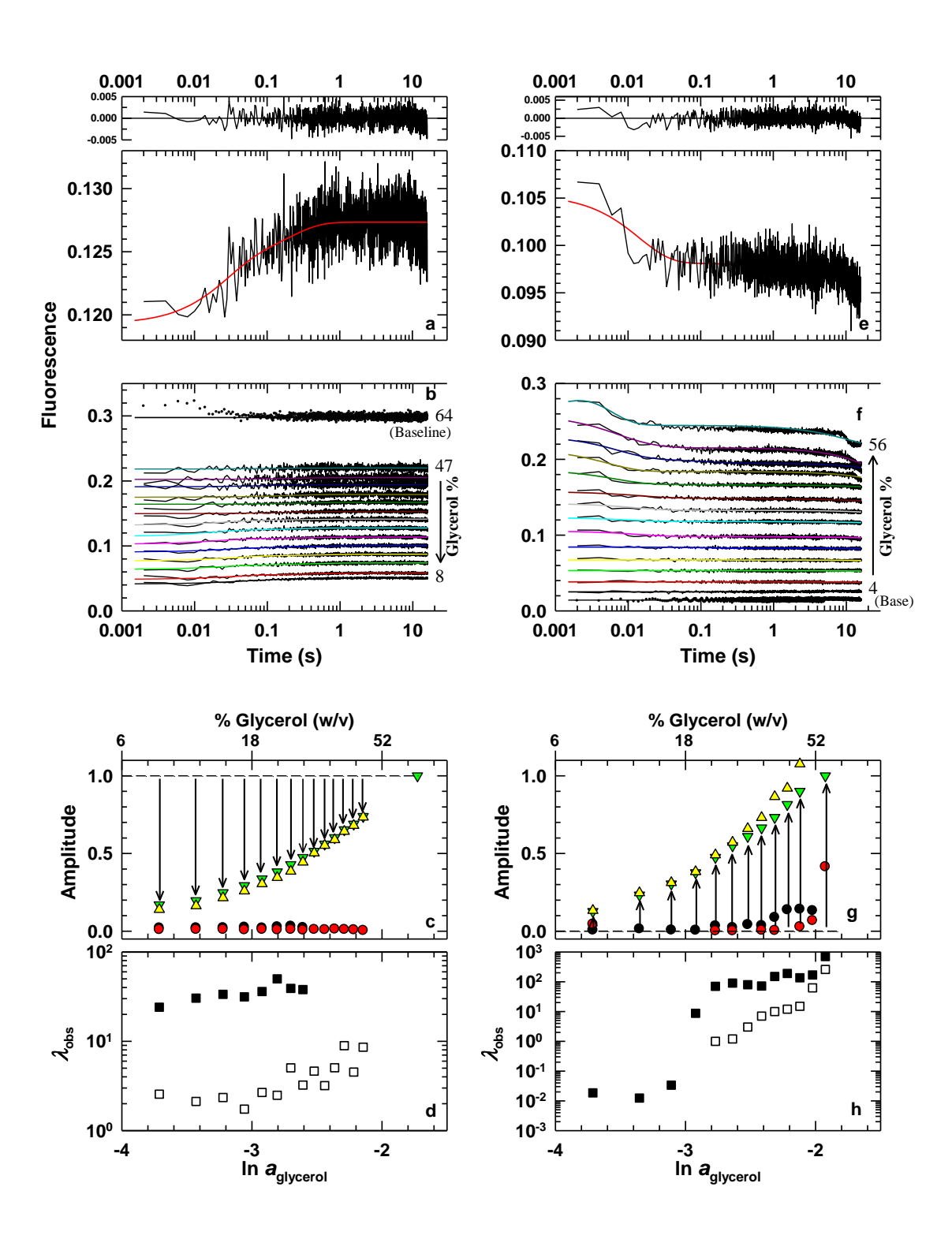


Figure 3.13. Fluorescence-monitored kinetics of conformational changes in cytochrome c upon transfer from water to water–glycerol and the reverse. (a) Two observed exponential phases of a trace (λ_1 and λ_2 , 39.11 and 5.04 s⁻¹, respectively) following a jump from 64% initial to 26% final glycerol. (b) Sample of traces shown relative to the signal for the initial protein solution in 64% glycerol. At higher glycerol (>35%) the traces fit to a single exponential. (c) Signal amplitudes: zero-time fluorescence, S₀ (yellow triangle), baseline fluorescence of traces, S_∞ (green inverted triangle), and amplitudes corresponding to the observable phases λ_1 and λ_2 (black and red circles, respectively). The arrows indicate glycerol dependence of the unobservable phase. (d) The observable phases λ_1 and λ_2 . Panels e–f show corresponding data for transfer of the protein from water (0% glycerol) to varying water–glycerol mixture. The description of symbol types and coloration are same as for panels c and d.

3.4. Discussion

3.4.1. Large-scale changes in protein structure in water-glycerol

The increase in secondary structure content of both lysozyme and cytochrome c starts to occur in as low as 2–5% glycerol and tends to saturate at ~60% glycerol. We believe additional secondary structure is a general property of proteins in water-glycerol medium. The details of the mechanism by which cosolvents enhance the secondary structural propensity of proteins are not certain. Many factors may contribute; the binding of the cosolvent may produce specific interactions between both polar and apolar side chains within the protein, and nonspecific interactions between charged side chains and helix dipoles. Earlier lattice simulation studies have predicted that molecular compactness can drive the propensity of both helices and sheets. This suggestion appears applicable at least for glycerol, which drives protein structures to more compact states. 22,52 But the finding that cytochrome c which expands in the presence of glycerol and yet rich in α -helix leads us to reason that it is not only the global compactness, but locally compact segments can also increase the helix propensity.

Regarding tertiary structural changes in water–glycerol we find two contrasting responses of the tertiary structure to water–glycerol. The changes, which begin to occur in as low as 2% glycerol and are completed in ~70% of the cosolvent, lead to molecular compaction of lysozyme, but expansion of cytochrome c. These changes are also reflected in the variation of their self diffusion coefficients, D_s (Figure 3.8). The observations sharply contradict the limited qualitative data of earlier studies of glycerol effect on lysozyme⁴¹ and cytochrome c^{62} whose tertiary structures were reported to change negligibly. We believe protein tertiary structures in general are strongly affected in water–glycerol mixture.

The different modes of structure development for lysozyme and cytochrome c in glycerol should arise from differences in their native state structures and the initial pH conditions employed. Native lysozyme is rich in both α - and β -structure contents and has four disulfide bonds which are stable at pH 3.8. But cytochrome c has no disulfides, and the secondary structure consists of four helices and three rudimentary β -turns. The development of additional β -structure for lysozyme but α -helix for cytochrome c in their quasi-native states may arise from the characteristic initial native-state secondary structures. Regarding the change in tertiary conformation with glycerol, the compaction of lysozyme may be due to constraints imposed by the disulfide bonds, the absence of which along with possible dissociation of the Fe²⁺–M80 bond in glycerol render large expansion of the cytochrome c chain (Figure 3.14).

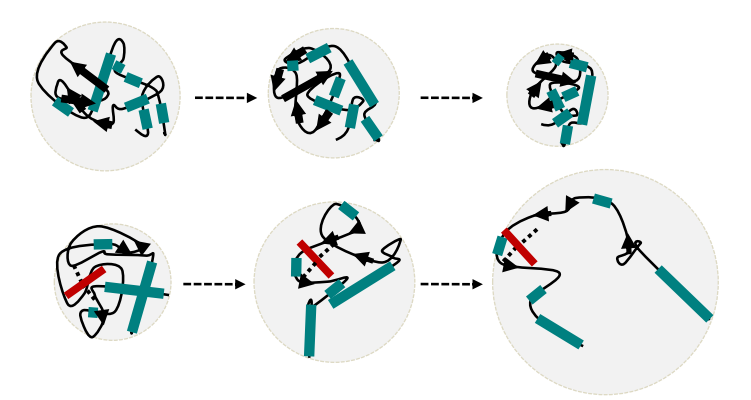


Figure 3.14. Coarse depiction of changes in structure and dimension of lysozyme, pH 3.8 (top), and cytochrome c, pH 7 (bottom). Disulfides of lysozyme are not shown. The heme is in red.

3.4.2. Ultrafast tertiary structure collapse and temporal intermediates in cytochrome c

About 95% of glycerol-induced tertiary structural changes in cytochrome c is completed in the submillisecond bin, and we call this regime ultrafast because conformational changes are limited by the diffusion of chain segments. When the N_w-state is taken to high glycerol the chain expands largely in the microsecond regime and then contracts marginally in milliseconds to produce the D_{gly} -state via a structural intermediate. These events are reversed when D_{gly} is driven to fold to N_w (Scheme 1). Submillisecond chain contraction and expansion coupled with transient contact formation between Fe²⁺ and the M80 ligand are known for the foldingunfolding of ferrocytochrome c. ^{63,64} But what is hard to know is the nature of this collapsed or expanded product, whether a specific barrier-limited structural intermediate or a nonspecific species produced by random collapse in response to the changing solvent condition. Since water is preferentially included, or equivalently, glycerol is preferentially excluded from the protein surface, it is very likely that the submillisecond species forms due to changes in Fe^{2+} -M80 ligation and protein chain-solvent interactions, and is therefore a nonspecific species unlike a true structural intermediate. Therefore, the collapsed species forms very likely due to ultrafast preferential hydration coupled to relieving the chain from interaction with glycerol. Yet the content of native-like tertiary structure in the contracted product cannot be dismissed, because nonspecific collapse often comprises more than one event which we do not resolve here. If the preferential hydration is the earliest event, the later event(s) may represent local structure formation and reorganization of the native-state topology.⁶⁵

We associate the millisecond kinetics with secondary structure reorganization and structure consolidation which give rise to excess α -helices in the $N_w \rightarrow D_{gly}$ process but restores the helicity to the initial normal level in the $D_{gly} \rightarrow N_w$ transition. The modes of secondary structure consolidation are expected to be slow for proteins the size of cytochrome c. The fact that millisecond kinetics entails two phases implies accumulation of a temporal intermediate whose structure remains to be studied.

3.4.3. Quasi-native states of proteins in glycerol

The resolution of structural changes listed above is good enough to state that glycerol binding brings about completely reversible $(N_w \rightleftharpoons D_{glv})$ major structural changes in the native state. But what do we call the structurally altered D_{gly} states? The glycerol-bound state is not unfolded, because the unfolded state is distinguished by a highly expanded and solvent exposed state that has little residual structure as obtained under strongly denaturing conditions. Is the glycerolbound state denatured because the structural changes are major and reversible $(N_w \rightleftharpoons D_{gly})$, and distinct from the initial native structure? These characteristic changes may appear to fit into the operational definition of denaturation due to Tanford. 66 But the problem lies in deciding what the original native structure is. The structures in glycerol cannot be compared to those of the proteins in dilute buffer solutions at fixed pH. Little is known of protein structures in extremely crowded conditions of the cell interior with very high concentration of macromolecules, but if any conditions are considered to be "native" it would be these. So, the glycerol-induced structural changes cannot really be compared to those of native proteins in dilute buffer solutions. But agreeing with Tanford, 66 we recognize that proteins remain active while undergoing tolerable structural changes in response to changes in environment. The states associated with such structural changes are "quasi-native states". In fact, the examples Tanford used to describe these states, cation- and pH-induced conformation changes, for example, are closely analogous to the glycerol-induced changes described here. The quasi-native states of enzymes in glycerol, for example, are functionally active.⁶⁷ However, based on the observations presented here it would appear that glycerol-induced quasi-native states are generally rich in α helices.

3.4.4. Factors that perturb protein structure in water-glycerol mixture

Unlike urea and guanidine hydrochloride that unfold proteins by interacting with both sidechain and backbone atoms by polyfunctional interactions, ⁶⁸ osmolytes are thought to spare the backbone atoms. ⁶⁹ Glycerol, for example, establishes electrostatic and hydrophobic interactions with limited surface groups ²² to perturb protein structure, but not to the extent of unfolding. Osmolytes are also found to affect the protein structure indirectly by altering the density, order, and hydrogen bonding of water^{30,69,70} both on the protein surface and in the bulk. The outcome is a reduction in protein flexibility.²⁶

We wish to mention the effect of static dielectric constant of water-glycerol mixture that has attracted less attention. It is a basic tenet of protein structure that side chain charges are generally located on the surface where they can be solvated favorably. Surface disposition of charges is preferred because their burial in the low-dielectric protein interior is energetically expensive simply because charge storage capacity is low there. In regard to the water-protein-glycerol (or polyol) system the surface charges are sandwiched by two low dielectric media. The static dielectric constant (ε) of the water-glycerol medium (~40% w/v glycerol) near 25°C is ~65⁷¹ and that of the protein interior is ~7,⁷² which suggests that surface charges should not be internalized. But the Coulombic repulsion involving unscreened surface charges becomes stronger in the water-glycerol medium relative to pure water whose dielectric constant is 80. In the experiments here, the net positive charges on lysozyme and cytochrome ε calculated by Protein Calculator v3.4 (protealc.sourceforge.net) are +16 and +9.6, respectively, which make the protein surfaces highly positively charged. Increased repulsion between positively charged regions, and hence the increase in electrostatic free energy in water-glycerol should destabilize the structure.

3.4.5. The free energy of transfer of proteins from water to glycerol

The reversibility of the native \rightleftharpoons quasi-native transition ($N_w \rightleftharpoons D_{gly}$) allows for a detailed thermodynamic treatment of the process. We find that the free energy for the $N_w \rightleftharpoons D_{gly}$ process, $\Delta G_{N,gly}$, measured by both secondary and tertiary structure probes of lysozyme and cytochrome c is $\sim 2(\pm 0.5)$ kcal mol⁻¹ (Table 1). This is the increase in the free energy of the glycerol-induced quasi-native state ($G_{D,gly}$) relative to that of the native state in water ($G_{N,w}$).

The condition $G_{D,gly} > G_{N,w}$ prevails because of a rise in the chemical potential of the protein due to glycerol binding when the protein is transferred from the aqueous to water-glycerol milieu. Thus $\Delta G_{N,gly} \sim \Delta G_{N,tr}$, where $\Delta G_{N,tr}$ is the free energy of transfer of the native protein from water to glycerol. The free energy of transfer for the unfolded state from water to glycerol ($\Delta G_{U,tr}$) is not known, and we use the free energies of unfolding in water

 $(\Delta G_{\rm w})$ and glycerol $(\Delta G_{\rm gly})$ to estimate $\Delta G_{\rm U,tr}$ for cytochrome c (Figure 3.15). From guanidinium chloride denaturation of cytochrome c we set $\Delta G_{\rm w}\sim 9$ and $\Delta G_{\rm gly}\sim 10$ kcal ${\rm mol}^{-1}$ (40% glycerol) to obtain $\Delta G_{\rm U,tr}\sim 3$ kcal ${\rm mol}^{-1}$, suggesting that unfolding of the protein structure has no major effect on the transfer free energy. This evidence is inconsistent with the longstanding belief that the Gibbs energy effect of osmolytes on unfolded proteins relative to that for native proteins is very large. The fact that $\Delta G_{\rm N,tr}\sim \Delta G_{\rm U,tr}$, for cytochrome c at least, suggests that unfolded proteins preferentially exclude glycerol only to a little larger extent than do native states.

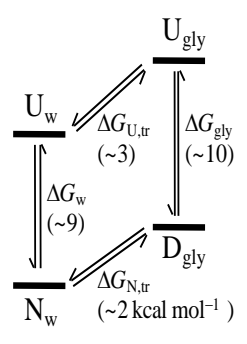


Figure 3.15. Thermodynamic box showing the free energy changes for reactions involving the states N_w , U_w , D_{gly} , and U_{gly} at 25°C, 40% glycerol.

3.4.6. Estimation of glycerol binding energy

In protein-glycerol binding the involvement of both hydrophobic and electrostatic interactions have been implicated. 22,74 If we assume binding of several glycerol molecules to independent but nearly identical sites on the protein surface an effective binding constant $K_{\rm B}$ can be estimated by using the self-diffusion data through 75

$$R_{\rm H} \sim R_{\rm H}^0 \left(1 + r^{a \to a_0} \frac{K_{\rm B} a}{1 + K_{\rm B} a} \right),$$
 (7)

where $R_{\rm H}$ is hydrodynamic radius of the protein, $R_{\rm H}^0$ is the $R_{\rm H}$ value in the absence of glycerol, a is activity of glycerol, and $r^{\rm a \to 1}$ is the relative change in $R_{\rm H}$ as the activity of glycerol approaches unity. Values of $R_{\rm H}$ were approximated from self-diffusion coefficients of lysozyme

and cytochrome c in water–glycerol mixtures (Figure 3.8) by the Stokes-Einstein relation, and the dependence of $R_{\rm H}$ on the activity of glycerol was fitted to equation 7 (Figure 3.16). The fits give $K_{\rm B}\sim16.4$ and 2.1 M⁻¹ for lysozyme and cytochrome c, respectively, and the binding energy ($-RT\ ln\ K_{\rm B}$) for glycerol-protein interaction thus is $\sim1(\pm0.6)$ kcal mol⁻¹. The binding energy approximated by this overly simplified approach is based on the analysis of binding isotherms, which is different from the preferential binding expressed as the number of moles of glycerol bound per mole of protein. The glycerol binding energy of ~1 kcal mol⁻¹ is roughly two-fold higher than the energy of methanol binding to proteins.

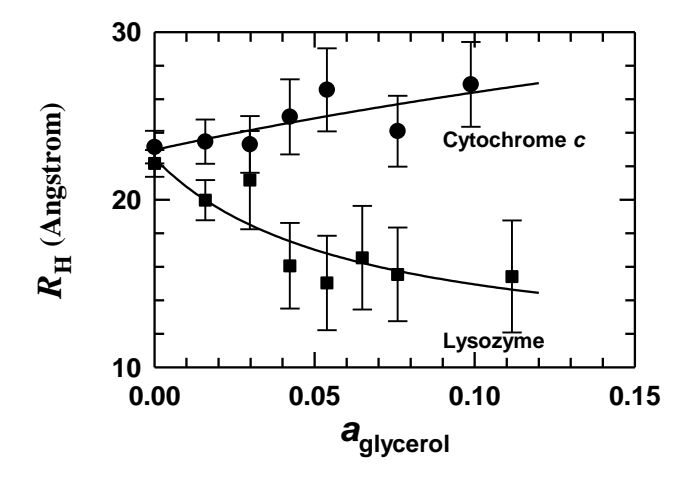


Figure 3.16. The functional dependence of R_h of lysozyme (\blacksquare) and cytochrome c (\bullet) on glycerol activity according to equation 7. The effective binding constants (K_B) for the binding of glycerol to lysozyme and cytochrome c are 16.4 and 2.1 M⁻¹, respectively.

3.4.7. Redistribution of water molecules in glycerol-bound protein

A key concept in glycerol stabilization of proteins is preferential hydration or preferential inclusion of water molecules at the cost of preferential exclusion of glycerol from the protein surface. Preferential exclusion means deficiency of glycerol on the protein surface relative to its concentration in the bulk solvent. By corollary, water is preferentially included on the protein surface, which should increase the density of water that is already denser by ~15% than the bulk water.⁷⁶

There has been confusion in the past concerning the interpretation of results obtained by using the Wyman relation (equation 6), whether the slope $\Delta \xi_1$ truly reflects the change in the water of hydration during a reaction. The equilibrium constant K_B for protein-glycerol interaction which leads to the native \rightleftharpoons quasi-native reaction ($N_w \rightleftharpoons D_{gly}$) is essentially an exchange equilibrium constant $K_B = K_{ex} = K_{gly}/K_W$, where K_{gly} and K_w are hypothetical equilibrium constants for the binding of glycerol and water, respectively, to vacant sites. The mutual inclusiveness of the two events leads to a redistribution of both glycerol and water on the protein surface, and this redistribution difference between the two states of the $N_w \rightleftharpoons D_{gly}$ equilibrium is obtained from equation 6. Because the number of glycerol molecules on the protein surface is far lower than the number of water molecules anywhere along the course of the reaction, we can neglect the redistribution of glycerol on the protein surface and retain the number of water molecules alone. Hence, $\Delta \xi_1$ in equation 6 represents the change in the effective number of water molecules across the $N_w \rightleftharpoons D_{gly}$ reaction.

What about myoglobin in water-glycerol? Of special interest is myoglobin whose dynamics and ligand binding properties in water-glycerol mixture have been reported vastly, and is still being studied to uncover the principles of protein motions and energy landscape. Recently, Hirai et al⁷⁰ used wide-angle x-ray and small-angle neutron scattering to study glycerol-induced solvation and thermal stability of myoglobin with reference to its structure content. Both cytochrome c and myoglobin are heme proteins, but the native state of the latter already has eight helices. The results of Hirai et al appear to indicate higher α -helical content in the presence of glycerol, consistent with the finding with cytochrome c here. The authors also implicate glycerol stabilization of tertiary structure of myoglobin in contrast with the expansion of cytochrome c reported here. Myoglobin should be studied with probes specific to the heme, and secondary and tertiary structures for a better understanding of glycerol effect. But it is our conviction that the heme iron of myoglobin will also be reduced by low concentration of glycerol to produce deoxymyoglobin, whose structure and conformation will be altered at high glycerol.

3.5. Conclusion and prospect

Glycerol elicits considerable conformational changes in proteins contrary to earlier belief. The protein is reversibly transformed to a quasi-native state of higher α -helical content, and the quasi-native state can be more compact or expanded than the native state in a protein specific manner. The conformational changes are ultrafast leaving only about 5% observable in the millisecond time bin. These observations have direct relevance to the use of glycerol as a cryoprotectant in storage and a medium of higher bulk viscosity for studies of protein reactions. In both applications the resultant protein conformation is extensively different from the native conformation. In both applications the resultant protein conformation is extensively different from the native conformation. Consequently, reactions rates, 67 ligand binding and relaxation properties, $^{2-9,80}$ and physical and chemical characteristics of proteins, myoglobin in particular, studied in glycerol are those of quasi-native states rather than the native state.

3.6. References

- 1. Bohon, R. L.; Conway, W. T. DTA studies on the glycerol-water system. *Thermochimica Acta.* **1972**, *4*, 321–341.
- 2. Austin, R. H.; Beeson, K. W.; Eisenstein, L.; Frauenfelder, H.; Gunsalus, I. C. Dynamics of ligand binding to myoglobin. *Biochemistry*. **1975**, *14*, 5355–5373.
- 3. Caliskan, G.; Kisliuk, A.; Tsai, A. M.; Soles, C. L.; Sokolov, A. P. Protein dynamics in viscous solvents. *J. Chem. Phys.* **2003**, *118*, 4230–4236.
- 4. Agmon, N. Coupling of protein relaxation to ligand binding and migration in myoglobin. *Biophys. J.* **2004**, *87*, 1537–1543.
- 5. Caliskan, G.; Mechtani, D.; Roh, J. H.; Kisliuk, A.; Sokolov, A. P.; Azzam, S.; Cicerone, M. T.; Lin-Gibson, S.; Peral, I. Protein and solvent dynamics: how strongly are they coupled. *J. Chem. Phys.* **2004**, *121*, 1978–1983.

- 6. Dirama, T. E.; Carri, G. A.; Sokolov, A. P. Coupling between lysozyme an glycerol dynamics: microscopic insights from molecular-dynamics simulations. *J. Chem. Phys.* **2005**, *122*, 244910.
- 7. Jansson, H.; Bergman, R.; Swenson, J. Role of solvent for the dynamics and the glass transition of proteins. *J. Phys. Chem. B.* **2011**, *115*, 4099–4109.
- 8. Ronsin, O.; Caroli, C.; Baumberger, T. Preferential hydration fully controls the renaturation dynamics in water–glycerol sovents. *Eur. Phys. J. E.* **2017**, *40*, 55.
- 9. Librizzi, F.; Carrotta, R.; Peters, J.; Cupane, A. The effects of pressure on the energy landscape of proteins. *Sci. Rep.* **2018**, *8*, 2037.
- De Rocha, M.; Loiko, M. R.; Gautério, G. V.; Tondo, E. C.; Prentice, C. Influence of heating, protein and glycerol concentrations of film-forming solution on the film properties of Argentine anchovy (*Engraulis anchoita*) protein isolate. J. *Food Engg.* 2013, 116, 666–673.
- Jarabak, J.; Seeds, A. E.; Talalay, P. Reversible cold inactivation of a 17β-hydroxysteroid dehydrogenase of human placenta: protective effect of glycerol.
 Biochemistry. 1966, 5, 1269–1279.
- 12. Ruwart, M. J.; Suelter, C. H. Activation of yeast pyruvate kinase by natural and artificial cryoprotectants. *J. Biol. Chem.* **1971**, *246*, 5990–5993.
- 13. Bradbury, S. L.; Jakoby, W. B. Glycerol as an enzyme-stabilizing agent: effect of aldehyde dehydrogenase. *Proc. Natl. Acad. Sci.* USA. **1972**, *69*, 2373–2376.
- 14. Myers, J. S.; Jakoby, W. B. Glycerol as an agent eliciting small conformational changes in alcohol dehydrogenase. *J. Biol. Chem.* **1975**, *250*, 3785–3789.
- 15. Gekko, K.; Timasheff, S. N. Mechanism of protein stabilization by glycerol: preferential hydration in gluycerol-water mixtures. *Biochemistry*. **1981**, *20*, 4667–4676.
- 16. Gekko, K.; Timasheff, S. N. Thermodynamics and kinetic examination of protein stabilization by glycerol. *Biochemistry*. **1981**, *20*, 4677–4686.

- 17. Xie, X.; Timasheff, S. N. Temperature dependence of the preferential interactions of ribonuclease A in aqueous co-solvent systems: thermodynamic analysis. *Protein Sci.* **1997**, *6*, 222–232.
- 18. Yancey, P. H. Organic osmolytes as compatible metabolic and counteracting cryoprotectants in high osmolarity and other stresses. *J. Exp. Biol.* **2005**, 208, 2819–2830.
- Dashnau, J. L.; Nucci, N. V.; Sharp, K. A.; Vanderkooi, J. M. Hydrogen bonding and the cryoprotective properties of glycerol/water mixtures. *J. Phys. Chem. B.* 2006, 110, 13670–13677.
- 20. Street, T. O.; Bolen, D. W.; Rose, G. D. A molecular mechanism for osmolyte-induced protein stability. *Proc. Natl. Acad. Sci.* USA. **2006**, *103*, 13997–14002.
- 21. Feng, S.; Yan, Y.–B. Effects of glycerol on the compaction and stability of the wild type and mutated rabbit muscle creatine kinase. *Proteins*. **2008**, *71*, 844–854.
- 22. Vegenende, V.; Yap, M. G. S.; Trout, B. L. Mechanism of protein stabilization and prevention of proein aggregation by glycerol. *Biochemistry*. **2009**, *48*, 11084–11096.
- 23. Weng, L. D.; Chen, C.; Zuo, J. G.; Li, W. Z. Molecular dynamics study of effects of temperature and concentration on hydrogen-bond abilities of ethylene glycol and glycerol: implications for cryopreservation. *J. Phys. Chem. A.* **2011**, *115*, 4729.
- Panuszko, A.; Bruździak, P.; Kaczkowska, E.; Stangret, J. General mechanism of osmolytes' influence on proein stability irrespective of the type of osmolyte cosolvent. *J. Phys. Chem. B.* 2016, 120, 1159–1169.
- 25. Sanfelice, D.; Temussi, P. A. Cold denaturation as a tool to measure protein stability. *Biophys. Chem.* 2016, 208, 4–8.
- 26. Pazhang, M.; Mehrnejad, F.; Pazhang, Y.; Falahati, H.; Chaparzadeh, N. Effect of sorbitol and glycerol on the stability of trypsin and difference between their stabilization effects in various solvents. *Biotechnol. Appl. Biochem.* **2016**, *63*, 206–213.

- 27. Farnum, M.; Zukoski, C. Effect of glycerol on the interactions and solubility of bovine pancreatic trypsin inhibitor. *Biophys. J.* **1999**, *76*, 2716–2726.
- 28. Van der Vegt, N. F. A.; Nayar, D. The hydrophobic effectand the role of cosolvents. *J. Phys. Chem. B.* **2017**, *121*, 9986–9998.
- 29. Mukherjee, M.; Mondal, J. Heterogeneous impacts of protein-stabilizing osmolytes on hydrophobic interactions. *J. Phys. Chem. B.* **2018**, *122*, 6922–6930.
- 30. Dubey, V.; Daschakraborty, S. Influence of glycerol on the cooling effect of pair hydrophobicity in water: relevance to proteins' stabilization at low temperature. *Phys. Chem. Chem. Phys.* **2019**, *21*, 800–812.
- 31. Santucci, R.; Polizio, F.; Desideri, A. Formation of a molten-globule-like state of cytochrome *c* induced by high concentrations of glycerol. *Biochimie*. **1991**, *81*, 745–751.
- 32. Bongiovanni, C.; Sinibaldi, F.; Ferri, T.; Santucci, R. Glycerol-induced formation of the moleten globule from acid-denatured cytochrome *c*: implication for hierarchical folding. *J. Protein Chem.* **2002**, *21*, 35–41.
- 33. Chen, X.; Bhandari, B.; Zhou, P. Insight into the effect of glycerol on stability of globular proteins in high protein model system. *Food Chem.* **2019**, 278, 780–785.
- 34. Bonincontro, A.; Risuleo, G. Dielectric spectroscopy as a probe for the investigation of conformational properties of proteins. *Spectrochim. Acta A.* **2003**, *59*, 2677–284.
- 35. Scharnagl, C.; Reif, M.; Friedrich, J. Stability of proteins: Temperature, pressure and the role of the solvent. *Biochim. Biophys. Acta.* **2005**, *1749*, 187–213.
- 36. Sreerama, N.; Woody, R. W. Computations and analysis of protein circular dichroism spectra. *Methods Enzymol.* **2004**, *383*, 318–351.
- 37. Wu, L–z.; Ma, B–l.; Sheng, Y–b.; Wang, W. Equilibrium and kinetic analysis on the folding of hen egg lysozyme in the aqueous-glycerol solution. *J. Mol. Struct.* **2008**, 891, 167–172.

- 38. Esquembre, R.; Sanz, J. M.; Wall, J. G.; del Monte, F.; Maeto, C. R.; Ferrer, M. L. Thermal unfolding and refolding of lysozyme in deep eutectic solvents and their aqueous dilutions. *Phys. Chem. Chem. Phys.* **2013**, *15*, 11248–11256.
- 39. Hahn, D. K.; Callis, P. R. Lowest triplet state of indole: an ab initio study. *J. Phys. Chem. A.* **1997**, *101*, 2686–2691.
- 40. Rao, M. T.; Bhuyan, A. K.; Venu, K.; Sastry, V. S. S. Nonlinear effect of GdnHCl on hydration dynamics of proteins: a ¹H magnetic relaxation dispersion study. *J. Phys. Chem. B.* 2009, *113*, 6994–7002.
- 41. Knubovets, T.; Osterhout, J. J.; Connolly, P. J.; Klibanov, A. M. Structure, thermostability, and conformational flexibility of hen egg-white lysozyme dissolved in glycerol. *Proc. Natl. Acad. Sci.* USA **1999**, *96*, 1262–1267.
- 42. Urry, D. W. Protein-heme interactions in heme proteins: cytochrome *c. Proc. Natl. Acad. Sci.* USA 1965, *54*, 640–648.
- 43. Marden, M. C.; Bon Hoa, G. H.; Stetzkowski-Marden, F. Heme protein fluorescence vs. pressure. *Biophys. J.* **1986**, *49*, 619–627.
- 44. Bhuyan, A. K.; Udgaonkar, J. B. Folding of horse cytochrome c in the reduced state. *J. Mol. Biol.* **2001**, *312*, 1135–1160.
- 45. Urry, D. W. The heme chromophore in the ultraviolet. *J. Biol. Chem.* **1967**, 242 4441–4448.
- 46. Blauer, G.; Sreerama, N.; Woody, R. W. Optical activity of hemoproteins in the Soret region. Cicular dichroism of the heme undecapeptide of cytochrome *c* in aqueous solution. *Biochemistry*. **1993**, *32*, 6674–6679.
- 47. Díaz-Álvarez, A. E.; Cadierno, V. Glycerol: a promising green solvent and reducing agent for metal-catalyzed transfer hydrogenation reactions and nanoparticles formation. *Appl. Sci.* **2013**, *3*, 55–69.

- 48. Kumar, R.; Bhuyan, A. K. Two-state folding of horse ferrocytochrome *c*: analyses of linear free energy relationship, chevron curvature, and stopped-flow burst relaxation kinetics. *Biochemistry*. **2005**, *44*, 3024–3033.
- 49. Gouterman, M. Study of the effects of substitution on the absorption spectra of porphin. *J. Chem. Phys.* **1959**, *30*, 1139–1161.
- 50. Altieri, A. S.; Hinton, D. P.; Byrd, R. A. Association of biomolecular systems via pulsed field gradient NMR self-diffusion measurements. *J. Am. Chem. Soc.* **1995**, *117*, 7566–7567.
- 51. Mohoberac, B. B.; Brill, A. S. Association of alcohols with heme proteins: optical analysis and thermodynamic models. *Biochemistry*. **1980**, *19*, 5157–5167.
- 52. Sashi, P.; Ramakrishna, D.; Bhuyan, A. K. Dispersion forces and the molecular origin of internal friction in protein. *Biochemistry*. **2016**, *55*, 4595–4602.
- 53. Schellman, J. A. The relation between the free energy of interaction and binding. *Biophys. Chem.* **1993**, *45*, 273–279.
- 54. Wyman, J. Linked functions and reciprocal effect in hemoglobin: a second look. *Adv. Protein Chem.* **1964**, *19*, 223–286.
- 55. Schellman, J. A. Selective binding and solvent denaturation. *Biopolymers*. **1987**, *26*, 549–559.
- Timasheff, S. N. Protein-solvent preferential interactions, protein hydration, and modulation of biochemical reactions by solvent components. *Proc. Natl. Acad. Sci.* USA 2002, 99, 9721–9726.
- 57. Huda, N.; Hossain, M.; Bhuyan, A. K., Complete observation of all structural, conformational, and fibrillation transitions of monomeric globular proteins at submicellar sodium dodecyl sulfate concentrations. *Biopolymers*. (2019). DOI:10.1002/bip.23255.

- 58. Facchiano, A. M.; Colonna, G.; Rogone, R. Helix stabilizing factors and stabilization of thermophilic proteins: an X-ray based study. *Protein Engg.* **1998**, *11*, 753–760.
- 59. Yakimov, A. P.; Afanuseva, A. S.; Khodorkovskiy, M. A.; Petukhov, M. G. Design of stable α-helical peptides and thermostable proteins in biotechnology and biomedicine. *Acta Nature*. **2016**, *8*, 70–81.
- 60. Chan, H. S.; Dill, K. A. Compact polymers. Macromolecules. **1989**, 22, 4559–4573.
- 61. Chan, H. S.; Dill, K. A. Origins of structure in globular proteins. *Proc. Natl. Acad. Sci.* USA **1990**, 87, 6388–6392.
- 62. De sanctis, G.; Maranesi, A.; Ferri, T.; Poscia, A.; Ascoli, F.; Santucci, R. Influence of glycerol on the structur and redox properties of horse heart cytochrome *c*, A circular dichroism and electrochemical study. *J. Protein Chem.* **1996**, *15*, 599–606.
- 63. Shastry, M. C. R.; Roder, H. Evidence for barrier-limited protein folding kinetics on the microsecond time scale. *Nature Struct. Biol.* **1998**, *5*, 385–392.
- 64. Kumar, R.; Prabhu, N. P.; Bhuyan, A. K. Ultrfast events in the folding of ferrocytochrome *c. Biochemistry*. **2005**, *44*, 9359–9367.
- 65. Munoz, V.; Cerminara, M. When fast is better: protein folding fundamentals and mechanisms from ultrafast approaches. *Biochem. J.* 2016, 473, 2545–2559.
- 66. Tanford, C. Protein denaturation. Adv. Protein Chem. 1968, 23, 121–282.
- 67. Sashi, P.; Bhuyan, A. K. Viscosity dependence of some protein and enzyme reaction rates: seventy-five years after Kramers. *Biochemistry*. **2015**, *54*, 4453–4461.
- 68. Bhuyan, A. K. Protein stabilization by urea and guanidine hydrochloride. *Biochemistry* **2002**, *41*, 13386–13394.

- 69. Bennion, B. J.; Daggett, V. Counteraction of urea-induced protein denaturation by trimethylamine N-oxide: a chemical chaperone at atomic resolution. *Proc. Natl. Acad. Sci.* USA **2004**, *101*, 6433–6438.
- 70. Hirai, M.; Ajito, S.; Sugiyama, M.; Iwase, H.; Takata, S–I.; Shimizu, N.; Igarashi, N.; Martel, A.; Porcar, L. Direct evidence for the effect of glycerol on protein hydration and thermal structural transition. *Biophys. J.* **2018**, *115*, 313–327.
- 71. Sedgwick, H.; Cameron, J. E.; Poon, W. C. K.; Egelhaff, S. U. Protein phase behavior and crystallization: effect of glycerol. *J. Chem. Phys.* **2007**, *127*, 125102.
- 72. Li, L.; Li, C.; Zhang, Z.; Alexov, E. On the dielectric "constant" of proteins: smooth dielectric function for macromoleular modeling and its implementation in DelPhi. J. Chem. *Theory Comput.* **2013**, *9*, 2126–2136.
- 73. Qu, Y.; Bolen, C. L.; Bolen, D. W. Osmolyte-driven contraction of a random coil protein. *Proc. Natl. Acad. Sci.* USA **1998**, *95*, 9268–9273.
- 74. Toal, S.; Amidi, O.; Schweitzer-Stenner, R. Conformational changes of trialanine induced by direct interactions between alanine residues and alcohols in binary mixtures of water with glycerol and ethanol. *J. Am. Chem. Soc.* **2011**, *133*, 12728–12739.
- 75. Sashi, P.; Yasin, U. M.; Bhuyan, A. K. Unfolding action of alcohols on a highly negatively charged state of cytochrome *c. Biochemistry*. **2012**, 51, 3273–3283.
- 76. Makarov, V.; Pettit, B. M.; Feig, B. M. Solvation and hydration of proteins and nucleic acids: a theoretical view of simulation and experiment. Acc. *Chem. Res.* **2002**, *35*, 376–384.
- 77. Colombo, M. F.; Rau, D. C.; Parsegian, V. A. Protein salvation in allosteric regulation: a water effect on hemoglobin. *Science*. **1992**, *256*, 655–659.
- 78. Courtenay, E. S.; Capp, M. W.; Anderson, C. F.; Record, M. T. Vapor pressure osmometry studies of osmolyte-protein interactions: implications for the action of

- osmoprotectants in vivo and for the interaction of "osmotic stress" experiments in vitro. *Biochemistry.* **2000**, *39*, 4455–4471.
- 79. Schellman, J. A. The thermodynamic stability of proteins. *Annu. Rev. Biophys. Biophys. Chem.* **1987**, *16*, 115–137.
- Frauenfelder, H.; Chen, G.; Berendzen, J.; Fenimore, P. N.; Jansson, H.; McMahon, B. H.; Stroe, I. R.; Swenson, J.; Young, R. D. A unified model of protein dynamics. *Proc. Natl. Acad. Sci.* USA 2009, 106, 5129–5134.

Glycerol-slaved volume fluctuation and NMR cross-relaxations in lysozyme

Abstract

Adiabatic compressibility, volume fluctuation, and ${}^{1}\text{H}{}^{-1}\text{H}$ nuclear cross-relaxation in lysozyme have been measured in variable glycerol viscosity to study self-diffusion, isotropic rigid-body rotational tumbling, and intramolecular motion at 298 K, pH 3.8. Compressibility and volume fluctuation as well as dynamics of lateral and rotational diffusions, and intramolecular cross-relaxation rates all show fractional viscosity dependence with a power law exponent κ in the 0.1–0.81 range. The diffusion coefficient D of glycerol itself is non-Stokesian with friction, having a fractional viscosity dependence on the medium viscosity ($D \sim \eta^{-\kappa}$, $\kappa \approx 0.61$). The concurrence and close similarity of the fractional viscosity dependence of glycerol diffusion on the one hand, and diffusion and intramolecular cross-relaxation rates of the protein on the other logically leads to infer that solvent relaxations and protein processes are coupled. The coupling leads to slaving of at least some of the protein motions by Debye relaxation of glycerol. The coupling also explains why an overwhelmingly large body of rate vs glycerol viscosity data shows overdamped Kramers behavior.

4.1. Introduction

The structural dynamics involving lateral self-diffusion and isotropic rotational tumbling of proteins in continuous interaction with the solvent can be described and quantified by the well-known principles of Brownian theory and energy dissipation. These overall diffusion motions can be measured by several methods, including dynamic light scattering, hydrodynamics, field-gradient NMR, and spin relaxation. But the area of internal dynamics is hazy, because several

hundreds of atoms in the congress can move individually or in groups of different sizes in $\sim 10^7 - 10^{13}$ Hz range of frequencies with distance amplitudes covering from ~ 0.4 to several angstroms. Time-averaged isotropic atomic displacements can be quantified by determining the Debye-Waller factor ($B = 8\pi^2 \langle x^2 \rangle$, where $\langle x^2 \rangle$ is mean square displacement, MSD) encoded in the X-ray scattering from each atom, ¹ but efforts are needed to measure collective motions where atom groups of variable size move in unison, each group having its own frequency and amplitude. For example, collective flipping of all hydrogens in an aromatic ring rotation or the rotation of a methyl group can be measured. ²⁻⁶ Collective motions involving atoms in sub-global dynamics and helical dynamics have also been observed by pump-probe laser spectroscopy and X-ray scattering in sub nanosecond regimes. ⁷⁻¹²

Some of the collective modes of motion, each of which can recruit a group of both bonded and non-bonded atoms are generally preserved, and they are thought to be functionally important. The other much larger group of collective motion is represented by the normal modes of vibrations of bonded atoms. A protein the size of lysozyme with ~1950 atoms has ~5844 vibrational modes, of which only a few, perhaps one or two, low-frequency (~1 cm⁻¹ ~3×10¹⁰ Hz) modes represent in-phase fluctuation of nearly all atoms in the molecule so as to produce small volume fluctuation necessary for maintenance of the native state. Modes with higher vibrational frequency are increasingly excited as the protein is increasingly denatured, producing larger volume fluctuations. All normal modes are thus not necessary, nor excited, for structure and stability of the native protein.

The above is only a précis with fewer citations from the vast area of protein dynamics that offers a myriad of questions and concerns to be addressed. Thermodynamics requires that the protein be hydrated, but how does the water of hydration control protein motions? For that matter, how do bulk solvent relaxations take control of local and collective motions in the protein interior? How effectively the internal fluctuations dissipate energy? What mechanism can explain the non-Stokesian performance of protein motions, self-diffusion, and rotational tumbling correlation in particular? Clearly, answers to such queries are sought not only as a part of academic pursuit, but also to prescribe conditions for stability and optimal functioning of proteins and enzymes.

To this end, we carried out a series of experiments to measure sound velocity in lysozyme and $^{1}\text{H}-^{1}\text{H}$ nuclear cross-relaxation rates by 2D-NOESY, both in glycerol-containing aqueous solvent. The sound velocity measurements provide values of the thermodynamic properties adiabatic compressibility and volume fluctuation, and the cross-relaxation rates provide information of intramolecular dynamics. The rationale of employing the water-glycerol mixture was to generate macroscopic viscosity so as to increase the protein tumbling correlation time, which displaces the time window for the observation of internal dynamics. The varying solvent viscosity also provides an opportunity to reexamine the extent to which solvent friction damps the motions, i.e., a reevaluation of Kramers stipulate. The use of glycerol as a viscogen in our experiments was also prompted by the relatively recent idea that Debye relaxations of glycerol can dictate motions and folding of proteins. The learly, many unknowns about how glycerol affects the thermodynamic stability, folding, fluctuations, and internal friction of proteins need to be explored.

4.2. Experimental section

Samples of 3 mM Lysozyme in D_2O were made in different concentrations of glycerol ranging from 0 to 40% (w/v). The pH of all samples was held at 3.8 by the use of minimal volume of HCl. Homonuclear 1H transient 2D NOE spectra of each sample was recorded at 298 K with mixing times 0.05, 0.09, 0.125, 0.150, 0.180, 0.210, 0.250, 0.300, 0.400 and 0.550 ms in a 500 MHz Bruker spectrometer. The spectra were processed and analyzed using Topspin. Further analyses were carried out with graphing softwares and codes written for the purpose. Solution density and velocity of sound wave (~4.8 MHz) were measured on aqueous samples of 15 μ M lysozyme prepared in different concentrations of glycerol ranging from (0 to 50% w/v). The pH of all solutions was 3.8, and the measurements were carried out at 298 K using a vibrating tube densitometer (DSA-5000M, Anton paar).

4.3. Results and Discussion

4.3.1. Compressibility of lysozyme in water-glycerol mixture

Since internal dynamics of macromolecules can be described to an extent by measuring bulk quantities such as hydrodynamics, compressibility, packing density, and elasticity coefficient of compression by pressure or viscosity, we first looked at the compressibility of lysozyme in the water-protein-glycerol system with the expectation that preferential exclusion of glycerol from the protein surface and hence its hydration will force it to adopt a more compact and ordered state. Sound velocity measurements on lysozyme samples in variable glycerol were carried out using a vibrating tube density meter at 293 K. The adiabatic compressibility of the solution and the solvent, β_s and β_o , respectively, are calculated from sound velocity (u) and density (ρ) by the Laplace formula $\beta = 1/\rho u^2$, and the adiabatic compressibility coefficient of the protein, β_p , is obtained from the difference of β_s and β_o . The β_p values are finally corrected for the compressibility of the protein-hydrating water (18×10⁻¹²cm² dyne⁻¹), which is nearly equal to the compressibility of ice. 20,21 As the details of the procedure and assumptions adopted for these calculations are found in several earlier studies on protein compressibility, 4,21-25 we avoid reproducing them here. The calculated values of $\beta_{\rm s}$, $\beta_{\rm o}$, and $\beta_{\rm p}$ in the 0–50% (w/v) range of glycerol are shown in Figure 4.1, where the difference of β_s and β_o dispenses with the compressional relaxation time of liquid glycerol and the mutually inclusive effect on the water structure, yielding adiabatic compressibility of the protein $\beta_{\rm p}$ alone.

The compressibility of lysozyme across the 0–50% range of glycerol decreases by ~1.3-fold (Figure 4.1c), suggesting a constraining effect of glycerol on the amplitudes of atom density fluctuations in the protein interior. The compressibility with glycerol presumably follows a power law dependence

$$\beta_{\rm p} = \frac{c}{\eta^{\kappa}} \tag{1}$$

with η being the solvent viscosity given in centipoise here. The value of the power law exponent ($\kappa \approx 0.15$) obtained from the fit (Figure 4.1c) indicates fractional solvent viscosity dependence of β_p . It is predominantly the effect of the bulk macroscopic viscosity which acts to diminish the

amplitudes of both large-scale conformational motions and individual vibrational fluctuation of atoms and their collective motions in the protein interior. Since collective motions involve large-amplitude fluctuations of a group of atoms in unison,²⁶ the bulk viscosity not only reduces the fluctuation amplitudes but also degrades the normal modes of vibrations causing the associated frequency spectrum to shift.¹⁵

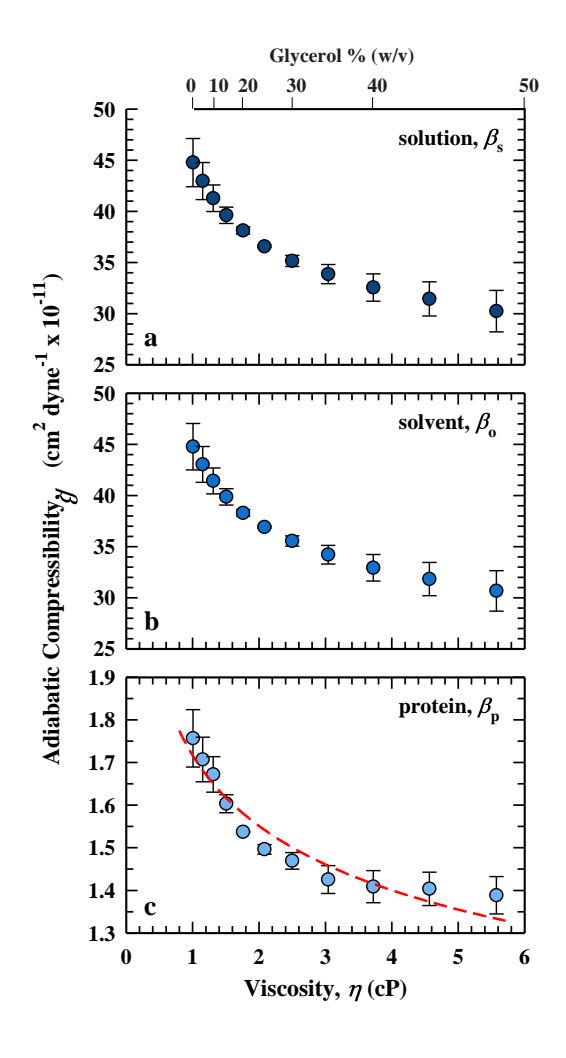


Figure 4.1. Adiabatic compressibility of water-protein-glycerol solution, β_s (a), water-glycerol solvent mixture, β_o (b), and the hydrated protein, β_p (c) with glycerol viscosity at 298 K, pH 3.8. Note: cm²dyne⁻¹=1 Pa⁻¹.

4.3.2. Root mean square volume fluctuation.

One of the utilities of adiabatic compressibility is to determine the volume fluctuation of a protein molecule by the rigorous thermodynamic relation ^{21,25,27}

$$\langle \delta V^2 \rangle = k_{\rm B} T V_{\rm M} \beta_{\rm T} \tag{2}$$

in which $\langle \delta V^2 \rangle$ is mean square volume fluctuation and $\beta_{\rm T}$ is isothermal bulk compressibility, which can be substituted with β_p when the volume coefficient of thermal expansion is far smaller than the heat capacity of the protein. This being the case in general, 21 we take $\beta_T \approx \beta_D$ in the relation above. The quantity $V_{\rm M}$, the intrinsic volume of a protein molecule is obtained from the sum of van der Waals volume of all protein atoms and the intramolecular void volumes; we find $V_{\rm M} \sim 1.8 \times 10^{-20} {\rm cm}^3$ for lysozyme by an approximate evaluation. The root mean square volume fluctuation ($\delta V_{\rm RMS} = \sqrt{\langle \delta V^2 \rangle}$) of lysozyme decreases from 39.79 to 35.37 cc mol⁻¹ when the glycerol content in the protein solution increases from 0 to 50% (Figure 4.2). This decrease also has a power law dependence on the solvent viscosity, $\kappa = 0.1$. A caveat in the determination of $\delta V_{\rm RMS}$ under variable solvent properties arises from the use of the same numerical value of the intrinsic volume of the protein molecule under all solvent conditions. If intramolecular void spaces in the protein change with the solvent glycerol, the value of $V_{\rm M}$ is also expected to change to an extent; we assume that $V_{\rm M}$ will change only marginally. The 1.13-fold change in $\delta V_{\rm RMS}$ observed here may appear only as a minor decrease in the volume of the protein in 50% glycerol; the hydrodynamic radius, however, decreases from ~22 to 15 Å. Since $\delta V_{\rm RMS}$ arises from the sum of all small-amplitude rapid internal fluctuations of varying frequencies, the decreasing $\delta V_{\rm RMS}$ with glycerol indicates reduced amplitude of all such motions to bring about constraints in the internal dynamics. It is noted that glycerol does not penetrate into the protein interior, but exerts its effect by its exclusion from the protein surface, leading to preferential hydration of the protein.^{29–31}

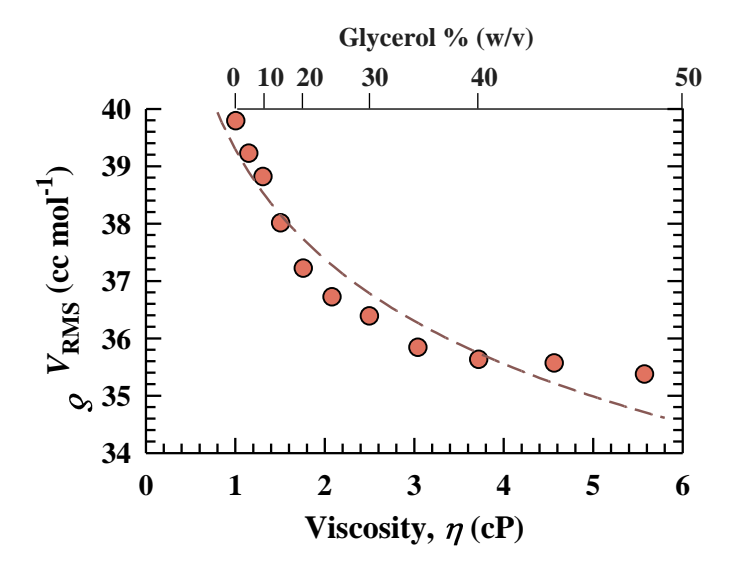


Figure 4.2. Glycerol viscosity dependence of root-mean-square volume fluctuation of lysozyme, 298 K, pH 3.8.

4.3.3. ¹H cross-relaxation rates in lysozyme in water-glycerol mixture

A convenient approach to analyze the glycerol-induced restrictions of internal motions is the measurement of nuclear cross-relaxations in water-glycerol solvent. The rationale is based on the fact that intramolecular motions significantly influence nuclear cross-relaxation rates. ^{32,33} For each level of glycerol in the lysozyme solution, transient NOESY spectra were obtained with different mixing times (τ_m) set in the 50–550 ms range. The $^1H^{N_-1}H^{\beta}$ region of a set of spectra obtained in 10% glycerol (Figure 4.3) shows increasing cross peak intensity with τ_m as NOE builds up, but decreases at longer τ_m due to auto-relaxation of the spins. Since the rotational tumbling time (or correlation time, τ_c) for the size of lysozyme dissolved in the viscous medium is sufficiently long, the slow-motion or spin diffusion limit ($\tau_c \omega_o \gg 1$, where $\omega_o = 5 \times 10^8$ Hz for the present) of time scale is assured. Accordingly, one expects the cross-peaks to be strong and positive as seen in the spectra.

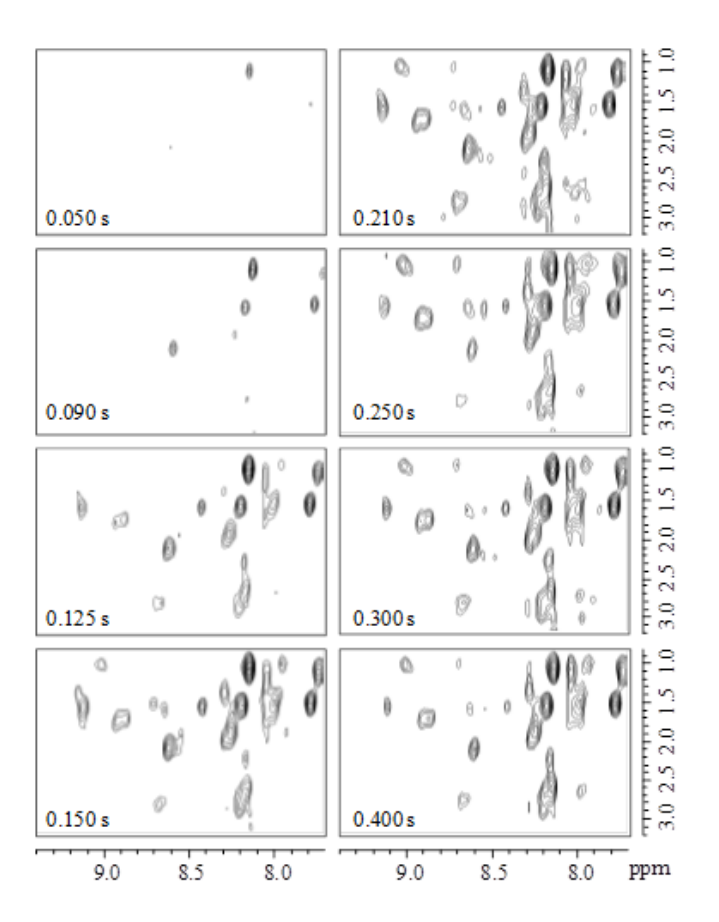


Figure 4.3. The ${}^{1}H^{N}_{-}{}^{1}H^{\beta}$ region of NOESY spectra of 1 mM lysozyme in 10% (w/v) glycerol, 298 K, pH 3.8 using the indicated mixing times.

To obtain the cross relaxation rate σ_{kl} we use the initial rate approximation

$$I_{kl} \approx \sigma_{kl} \tau_{\rm m}$$
 (3)

where I_{kl} is the relative intensity of the cross peak arising from spins k and l with shorter mixing times $\tau_{\rm m}$. The I_{kl} vs $\tau_{\rm m}$ plots each with variable glycerol

are provided in Figure 4.4 along with the assignments of the cross-relaxing nuclei depicted in Table 1. The decrease in σ_{kl} with glycerol for each of these cross-relaxing pairs shows a fractional solvent viscosity dependence with the power law coefficient $\kappa = 0.58$ (Figure 4.5), suggesting that the internal friction is not the dominant reason.

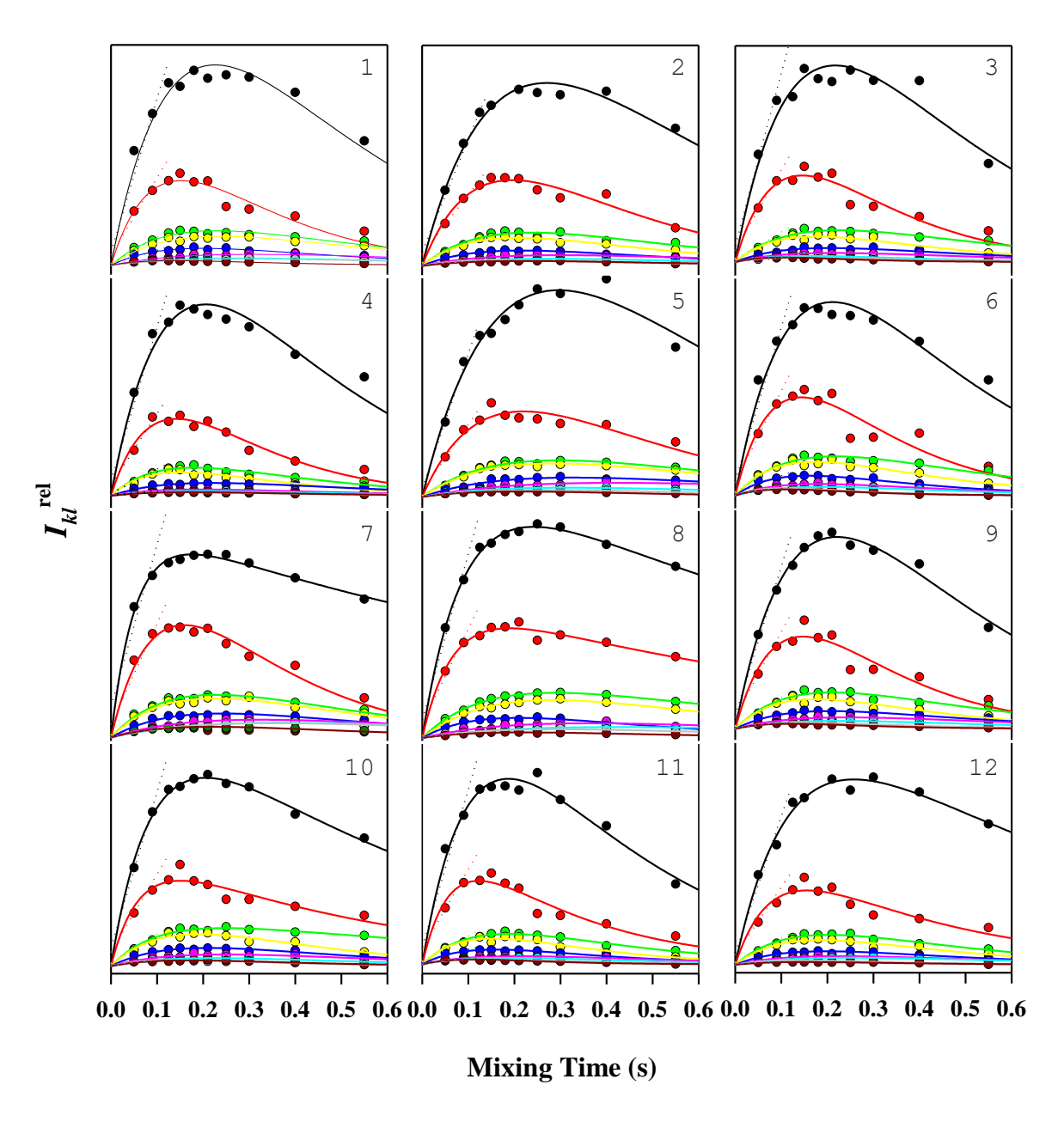


Figure 4.4 The $\tau_{\rm m}$ dependence of cross peak intensities. Assignments of the peaks indicated by 1 to 12 are given in Table 1.

Cross-peak	Assignment	
1	M12 (NH)	K13 ($C^{\beta}H$)
2	unassigned	
3	W28 (N1H)	$Y23 (C^{\beta}H)$
4	R112 (NH)	W108 ($C^{\beta}H$)
5	S24 (NH)	Y23 ($C^{\beta}H$)
6	G26 (NH)	$C30 (C^{\beta}H)$
7	I78 (NH)	C64 ($C^{\alpha}H$)
8	N65 (NH)	C64 ($C^{\alpha}H$)
9	D66 (NH)	S60 ($C^{\alpha}H$)
10	T51 (NH)	S60 ($C^{\alpha}H$)
11	W63 (N1H)	W63 ($C^{\alpha}H$)
12	V2 (NH)	N39 ($C^{\alpha}H$)

Table 1. Assignment of cross-relaxing nuclei

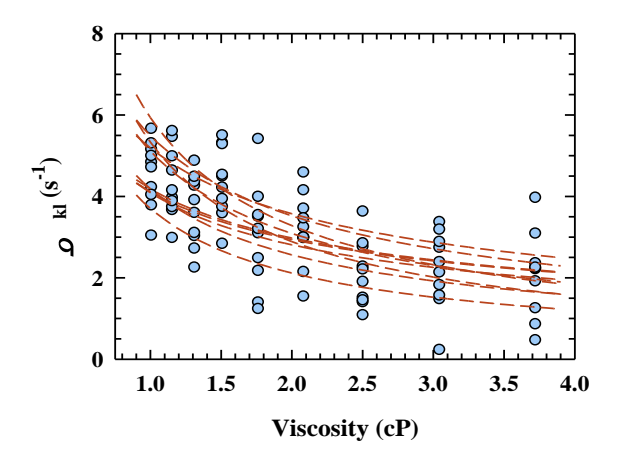


Figure 4.5. Fractional viscosity dependence of σ_{kl} shown for 10 cross peaks without labeling; the assignments are given in Supplementary Information (Table S1). The dashed lines represent a power law fit to $\sigma_{kl} = c/\eta^{\kappa}$ with κ varying from 0.49 to 0.81 for the 10 peaks.

4.3.4. Inter-nuclear distances of some cross-relaxing proton pairs

For further analysis, we briefly recall the basis of relating σ_{kl} to spatial distance between the spins k and l, r_{kl} . Cross relaxation within the energy eigenstates corresponding to the four product functions $|\alpha_k\alpha_l\rangle$, $|\alpha_k\beta_l\rangle$, $|\beta_k\alpha_l\rangle$, and $|\beta_k\beta_l\rangle$ can occur by zero-quantum ($|\alpha_k\beta_l\rangle \rightleftharpoons |\beta_k\alpha_l\rangle$) and double-quantum ($|\alpha_k\alpha_l\rangle \rightleftharpoons |\beta_k\beta_l\rangle$) transitions with the respective transition rates W_0 and W_2 given by

$$W_{\rm o} = \frac{1}{2} q_{kl} J_{kl} (\omega_{\rm ok} - \omega_{\rm ol})$$

$$W_2 = 3q_{kl}J_{kl}(\omega_{ok} + \omega_{ol}) \tag{4}$$

The magnetic dipolar coupling constant q_{kl} in these rate expressions can be evaluated by

$$q_{kl} = \left(\frac{\mu_0}{4\pi}\right)^2 \frac{1}{10} \gamma_k^2 \gamma_l^2 \hbar^2 \langle r_{kl}^{-6} \rangle \sim 75.468 \times 10^{-26} \langle r_{kl}^{-6} \rangle \text{ rad m}^3 \text{s}^{-1}$$
 (5)

where μ_0 is magnetic permeability of free space $(4\pi \times 10^{-7} \text{ T m A}^{-1})$. The numerical value of q_{kl} given above is valid when both k and l spins are ^1H . The reduced spectral density functions J_{kl} are

$$J_{kl}(\omega_{0k} - \omega_{0l}) = J(0) = 2\tau_{c}$$

$$J_{kl}(\omega_{0k} + \omega_{0l}) = J(2\omega_0) = \frac{2\tau_c}{1 + 4\omega^2 \tau_c^2}$$
(6)

Since the cross relaxation rate $\sigma_{kl} = (W_2 - W_0)$, eq 4–6 yield

$$\sigma_{kl} = 75.468 \times 10^{-26} \left[-\tau_{c} + \frac{6\tau_{c}}{1 + 4\omega_{0}^{2}\tau_{c}^{2}} \right] \left\langle \frac{1}{r_{kl}^{6}} \right\rangle \tag{7}$$

which formally relates σ_{kl} to r_{kl} for a rigid molecule.

The calculation of r_{kl} now requires the rotational correlation time τ_c of lysozyme in glycerol solutions that are obtained from earlier studies of the hydrodynamic radius R_H of the protein^{28,34,35} by the use of the Debye-Stokes-Einstein relation

$$\frac{1}{6\tau_{\rm c}} = \frac{k_{\rm B}T}{8\pi\eta R_{\rm H}^3} \tag{8}$$

The viscosity dependence of τ_c is described by the inverse power law relation

$$r_{kl}(\eta) = \frac{c}{n^{\kappa}} \tag{9}$$

with $\kappa = -0.81$ (Figure 4.6a), asserting on a fractional coupling of solvent viscosity with global tumbling. The distances between k and l for the 12 cross-relaxing kl proton pairs (Table 1) calculated by using these τ_c values are plotted in Figure 4.6b, showing an inverse power law dependence of r_{kl} on η with the exponent κ ranging from -0.20 to -0.29, meaning an increasing internuclear distance with fractional solvent viscosity dependence.

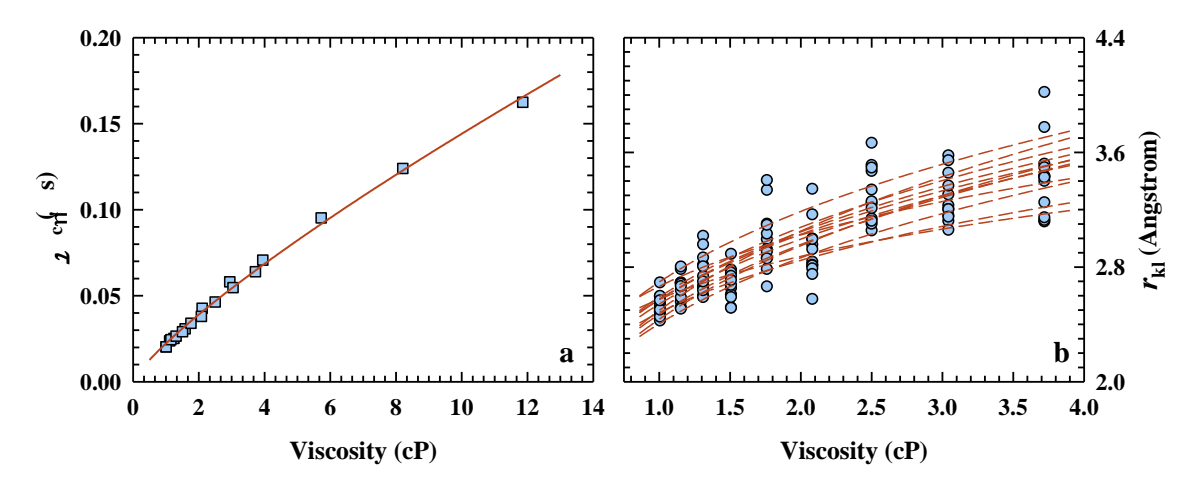


Figure 4.6. (a) Fractional viscosity dependence of the overall tumbling time τ_c with viscosity, described by the inverse power law exponent $\kappa = -0.81$. (b) Power law dependence of the increase in internuclear distance shown for 12 unlabeled cross peaks with solvent viscosity. The value of κ obtained from the 12 fits lie in the range -0.20 to -0.29.

4.3.5. Relative order parameter with viscosity

The above result that the solvent viscosity produces an increase of average inter-nuclear distance of the cross-relaxing proton pairs suggests an increase in intramolecular mobility, which appears contrary to that of the compressibility results that are interpreted to mean that solvent viscosity promotes constraints on the amplitudes of internal motion. Whether intramolecular mobility increases or not can be analyzed by factoring the overall correlation function for the kl pair of cross-relaxing nuclei into the global rotational correlation, $C_{kl}^{\text{global}}(t)$, and internal correlation functions $C_{kl}^{\text{internal}}(t)$

$$C_{kl}(t) = C^{\text{global}}(t)C_{kl}^{\text{internal}}(t)$$
(10)

which can be integrated to obtain

$$\frac{1}{\tau_{\text{total}}} = \frac{1}{\tau_c} + \frac{1}{\tau_{kl}} \tag{11}$$

The contribution of τ_{kl} to the cross-relaxation rate is, however, conditional. If the internal correlation time corresponding to the kl internuclear vector is sufficiently small ($\tau_{kl} \ll \tau_c$), the contribution of τ_{kl} will be considerable only when $C_{kl}^{internal}(t)$ decays within a finite time.³⁶ This is not always the case, especially for large molecules where global and local intramolecular motions are rarely correlated. The lack of a well-defined model of internal motion renders τ_{kl} not readily interpretable because it depends on both the frequency and amplitude of internal motion faster than τ_c . We assume that τ_{kl} contributes little to the cross-relaxation of the kl pair because of its smallness compared to τ_c by at least three-orders of magnitude. This assumption allows one to introduce a τ_c -based generalized order parameter S_{kl}^2 by

$$\sigma_{kl} = \langle r_{kl} \rangle^6 \langle r_{kl}^{-6} \rangle S_{kl}^2 \sigma_{kl}^{\text{ref}} \tag{12}$$

which relates the actual cross-relaxation rate constant σ_{kl} to a reference cross-relaxation rate constant σ_{kl}^{ref} of a relatively rigid state of the protein molecule with the average inter-nuclear distance $\langle r_{kl} \rangle$. Since the objective is to determine the dynamics of the protein in water-glycerol solutions relative to that in water alone, the cross-relaxation rate constant in the aqueous solution without glycerol can be taken as the reference.

The variation of the relative order parameter with viscosity is shown in Figure 4.7. The order parameter reflects the extent of spatial restriction of the kl internuclear vector; $S_{kl}^2 = 1$ for completely restricted mobility, and $S_{kl}^2 = 0$ for completely unrestricted motion. In Figure 4.7, $S_{kl}^2 = 1$ for all internuclear vectors specifying the cross-relaxing nuclei, because the motional order at various levels of glycerol viscosity is being scaled with reference to the viscosity of water. The S_{kl}^2 values greater than unity are outliers, arising from error in data. The inverse power law fit obtained by using the viscosity specific mean of S_{kl}^2 yields a power law exponent $\kappa = 0.58$, indicating fractional viscosity dependence of internal motion. It is this internal dynamic disorder that gives rise to an increasing r_{kl} with solvent viscosity.

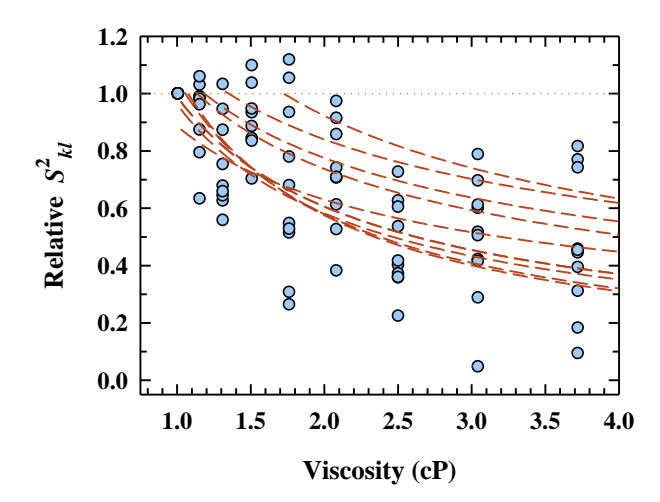


Figure 4.7. Fractional viscosity dependence of the generalized order parameter, relative to that in the absence of glycerol, characterizing the fluctuation of internuclear distance for ten r_{kl} vectors (labels not included). The value of the power law exponent κ in $\sigma_{kl} = c/\eta^{\kappa}$ obtained by fitting the data for 10 pairs of cross-relaxing nuclei (see Table 1) are in the 0.46–0.89 range. The data points exceeding unity are outliers.

It is also useful to look at the dependence of the cross relaxation rate constant on rotational tumbling correlation time τ_c and S_{kl}^2 . In Figure 4.8, the y-axis is generated by multiplying σ_{kl} with $\omega_0 q \langle 1/r_{kl}^6 \rangle^{-1}$, and the abscissa is the $\tau_c \omega_0$ scale. In this mode of plotting results, each $\tau_c \omega_0$ will have cross-relaxation rate constants from all assigned pairs of cross-relaxing nuclei. The fits according to equation 7 and 12 with those values of S_{kl}^2 that have been calculated above are also shown in Figure 4.8. The spread of the curves indicates the influence of S_{kl}^2 on the cross-relaxation rate. The tapering of the spread with larger values of τ_c of lysozyme, i.e., with higher solvent viscosity, indicates that the cross-relaxation rate tends to be independent of S_{kl}^2 as the tumbling correlation time increases. This result is a manifestation of the fact that the time scale of intramolecular mobility becomes insignificant with largeness of the tumbling time.

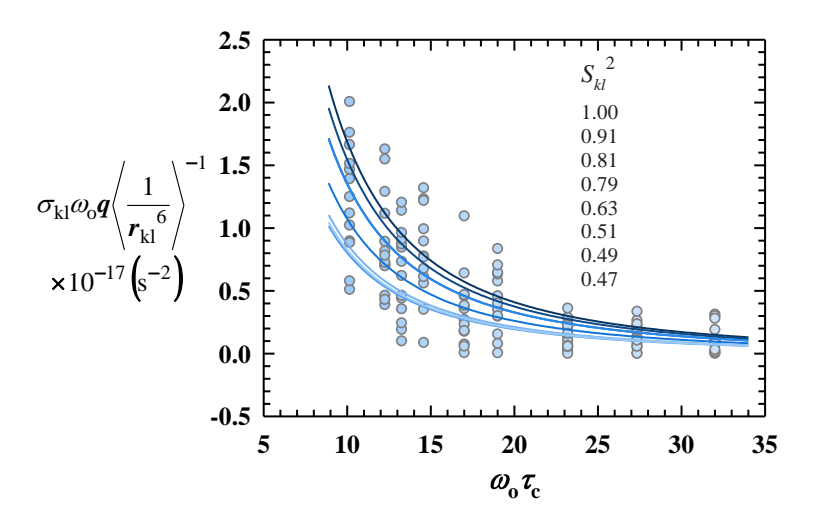


Figure 4.8. Effect of $\omega_0 \tau_c$ on dynamic σ_{kl} for the indicated values of S_{kl}^2 . The fits are not according to eq 12 to emphasize on the influence of fluctuation of the r_{kl} on cross-relaxation rate.

4.3.6. Fractional viscosity dependence of glycerol diffusion

Properties of individual components of a binary or a ternary mixture consisting of water:protein:effector, in which the effector component is glycerol here, often change in a mutually inclusive manner. The results above already establish the variation in protein properties with the level of glycerol. To find out the changes in hydrodynamic properties of water and glycerol in their binary mixture, we used pulsed-field gradient NMR measurements to calculate the self-diffusion coefficient of glycerol (D_S) with increasing level of glycerol at pH 3.5, 298 K (Figure 8). One finds the power law dependence of D_S on glycerol viscosity as well ($\kappa = 0.62$). We also read a dataset on glycerol concentration dependence of D_S from literature³⁷ to find the power law exponent ($\kappa = 0.66$), sufficiently consistent with that determined here (Figure 4.9, inset). Others (ref 38, for example) also quote a κ -value near ~0.7.

This result suggests a deviation of D_S of glycerol in ambient temperature from what Stokes-Einstein relation predicts. We dub this underdamped self-diffusion of glycerol 'diffusion heterogeneity', where 'heterogeneity' refers to isotropic spatial heterogeneity in the diffusion

with variable solution composition or changing pressure and temperature. The implication of diffusion heterogeneity of the water-glycerol mixture is that the dynamics of the solvent system enslaves the dynamic properties of the protein solute in the water-protein-glycerol system. This is the central result to explain the fractional viscosity dependence of protein dynamics.

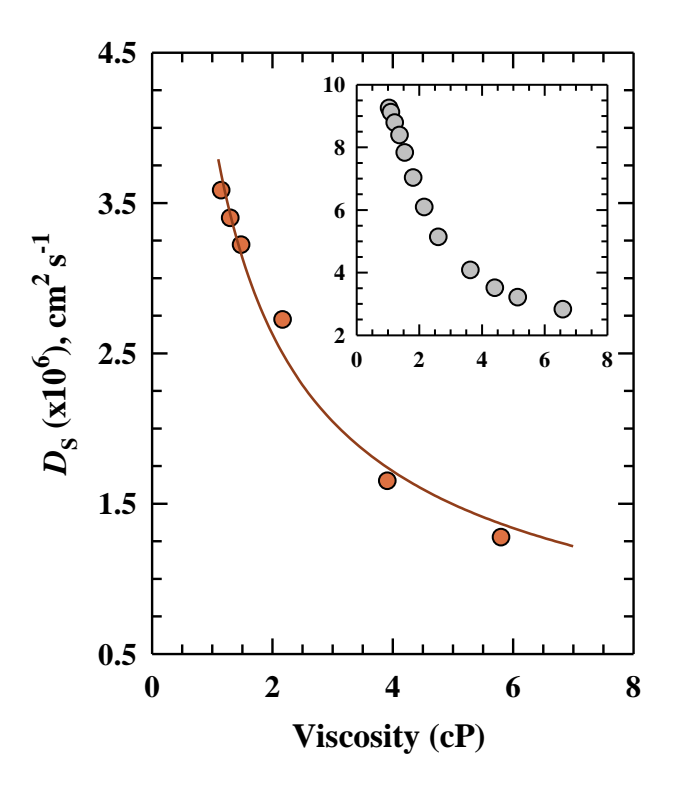


Figure 4.9. Self-diffusion coefficient of glycerol with solvent viscosity determined by NMR (plotted in hue). The fit yields $\kappa = 0.62$. *Inset*, fit of the data from Yasunori and Gerald³⁷ yields $\kappa = 0.66$.

4.4. Discussion

4.4.1. Mutual exclusion of components in water-glycerol mixture

The adiabatic compressibility β_p and its corollary the root mean square volume fluctuation $\delta V_{\rm RMS}$ are two of the thermodynamic properties whose values at constant temperature are perturbed by glycerol viscosity. One therefore seeks an account based on the thermodynamic interaction between the solvent components in the water-lysozyme-glycerol system before considering the

fallout on the protein. A motivating observation we have made with the water:glycerol mixture is the exclusion of the components from each other's vicinity, a phenomenon of thermodynamic exclusion common to mixtures of polar:apolar substances. If water and glycerol molecules both obey the van der Waals equation of state, then they share similar variation of their thermodynamic properties in response to a variable at the same reduced pressure and temperature. This is the outcome of the generalized corresponding state principle (CSP) that states that the thermodynamic behavior of the two mutually excluding components will vary in a similar manner.³⁹ For example, the decrease in the surface tension γ of glycerol with a rise of its mole fraction⁴⁰ is accompanied by a slight decrease in the γ of water as well.²⁹ The decrease in the γ of water per se is counterproductive to preferential hydration of the protein surface.³⁰ Instead, the reduced surface tension lowers the Gibbs free energy barriers for both water clustering and glycerol aggregation, leading to exclusion of glycerol from the surface of the protein whose solvation shell will now have improved density of water at the protein-water interface. This argument is similar to those stated earlier in the context of protein stabilization by glycerol.^{29,31}

The preferential exclusion of glycerol leading to improved protein solvation can also be discussed with reference to the principle of composition fluctuation⁴¹ applied to the water:glycerol binary system. The thermodynamic interaction between the two should cause one component, say glycerol, to produce composition fluctuation with respect to the other to the same extent as that with respect to the former. Denoting the water and glycerol by '1' and '2', the individual excess chemical potentials can be given by

$$\mu_i = \mu_i^0(T, P) + \log \gamma_i c_i \tag{13}$$

with $\log \gamma_1 = A_{11}c_1 + A_{12}c_2$ and $\log \gamma_2 = A_{21}c_1 + A_{22}c_2$, in which the thermodynamic interaction coefficients A_{11} , A_{12} , A_{21} , and A_{22} measure the perturbation of γ of one component by the other in the mixture. The off-diagonal terms in the coefficient matrix arise from intercomponent thermodynamic interactions, and they are predicted to be negative if glycerol and water mutually exclude each other.

4.4.2. Protein compressibility and molecular fluctuation

The above thermodynamic interactions between water and glycerol are expected to drive the native-state of the protein ensemble to less flexible states³¹ that have larger intramolecular density and reduced compressibility (Figure 4.1c), which merits evaluation in terms of the number of fluctuating protein molecules N about an average $\langle N \rangle$. The basic analysis is approached with the Grand Canonical Ensemble theory of Kirkwood and Buff⁴² that can relate the variance of the isothermal compressibility β_T ($\approx \beta_P$) to the distribution of the number of protein molecules whose average value is the Avogadro number on a molar basis. Denoting the total number of lysozyme molecules by N and the volume V, it can be shown that⁴³

$$\frac{\langle N^2 \rangle - \langle N \rangle^2}{\langle N \rangle^2} = \frac{\sigma_N^2}{\langle N \rangle^2} \cong \frac{k_{\rm B} T \, \beta_{\rm T}}{V} \tag{14}$$

where σ_N^2 is the variance. We have already determined β_T ($\approx\beta_P$) with increasing mole fraction of glycerol. Taking the volume as the molar volume of lysozyme (\sim 14000 cm³ mol⁻¹), one can calculate the standard deviation σ for each value of β_T , i.e., as a function of glycerol viscosity (Figure 4.10a). The probability distribution P(N) calculated as a normalized Gaussian distribution for N

$$P(N) = \frac{1}{\sigma\sqrt{2\pi}} e^{-0.5\left(\frac{N-\langle N\rangle}{\sigma}\right)^2}$$
 (15)

is shown in Figure 4.10b for each value of β_T . The width of the distribution ($FWHM = 2\sigma\sqrt{\ln 2}$) is centered about the mean value $\langle N \rangle = 6.022 \times 10^{23}$. By comparing N with σ , one finds that the fluctuations in the number of protein molecules are just one part in 1.3×10^{14} in water alone and one part in 1.6×10^{14} in the presence of 50% glycerol, implying that the fluctuating molecules decrease with increase in glycerol viscosity. We should also note that the compressibility decrease with glycerol viscosity that appears to follow a power law dependence (Figure 4.1) should have contributions from average compressional relaxation time of liquid glycerol as well. The same argument applies to volume fluctuation (Figure 4.2). Because lower compressibility constrains atom density fluctuations, 44,45 the volume fluctuation quantified by δV_{RMS} decreases.

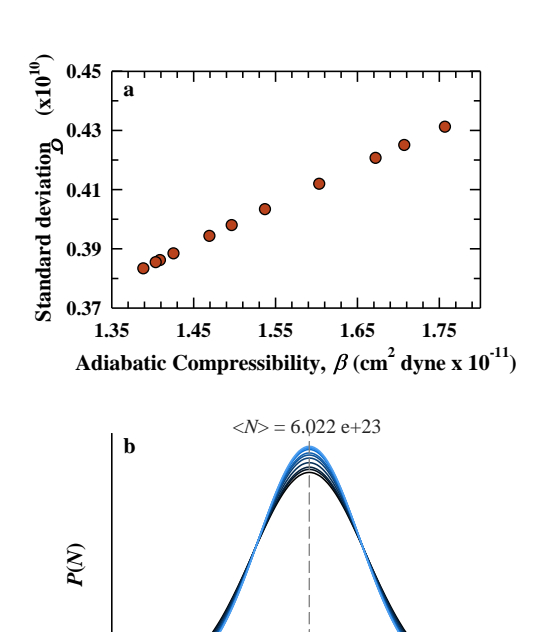


Figure 4.10. (a) Standard deviation (σ) associated with adiabatic compressibility of lysozyme, 298 K, pH 3.8. Note that σ decreases as the compressibility decreases with higher solvent viscosity because the volume fluctuation decreases. (b) The probability distribution function P(N) for the number of fluctuation molecules N.

N (x 10⁻¹⁰)

0.5

1.5

-0.5

4.4.3. Fractional viscosity dependence of protein motions

-1.5

As this discussion will be based on results, evidences, and postulates of glycerol effect on protein motions, it is convenient to present the premises in subsections. We keep in mind while progressing that studies of viscosity and relaxation, and thermodynamics of glycerol date back several decades and are still in flux.

4.4.3.1. Power law dependence of glycerol dielectric loss on frequencies.

The conduction of alternating current (AC) by dielectric substances can be expressed to have contributions from both DC and effective AC components

$$\sigma(\omega) = \sigma_0 + \omega \varepsilon''(\omega) \tag{16}$$

where $\sigma(\omega)$ is the conductivity and ε'' is the AC contribution to the conductivity, i.e., the dielectric loss. Empirical analysis of a large set of dielectric spectra has already shown that $\varepsilon''(\omega)$ universally exhibits a power law dependence on frequency, $\varepsilon''(\omega) \propto \omega^{n-1}$, $0.6 < n < \infty$ 1.46 Specific to glycerol, most recent experiments show power law frequency dependence for low-frequency orientational-relaxation, called α -loss ($\nu^{-\kappa}$, $\kappa \approx 0.5$), as well as high-frequency caged rattling motion, called β -loss ($\nu^{-\kappa}$, κ in 0.1–0.2 range), at low temperature.⁴⁷ We note that the power law dielectric loss represents the frequency response of motional relaxation, unlike the inhomogeneously broadened Gaussian molecular spectrum calculated from the electronic transition dipoles of molecules in different environment, 33 and may arise from both bulk as well as barrier responses due to a variety of dipole reorganization motions. 46 Moreover, the motions of viscous flow, i.e., orientation and translation, may not be executed by all molecules uniformly across the sample volume. Bulk inhomogeneity should mean spatial inhomogeneity in the macroscopic viscosity which is measured as an average over the entire volume of the liquid. We suggest that the local macroscopic viscosity appears to present the viscosity of glycerol as an extrinsic property, arising from its aggregation tendency. To summarize, the dependence of dielectric loss of glycerol on fractional power of frequency originates from dynamic heterogeneity of the macroscopic viscosity of glycerol across the volume of the liquid.

4.4.3.2. Power law dependence of glycerol self-diffusion on glycerol viscosity

The dynamic heterogeneity in the macroscopic viscosity of glycerol proposed above should lead to a non-Stokesian performance of isotropic diffusion of glycerol (Figure 4.9). Indeed so, results from molecular and Langevin dynamics simulations with a glass forming liquid have also shown that the diffusion coefficient D_s of the liquid does not vary linearly with viscosity as predicted, but follows a fractional viscosity dependence with a power law exponent $\kappa \sim 0.85$. This study shows further that the rate of loop formation in a polymer embedded in the glass forming liquid also has a fractional viscosity dependence with a κ -value nearly identical to that obtained for the diffusion coefficient of the liquid against its viscosity. We note from our earlier studies that the rate of intrachain loop formation with microscopic internal friction coefficient also deviates from

linearity; increase of internal friction reduces the rate of polypeptide relaxation,⁴⁹ but whether in accordance with a power law or not remains to be verified. However, the indications that dynamic heterogeneity of glycerol gives rise to a power law dependence of its diffusion on macroscopic viscosity should also lead to a power law dependence of protein motions, at least the orientational and translational modes that are directly related to the viscous flow.

4.4.3.3. Power law dependence of protein motions on glycerol viscosity

The concurrence of fractional viscosity dependence of the bulk solvent component and the protein solute logically leads to the conception that at least some of the protein motions will be coupled to the relaxation of the solvent. The protein motions and folding are said to be slaved by dielectric relaxations of glycerol, ^{17,19} an approximate mechanics-based theory of which has also been given. ¹⁸ If the rate coefficients of protein fluctuations are assumed proportional, although smaller by ~5-orders of magnitude, to the orientational and translational relaxation rates of glycerol and the latter shows fractional viscosity dependence, the overdamped Kramers behavior observed on numerous occasions of protein and enzyme reaction rates with glycerol viscosity ¹⁶ can also be explained. One may note that the rate × 1/viscosity relation predicted by Kramers theory, ^{50,51} which is based on the extent to which the frictional damping rate affects the degree of interaction of the reaction coordinate with the remaining degrees of freedom of the system, is decisive in both classical and quantum regimes. ⁵¹ The overdamped 'artifact' observed for numerous protein processes in solutions arises mainly from overdamped relaxation of glycerol molecules.

We end this section by stating that solvent slaving refers to the coupling of not only glycerol relaxation, but also the fluctuation of bulk and hydration water to protein dynamics. ^{17,52} Therefore, if water and glycerol exclude each other purely on the thermodynamic ground so as to enrich the protein hydration layer in terms of water density and water-protein hydrogen bonding, the salving of some of the intra-protein motions by water is also expected to change.

4.4.3.4. Solvent slaving of NMR cross-relaxation rate.

The rate of cross relaxation between nuclear spins k and l is inversely proportional to the average of the sixth root of the distance between them $(\sigma_{kl} \propto \langle r_{kl}^{-6} \rangle)$, for which the fluctuation of the kl internuclear vector (r_{kl}) may be considered. We have found that proton crossrelaxation rates show fractional viscosity dependence with a power law exponent $\langle \kappa \rangle = 0.65$, SD 0.15 (Figure 4.5), implying that r_{kl} fluctuations are also slaved by the bulk solvent fluctuations and hence macroscopic viscosity. Although the result presented is conclusive, the interpretation may not seem as straightforward as it reads, because the slaving model is presumably not reliant on internal dissipation of energy.¹⁹ There are two approaches to analyze the validity of the interpretation. One, we concluded in an earlier study with no reference to the slaving concept that internal collective motions in protein, viz. ring flip rate, are damped by internal friction arising from dispersion interactions and London-van der Waals forces between nonbonded atoms.⁴ That study used glycerol to reduce the $\delta V_{\rm RMS}$, leading to an increase in internal friction. In this setup, the internal friction may be thought as a delegate of the macroscopic viscosity, even though no dielectric relaxation can occur in the intraprotein milieu because glycerol cannot penetrate into the protein interior. Nevertheless, since the bulk solvent influences σ_{kl} , plausibly by increasing the density of the hydration shell, it may be stated that the internal fluctuations are also slaved by solvent relaxations. Two, σ_{kl} is generally insensitive to internal motions when the internal correlation time is smaller than the rotational tumbling correlation time ($\tau_i \ll \tau_c$), which is almost always the case. In the viscous medium, longer τ_c invariably leads to the spin diffusion limit, which means the cross relaxation rate depends on the relative tumbling correlation time $\omega_0 \tau_c$, where ω_0 is the Larmor frequency. We also notice from Figure 4.8 that the cross relaxation rate does not show a power law dependence on τ_c , suggesting that the global tumbling motion does not slave the internal motion even if the former is slaved by solvent relaxation.

4.4.3.5. Glycerol-induced disorder and internal distance fluctuations

A difficulty may appear when the decrease of nuclear cross-relaxation rate σ_{kl} , and hence a decrease in the spatial restriction of the two cross-relaxing nuclei, with increasing glycerol viscosity is considered (Figures 4.5, 4.6). Moreover, the value of the generalized order parameter S_{kl}^2 characterizing the spatial restriction of the r_{kl} vector decreases with glycerol (Figure 4.7),

suggesting increasing fluctuations in the protein interior. This result may appear incompatible with glycerol-induced reduction in the compressibility and volume fluctuation (Figures 4.1, 4.2), both of which are expected to decrease the respective amplitudes of internal fluctuations.⁴ There should be no confusion, however; glycerol generally does not preserve the native state of a protein, but induces a reversible transition from the native to a less stable quasi-native state whose tertiary structure is less stable with increased fluctuations.²⁸ Steady-state experiments may still indicate compaction of lysozyme, ^{28,35,53} but this added compaction is related to the four disulfide bridges of lysozyme that are stable near pH 4.

4.4.3.6. Water-glycerol medium as the viscogen: a catch-22 condition

Our initial idea of varying the tumbling correlation of the protein by changing glycerol viscosity so as to displace the time-scale bin for the observation of intramolecular dynamics by NMR is indeed useful, but the above mentioned structural changes induced by glycerol come as a setback. To what extent the dynamics and relaxation of a protein in glycerol can be associated with its native state is questionable, even though glycerol is universally used as a viscogen in a plethora of protein studies. Nevertheless, dielectric relaxations (losses) of glycerol, however complex they could be, ^{47,54,55} have yielded to the development of the solvent slaving concept of protein motions. ^{17–19,56–60}

4.5. Conclusion

In the three-component system water-protein-glycerol, both glycerol and protein exhibit non-Stokesian self-diffusion showing a fractional viscosity dependence with similar values of the power law exponent. This resemblance of fractional viscosity dependence leads to the thinking that some protein processes should be slaved by glycerol. By connecting this premise to earlier reports of the slaved dynamics model, we find that root-mean-square volume fluctuation and NMR cross relaxation rates are also slaved by dielectric relaxation of glycerol. It is suggested that solvent slaving of protein properties (dynamics) can explain the overdamped Kramers

behavior observed for numerous studies of solvent viscosity dependence of protein and enzyme reaction rates.

4.6. References

- 1. Petsko, G. A.; Ringe, D. Fluctuations in Protein Structure from X-Ray Diffraction. *Annu. Rev. Biophys. Bioeng.* **1984**, *13*, 331–371.
- Rao, D. K.; Bhuyan, A. K. Complexity of Aromatic Ring-Flip Motions in Proteins: Y97
 Ring Dynamics in Cytochrome c Observed by Cross-Relaxation Suppressed Exchange
 NMR Spectroscopy. J. Biomol. NMR 2007, 39, 187–196.
- 3. Rodríguez-Molina, B.; Pérez-Estrada, S.; Garcia-Garibay, M. Amphidynmic Crystals of Steroidal Bicyclo[2.2.2]octane Rotor: A Highly Symmetric Group that Rotates Faster than Smaller Methyl and Methoxy Groups. *J. Am. Chem. Soc.* **2013**, *135*, 10388–10395.
- 4. Sashi, P.; Ramakrishna, D., Bhuyan, A. K. Dispersion Forces and the Molecular Origin of Internal Friction in Protein. *Biochemistry* **2016**, *55*, 4595–4602.
- Pérez, L. M.; Ielasi, F. S.; Bessa, L. M.; Maurin, D.; Kragelj, J.; Blackledge, M.; Salvi, N.;
 Bouvignies, G.; Palencia, A.; Jensen, M. R. Visualizing Protein Breathing Motions
 Associated with Aromatic Ring Flipping. *Nature* 2022, 602, 695–700.
- 6. Akke, M.; Weininger, U. NMR Studies of Aromatic Ring Flips to Probe Conformational Fluctuations in Proteins. *J. Phys. Chem. B* **2023**, *127*, 591–599.
- 7. Ansari, A.; Jones, C. M.; Henry, E. R.; Hofrichter, J.; Eaton, W. A. The Role of Solvent Viscosity in the Dynamics of Protein Conformational Changes. *Science* **1992**, *256*, 1796–1798.

- 8. Kim, K. H.; Muniyappan, S.; Oang, K. Y.; Kim, J. G.; Nozawa, S.; Sato, T.; Koshihara, S.; Henning, R.; Kosheleva, I.; Ki, H.; Kim, Y.; Kim, T. W.; Kim, J.; Adachi, S.; Ihee, H. Direct Observation of Cooperative Structural Dynamics of Homodimeric Hemoglobin from 100 ps to 10 ms with Pump-probe X-Ray Solution Scattering. *J. Am. Chem. Soc.* **2012**, *134*, 7001–7008.
- 9. Brinkmann, L. U. L.; Hub, J. S. Ultrafast Anisotropic Protein Quake Propagation after CO Photodissociation in Myoglobin. *Proc. Natl. Acad. Sci. USA* **2016**, *113*, 10565–10570.
- Kovacs, G. N.; Colletier, J-P.; Grünbein, M. L.; Yang, Y.; Stensitzki, T.; Batyuk, A.; Carbajo, S.; Doak, R. B.; Ehrenberg, D.; Foucer, L.; Gasper, R.; Gorel, A.; Hilpert, M.; Kloos, M.; Koglin, J. E.; Reinstein, J.; Roone, C. M.; Schlesinger, R.; Seaberg, M.; Shoeman, R. L.; Stricker, M.; Boutet, S.; Haacke, S.; Heberle, J.; Heyne, K.; Domratcheva, T.; Barends, T. R. M.; Schlichting, I. Three-Dimensional View of Ultrafast Dynamics in Photoexcited Bacteriorhodopsin. *Nat. Commun.* 2019, 10, 3177.
- 11. Ghosh, A.; Ostrander, J. S.; Zanni, M. T. Watching Protein Wiggle: Mapping Structures with Two-Dimensional Infrared Spectroscopy. *Chem. Rev.* **2017**, *117*, 10726–10759.
- Lee, Y.; Kim, J. G.; Lee, S. J.; Muniyappan, S.; Kim, T. W.; Ki, H.; Kim, H.; Jo, J.; Yun, S. R.; Lee, H.; Lee, K. W.; Kim, S. O.; Cammarata, M.; Ihee, H. Ultrafast Coherent Motion and Helix Rearrangement of Homodimeric Hemoglobin Visualized with Femtosecond X-Ray Solution Scattering. *Nat. Commun.* 2021, 12, 3677.
- 13. Frauenfelder, H.; Sligar, S. G.; Wolynes, P. G. The Energy Landscapes and Motions of Proteins. *Science* **1991**, *254*, 1598–1603.
- 14. Phillips, D. C. The Three-Dimensional Structure of an Enzyme Molecule. *Sci. Am.* **1966**, 215, 78–90.

- 15. Swarupini, D. S.: Joshi, K.; Bhuyan, A. K. Negative Thermal Expansion of a Disordered Native Protein. *Chem. Phys.* **2022**, *560*, 111569.
- 16. Sashi, P.; Bhuyan, A. K. Viscosity Dependence of some Protein and Enzyme Reaction Rates: Seventy-Five Years after Kramers. *Biochemistry* **2015**, *54*, 4453–4461.
- 17. Fenimore, P. W.; Frauenfelder, H.; McMahon, B. H.; Parak, F. G. Slaving: Solvent Fluctuations Dominate Protein Dynamics and Fluctuations. *Proc. Natl. Acad. Sci. USA* **2002**, *99*, 16047–16051.
- 18. Lubchenko, V.; Frauenfelder, H.; Wolynes, P. G. Mosaic Energy Landscapes of Liquids and the Control of Protein Conformational Dynamics by Glass-forming Solvents. *J. Phys. Chem. B* **2005**, *109*, 7488–7499.
- 19. Frauenfelder, H.; Fenimore, P. W.; Chen, G.; McMahon, B. H. Protein Folding is Slaved to Solvent Motions. *Proc. Natl. Acad. Sci. USA* **2006**, *103*, 15469–15472.
- 20. Gekko, K.; Noguchi, H. Compressibility of Globular Proteins in Water at 25°C. *J. Phys. Chem.* **1979**, *83*, 2706–2714.
- 21. Eden, D.; Matthew, J. B.; Rosa, J. J.; Richards, F. M. Increase in Apparent Compressibility of Cytochrome *c* upon Oxidation. *Proc. Natl. Acad. Sci. USA* **1982**, *79*, 815–819.
- 22. Gekko, K.; Hasegawa, Y. Effect of Temperature on the Compressibility of Native proteins. *J. Phys. Chem.* **1989**, *93*, 426–429.
- 23. Gekko, K.; Yamagani, K. Flexibility of Food Protein as Revealed by Compressibility. *J. Agric. Food Chem.* **1991**, *39*, 57–62.
- 24. Kharakoz, D. P. Volumetric Properties of Proteins and their Analogues in Diluted Water Solutions. 2. Partial Adiabatic Compressibilities of Amino Acids at 15–70°C. *J. Phys.*

- Chem. 1991, 95, 5634–5642.
- 25. Taulier, N.; Chalikian, T. V. Compressibility of Protein Transitions. *Biochim. Biophys. Acta* **2002**, *1595*, 48–70.
- 26. Ringe, D.; Petsko, G. A. Study of Protein Dynamics by X-Ray Diffraction. *Methods Enzymol.* **1986**, *131*, 389433.
- 27. Cooper, A. Thermodynamic Fluctuations in Protein Molecules. *Proc. Natl. Acad. Sci. USA* **1976**, *73*, 2740–2741.
- 28. Joshi, K.; Bhuyan, A. K. Quasi-native Transition and Self-Diffusion of Protein in Water-Glycerol Mixture. *Biophys. Chem.* **2020**, 257, 106274.
- 29. Gekko, K.; Timasheff, S. N. Mechanism of Protein Stabilization by Glycerol: Preferential Hydration in Glycerol-Water Mixtures. *Biochemistry* **1981**, *20*, 4667–4676.
- Sinibaldi, R.; Ortore, M. G.; Spinozzi, F.; Carsughi, F.; Frielinghaus, H.; Cinelli, S.; Onori,
 G.; Mariani, P. Preferential Hydration of Lysozyme in Water/glycerol Mixtures: a Small-Angle Neutron Scattering Study. *J. Chem. Phys.* 2007, 126, 235101.
- 31. Vagenende, V.; Yap, M. G. S.; Trout, B. L. Mechanism of Protein Stabilization and Prevention of protein Aggregation by Glycerol. *Biochemistry* **2009**, *48*, 11084–11096.
- 32. Ernst, R. R.; Bodenhausen, G.; Wokaun, A. *Principles of Nuclear Magnetic Resonance in One and Two Dimensions*; Oxford University Press: Oxford, 1988.
- 33. Bhuyan, A. K. *Fundamental Concepts of Molecular Spectroscopy*; CRC Press, Taylor & Francis Group: Boca Raton, Fl, 2023.
- 34. Bonincontro, A.; Calandrini, V.; Onori, G. Rotational and Translational Dynamics of

- Lysozyme in Water-Glycerol Solution. *Colloids Surf. B: Biointerfaces* **2001**, 21, 311–316.
- 35. Bonincontro, A.; Risuelo, G. Dielectric Spectroscopy as a Probe for the Investigation of Conformational Properties of Proteins. *Spectrochim. Acta A* **2003**, *59*, 2677–2684.
- 36. Brüschweiler, R.; Roux, B.; Blackledge, M.; Griesinger, C.; Ernst, R. R. Influence of Rapid Intramolecular Motion on NMR Cross-Relaxation Rates. A Molecular Dynamics Study of Antmanide in Solution. *J. Am. Chem. Soc.* **1992**, *114*, 2289–2312.
- 37. Yasunori, N.; Gerald, O. Diffusion in Glycerol-Water Mixture. *Bull. Chem. Soc. Japan* **1960**, *33*, 1649–1651.
- 38. Gavish, B.; Yedgar, S. Solvent Viscosity Effect of Protein Dynamics: Updating the Concepts. In *Protein-Solvent Interactions*; Gregory, R. B., Ed.; Marcel Dekker, Inc: New York, 1995; pp 343–373.
- 39. Rice, P.; Teja, A. S. A Generalized Corresponding-States Method for the Prediction of Surface Tension of Pure Liquids and Liquid Mixtures. *J. Colloid Interface Sci.* **1982**, *86*, 158–163.
- 40. Takamura, K.; Fischer, H.; Morrow, N. R. Physical Properties of Aqueous Glycerol Solutions. *J. Petroleum Sci. Engg.* **2012**, *98*–*99*, 50–60.
- 41. Kirkwood, J. G.; Goldberg, R. J. Light Scattering Arising from Composition Fluctuations in Multicomponent Systems. *J. Chem. Phys.* **1950**, *18*, 54–57.
- 42. Kirkwood, J. G.; Buff, F. P. The Statistical Mechanical Theory of Solutions. *J. Chem. Phys.* **1951**, *19*, 774–777.
- 43. Newman, K. E. Kirkwood-Buff Solution Theory: Derivation and Applications. *Chem. Soc. Rev.* **1994**, *23*, 31–40.

- 44. Phelps, D. K.; Post, C. B. A Novel Basis for Capsid Stabilization by Antiviral Compounds. *J. Mol. Biol.* **1995**, 254, 544–551.
- 45. Halle, B. Flexibility and Packing in Proteins. *Proc. Natl. Acad. Sci. USA* **2002**, *99*, 1274–1279.
- 46. Jonscher, A. K. A New Understanding of the Dielectric Relaxation of Solids. *J. Mater. Sci.* **1981**, *16*, 2037–2060.
- 47. Ngai, K. L.; Capaccioli, S.; Lunkenheimer, P.; Loidl, A. Arriving at the Most Plausible Interpretation of the Dielectric Spectra of Glycerol with Help From Quasielastic γ-Ray Scattering Time-Domain Interferometry. *Phys. Rev. E* **2022**, *105*, 054609.
- 48. Kwon, S.; Cho, H. W.; Kim, J.; Sung, B. J. Fractional Viscosity Dependence of Reaction Kinetics in Glass-Forming Liquids. *Phys. Rev. Lett.* **2017**, *119*, 087801.
- 49. Yasi, U. M.; Sashi, P.; Bhuyan, A. K. Expansion and Internal Friction in Unfolded Protein Chain. *J. Phys. Chem. B* **2013**, *117*, 12059–12064.
- 50. Kramers, H. A. Brownian Motion in a Field of Force and the Diffusion Model of Chemical Reactions. *Physica* **1940**, *7*, 284–304.
- 51. Hangii, P.; Talkner, P.; Borkovec, M. Reaction Rate Theory: Fifty Years After Kramers. *Rev. Mod. Phys.* **1990**, *62*, 251341.
- 52. Mattos, C. Protein-Water Interactions in a Dynamic World. *Trends Biochem. Sci.* **2002**, 27, 203–208.
- 53. Filianina, M.; Bin, M.; Berkowicz, S.; Reiser, M.; Li, H.; Timmermann, S.; Blankenburg, M.; Amann-Winkel, K.; Gutt, C.; Perakis, F. Nanocrystallites Modulate Intermolecular

- Interactions in Cryoprotected Protein Solutions. J. Phys. Chem. B 2023 (arXiv:2304.05802).
- 54. Farrell, A. J.; González-Jiménez, M.; Ramakrishnan, G.; Wynne, K. Low-Frequency (Gigahertz to Terahertz) Depolarized Raman Scattering Off n-Alkanes, Cycloalkanes, and Six-Membered Rings: A Physical Interpretation. *J. Phys. Chem. B* **2020**, *124*, 7611–7624.
- 55. Saito, M.; Kurokuzu, M.; Yoda, Y.; Seto, M. Microscopic Observation of Hidden Johari-Goldstein-β process in glycerol. *Phys. Rev. E* **2022**, *105*, L012605.
- 56. Bellissent-Funel, M-C.; Hassanali, A.; Havenith, M.; Henchman, R.; Pohl, P.; Sterpone, F.; van der Spoel, D.; Xu, Y.; Garcia, A. E. Water Determines the Structure and Dynamics of Proteins. *Chem. Rev.* **2016**, *116*, 7673–7697.
- 57. Marques, B. S.; Stetz, M. A.; Jorge, C.; Valentine, K. G.; Wand, A. J.; Nucci, N. V. Protein Conformational Entropy is not Slaved to Water. *Sci. Rep.* **2020**, *10*, 17587.
- 58. Caliskan, G.; Kisliuk, A.; Sokolov, A. P. Dynamic Transition in Lysozyme: Role of a Solvent. *J. Non-Cryst. Solids* **2002**, *307–310*, 868–873.
- Caliskan, G.; Mechtani, D.; Roh, J. H.; Kisliuk, A.; Sokolov, A. P.; Azzam, S.; Cicerone, M. T.; Lin-Gibson, S. Protein and Solvent Dynamics: How Strongly are they Coupled. *J. Chem. Phys.* 2004, *121*, 1978–1983.
- 60. Dirama, T. E.; Carri, G. A.; Sokolov, A. P. Coupling Between Lysozyme and Glycerol Dynamics: Microscopic Insights From Molecular-Dynamics Simulations. *J. Chem. Phys.* **2005**, *122*, 244910.

Publications

- 1. Joshi, K.; Bhuyan, A. K. Quasi-native transition and self-diffusion of protein in water-glycerol mixture. *Biophysical Chemistry*. **2020**, *257*, 106274.
- 2. Swarupini, D. S.; Joshi, K.; Bhuyan, A. K. Negative thermal expansion of a disordered native protein. *Chemical Physics.* **2022**, *560*, 111569.

Presentations

- 1. Poster: "The effect of Glycerol on the structure of protein", at CHEMFEST 2019: Annual In-house symposium at School of Chemistry, University of Hyderabad.
- 2. Presentation: "NMR and Optical Spectroscopic studies on binary and ternary aqueous system containing glycerol as a component" at CHEMFEST 2021: Annual In-house symposium at School of Chemistry, University of Hyderabad.

Plagiarism-free statement

This is to certify that the thesis titled "Proton-Catalyzed Oligomerization, non-Stokesian Diffusion and the Slaving Effect of Glycerol on Protein Folding and Dynamics" has been screened by the Turnitin software at the Indian Gandhi Memorial Library of University of Hyderabad.

The software shows a similarity index of 35%, out of which 31% is from student's own article related to the thesis which is available online as

1. Kirthi Joshi, Abani K. Bhuyan. Quasi-native transition and self-diffusion of proteins in water-glycerol mixture. *Biophysical Chemistry*. **2020**, *257*, 106274.

Thus after excluding student's own research article, the effective similarity index is 4% (35% - 31%) which is less than the stipulated 10% as per the university guidelines.

Therefore this thesis is considered free from plagiarism as per the guidelines.

27 07 2023

Signature of the Supervisor

ABANI K. BHUYAN, Ph.D. Professor

University of Hyderabad School of Chemistry Hyderabad - 500 046.

Proton-Catalyzed Oligomerization, non-Stokesian Diffusion, and the Slaving Effect of Glycerol on Protein Folding and Dynamics

by Kirthi Joshi

Submission date: 26-Jul-2023 12:15PM (UTC+0530)

Submission ID: 2136998168

File name: Kirthi Joshi Thesis for Plagiarism Check 17CHPH02.pdf (1.06M)

Word count: 18912 Character count: 98379

Proton-Catalyzed Oligomerization, non-Stokesian Diffusion, and the Slaving Effect of Glycerol on Protein Folding and Dynamics

ORIGINALITY REPORT SIMILARITY INDEX INTERNET SOURCES **PUBLICATIONS** STUDENT PAPERS PRIMARY SOURCES Kirthi Joshi, Abani K. Bhuyan. "Quasi-native transition and self-diffusion of proteins in water-glycerol mixture", Biophysical ABANI K. BHUYAN, Ph.D. Chemistry, 2020 Professor University of Hyderabad Publication School of Chemistry Hyderabad - 500 046. www.ncbi.nlm.nih.gov Internet Source Pulikallu Sashi, Dasari Ramakrishna, Abani K. 3 Bhuyan. "Dispersion Forces and the Molecular Origin of Internal Friction in Protein", Biochemistry, 2016

Brueschweiler, R., B. Roux, M. Blackledge, C. Griesinger, M. Karplus, and R. R. Ernst. "Influence of rapid intramolecular motion on NMR cross-relaxation rates. A molecular dynamics study of antamanide in solution", Journal of the American Chemical Society, 1992.

Publication

Publication



11	worldwidescience.org Internet Source	<1%
12	Andrew N. LANE. "The influence of tryptophan on mobility of residues in the trp repressor of Escherichia coli", European Journal of Biochemistry, 6/1989 Publication	<1%
13	www.researchgate.net Internet Source	<1%
14	Matthew B. Seefeldt, Yong-Sung Kim, Kevin P. Tolley, Jim Seely, John F. Carpenter, Theodore W. Randolph. "High-pressure studies of aggregation of recombinant human interleukin-1 receptor antagonist: Thermodynamics, kinetics, and application to accelerated formulation studies", Protein Science, 2005 Publication	<1%
15	Submitted to Osmania University, Hyderabad Student Paper	<1%
16	pure.rug.nl Internet Source	<1%
17	Mitsuhiro Hirai, Satoshi Ajito, Tatsuo Iwasa, Durige Wen, Noriyuki Igarashi, Nobutaka Shimizu. "Short-Distance Intermolecular Correlations of Mono- and Disaccharides in	<1%

Condensed Solutions: Bulky Character of Trehalose", ACS Omega, 2020

Publication

18	argops.psu.edu Internet Source	<1%
19	cpi.vm.uni-freiburg.de Internet Source	<1%
20	erewhon.superkuh.com Internet Source	<1%
21	Abani K. Bhuyan. "Off-Pathway Status for the Alkali Molten Globule of Horse Ferricytochrome", Biochemistry, 2010 Publication	<1%
22	C. T. Farrar. "Mechanism of dynamic nuclear polarization in high magnetic fields", The Journal of Chemical Physics, 2001 Publication	<1%
23	www.meritnation.com Internet Source	<1%

Exclude quotes On Exclude bibliography On

Exclude matches

< 14 words